THE EARLY STAGES OF *CLOSTRIDIOIDES DIFFICILE* SPORE GERMINATION

A Dissertation

by

Marko Baloh

Submitted to the Graduate and Professional School of

Texas A&M University

in partial fulfillment of the requirements for the degree of

DOCTOR OF PHILOSOPHY

Chair of Committee,	Joseph A. Sorg
Committee Members,	Jerome Menet
	Beiyan Nan
	Paul Straight
Head of Department,	Alex Keene

August 2022

Major Subject: Microbiology

ABSTRACT

Clostridioides difficile is a Gram-positive, obligately anaerobic microorganism that is of considerable medical concern as a nosocomial and community-acquired human pathogen. *C. difficile* is an endospore-forming organism and spores are commonly introduced into a host via fecal-oral route. The spore is metabolically dormant and exhibits considerable resistance to environmental conditions (*e.g.,* oxygen, heat, UV, and commonly used disinfectants). The toxin-producing, vegetative form develops from the germinated spore and the toxins damage the lower gastrointestinal tract epithelium. Spore germination is an irreversible and tightly regulated process. Spore germination begins upon the detection of small-molecule germinants and ends with the release of the large depot of calcium dipicolinic acid (DPA) from the core, core rehydration and the resumption of metabolic activities. Here, using EM immunolabeling, we determined the location of the CspB, CspA, and CspC, and SleC proteins. Also using a split-luciferase system, we determined that the products of the *spoVA* operon, which are responsible for DPA packaging into the spore core during sporulation, interact and are localized to the inner spore membrane. The combined data is the first to determine how the SpoVA proteins interact and to determine the location of the *C. difficile* ‘germinosome’ components.

DEDICATION

To Andrea, Alice, Mia, Albus, and Chloe. Couldn’t have done it without you.

CONTRIBUTORS AND FUNDING SOURCES

Contributors

This work was supervised by a dissertation committee consisting of Professor Joseph A. Sorg, Professor Jerome Menet, and Professor Beiyan Nan of the Department of Biology and Professor Paul Straight of the Department of Biochemistry and Biophysics.

In Chapter 2, Hailee N. Nerber from Texas A&M University performed experiments and contributed significantly to this work for which they were authors on this publication. All other work conducted for the dissertation was completed by the student independently.

Funding Sources

This project was supported by awards 5R01AI116895 and 1U01AI124290 to J.A.S. from the National Institute of Allergy and Infectious Diseases. The content is solely the responsibility of the authors and does not necessarily represent the official views of the NIAID. The funders had no role in study design, data collection and interpretation, or the decision to submit the work for publication.

NOMENCLATURE

AD	activation domain
ANOVA	analysis of variance
aTc	anhydrotetracycline
BACTH	Bacterial Adenylate Cyclase-based Two-Hybrid
BHI	brain heart infusion medium
BHIS	brain heart infusion medium supplemented with yeast extract
CaDPA	chelate of Ca^{2+} with pyridine-2,6-dicarboxylic acid
cAMP	cyclic adenosine monophosphate
CAP	catabolite activator protein
CCD	charge-coupled device
CCTOPS	consensus constrained topology prediction web server
CDI	*Clostridioides difficile* infection
CDT	*C. difficile* binary toxin
CDMM	*C. difficile* defined minimal medium
CRISPR	clustered regularly interspaced short palindromic repeats
DNA	deoxyribonucleic acid
DNA-BD	DNA binding domain
DO	dropout medium
DDO	double dropout medium
DPA	dipicolinic acid
EM	electron microscopy
EMS	ethyl methanesulfonate
FEG	field emission gun
FLAG	polypeptide protein tag with DYKDDDDK sequence
FOA	5-fluoroorotic acid
GCW	germ cell wall
GI	gastrointestinal

gRNA	guide RNA
GTPase	guanosine triphosphate (GTP) hydrolase
HEPES	2-[4-(2-hydroxyethyl) piperazin-1-yl] ethanesulfonic acid
HMDS	hexamethyldisilazane
HM20	Lowicryl HM20 acrylic resin
HPF	high pressure freezing
IM	inner membrane
K4M	Lowicryl K4M acrylic resin
LB	lysogeny broth
MCS	multicloning site sequence
MDL	muramic-δ-lactam
OD	optical density
OM	outer membrane
PaLoc	pathogenicity locus
PBS	phosphate buffered saline
PCR	polymerase chain reaction
PLT	progressive lowering of temperature
PVDF	polyvinylidene difluoride
QDO	quadruple dropout medium
RBS	ribosome binding site
RNA	ribonucleic acid
RT	room temperature
SASP	small acid-soluble spore proteins
SD	synthetic minimal medium
SDS-PAGE	sodium dodecyl sulfate polyacrylamide gel electrophoresis
SCLE	spore cortex lytic enzymes
SEM	scanning electron microscopy
TA	taurocholic acid

TBST	tris-buffered saline supplemented with 1% (vol / vol) Tween 20
TEM	transmission electron microscopy
TY	tryptone yeast medium
UV	ultraviolet
WT	wild type
YPDA	yeast peptone dextrose adenine medium
Y2A	yeast two-hybrid

TABLE OF CONTENTS

LIST OF FIGURES

Page

LIST OF TABLES

Page

INTRODUCTION TO *C. DIFFICILE*

1.1. Epidemiology

Clostridioides difficile is an endospore-forming, strictly anaerobic, Gram-positive, bacterium that is opportunistically pathogenic in humans. According to the most recent report by the Centers for Disease Control and Prevention, issued in 2019, it is estimated that 223,900 cases of *C. difficile* occurred in 2017 (1, 2)**.** Of these, 12,800 deaths can be directly attributed to *C. difficile*, with the majority of deaths occurring among people aged 65 and older. In recent years, there has been an emergence of antibiotic-resistant strains, as well as strains with increased virulence making *C. difficile* a leading cause of hospital-associated infections with an estimated $5 billion in annual treatment-associated cost for *C. difficile* infections (CDI) in US hospitals alone (3, 4). *C. difficile* vegetative cells secrete toxins responsible for the primary symptoms of CDI, but they are susceptible to oxygen and therefore incapable of surviving outside of a host. Moreover, they are a poor competitor with the native gut microbiota of healthy host individuals. The spore is the infective agent due to its ability to survive outside of the host in the aerobic environment, and due to its remarkable resistance to environmental insults. *C. difficile* infection follows the fecal-oral route, that is, spores that are ingested by the susceptible host will pass through the upper digestive tract. Once in the colon, it will germinate to form the toxin-secreting vegetative cell. CDI is generally initiated by germination of dormant spores within the gastrointestinal tract (GI) upon disruption to the normally protective microbiota, commonly due to broad spectrum antibiotic use (5-8)**.** The antibiotics that are prescribed to treat CDI (*i.e.* vancomycin or fidaxomicin) affect the vegetative cells, but patients frequently relapse with recurring CDI due to the

continued disruption to the colonic microbiota and the presence of antibiotic-resistant spores that remain in the gastrointestinal tract or in the re-inoculation of spores from surrounding environment (9)**.** (**Figure 1.1.**).

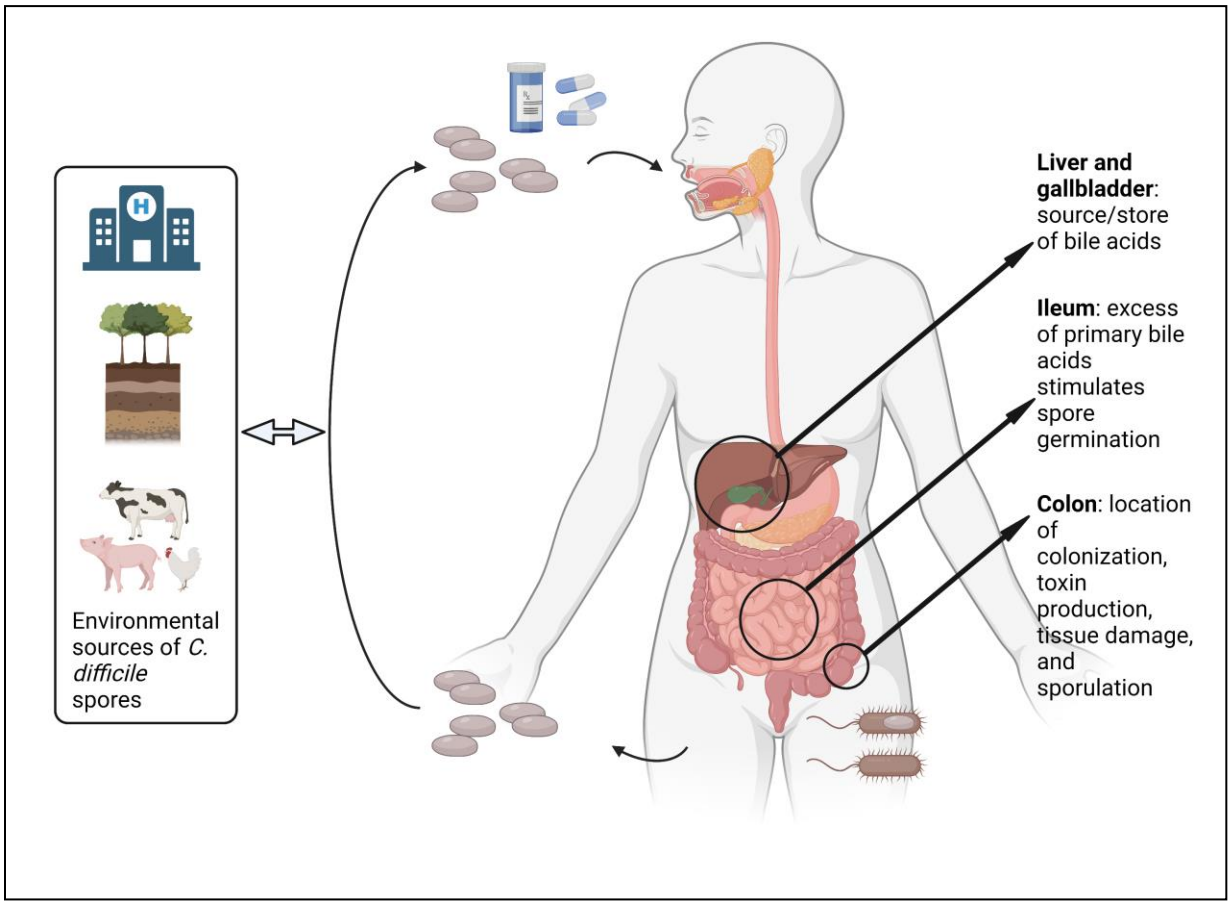

Figure 1.1. *C. difficile* fecal-oral route of transmission

Dormant spores from environmental sources (e.g., hospital settings, soil, animals) are ingested. Bile acids are produced in the liver, stored in the gallbladder, released to aid digestion of lipids, with a fraction reaching the ileum, where they are further modified by native gut microbiota. Disruption to the gut microbiota eliminates secondary bile acid production resulting in an abundance of primary bile acids in the GI. *C. difficile* vegetative cells secrete toxins that damage intestinal epithelium, resulting in the symptoms of CDI. A fraction of the cells sporulate and are released via diarrhea into the surrounding environment.

Symptoms of CDI are mainly the consequence of the action of two toxins secreted by the vegetative cell, TcdA and TcdB. TcdA is an enterotoxin and TcdB is a cytotoxin and both are a part of the pathogenicity locus (PaLoc) that also encodes additional toxin regulatory elements (*i.e.,* an alternative RNA-polymerase sigma factor, TcdR, a holin-like protein, TcdE, and an anti-sigma factor, TcdC) (10-12). A third toxin, CDT, is encoded by some *C. difficile* strains, and its role in the CDI development is unclear, but there is some evidence that is associated with poorer clinical outcomes in patients (13). The mechanisms by which TcdA and TcdB cause CDI symptoms is well-established. Both toxins catalyze the glycosylation of the Rho family GTPases, which leads to their inactivation, subsequent cell death, loss of barrier function in host colonic epithelium, and diarrhea (14).

1.2. Spore structure

C. difficile spores have a complex structure that allows them to adhere to surfaces and resist adverse environmental conditions (15-17). The outermost exosporium layer is composed of proteins and glycoproteins (*i.e.*, BclA1, BclA2, BclA3, CdeA, CdeC, and CdeM). It is of variable thickness and is believed to have a role in the spore interaction and attachment with the host intestinal epithelium (18-21). The exosporium surrounds the coat layer, which is composed of layers of protein serving as a barrier for enzymes and damaging chemicals (22). The coat is built upon the outer spore membrane, a membrane that is thought to be largely permeable during spore dormancy (23, 24). The outer spore membrane surrounds the cortex, a thick layer of modified peptidoglycan (25). Under the cortex is the germ cell wall, a peptidoglycan layer destined to become the cell wall during outgrowth of a vegetative cell from a germinated spore, and the

inner spore membrane, an immobile, low-permeability membrane that serves as a barrier to damaging chemicals (26, 27). The spore core contains DNA, RNA, proteins, and other components necessary for re-establishment of metabolic processes upon germination. The core has a low water content and increased levels of 1:1 chelate of Ca^{2+} with pyridine-2,6-dicarboxylic acid (CaDPA), which provide *C. difficile* (and spores derived from all other studied endospore forming bacteria) with remarkable heat resistance (28-33) . (**Figure 1.2.)**

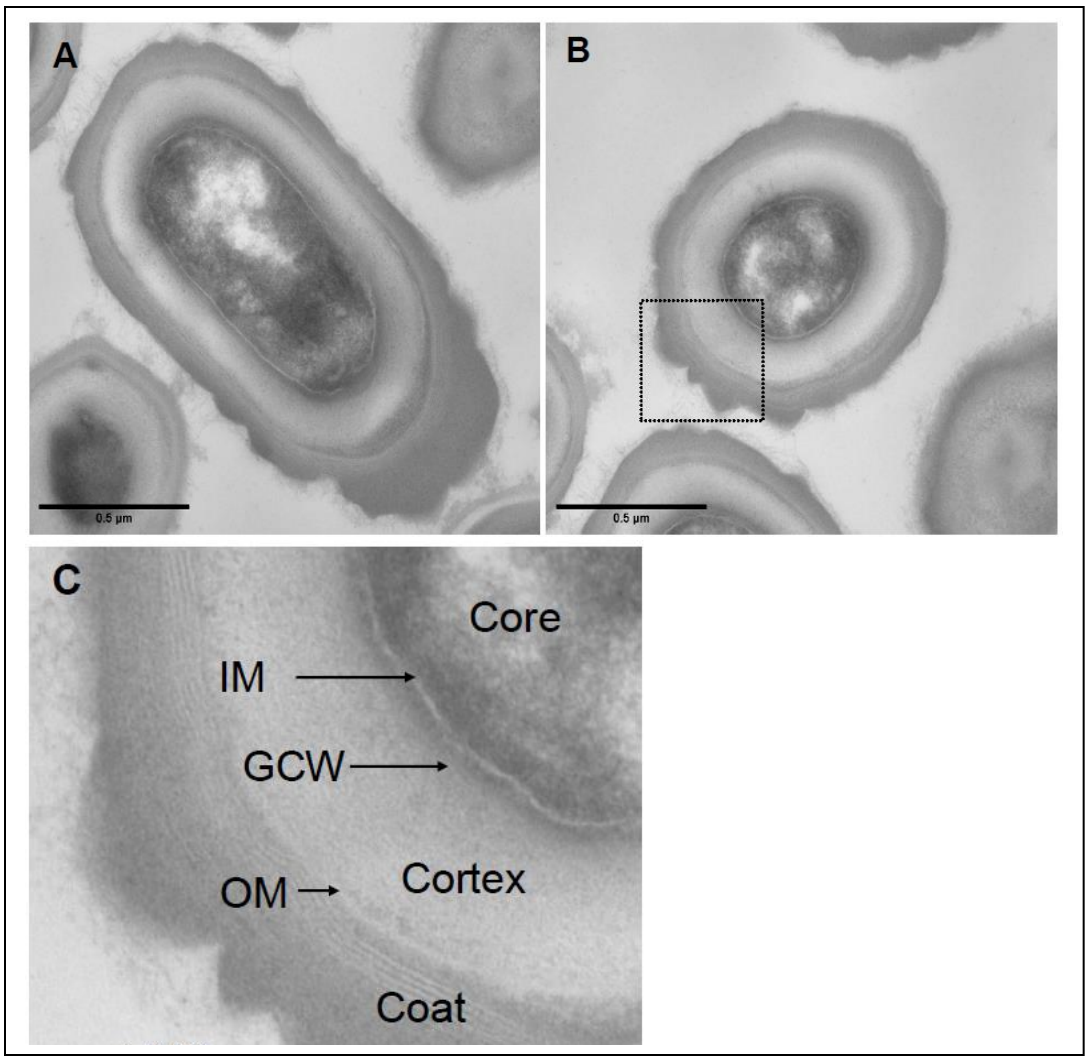

Figure 1.2. *C. difficile* spore structure visualized by TEM.

Spores derived from *C. difficile* R20291 strains were embedded in epoxy resin, sectioned, and imaged by TEM. (A) and (B) Longitudinal and cross-section images, respectively, of dormant spore. The black box indicates a region containing all the spore structures (magnified in C). (C) Components of spore structure. IM - inner membrane, GCW - germ cell wall, OM - outer membrane

1.3. Germinants

Germination by *C. difficile* spores is an essential step in its pathogenesis, and, like all endospore-forming bacteria, *C. difficile* spores require the presence of small molecule compounds, germinants, to stimulate the cascade of events that trigger germination (34, 35). *C. difficile* spores activate germination in response to host-derived bile acids (36, 37). Bile acids are synthesized in the liver using cholesterol as a scaffold. The two primary bile acids, cholate and chenodeoxycholate, are further modified via conjugation with either taurine or glycine (*e.g.*, taurocholate is generated from cholate and taurine) (38, 39). Cholate-derivatives are the most effective bile acid germinants, while chenodeoxycholate is a competitive inhibitor of cholic acid-mediated germination (36, 37, 40-44). During GI transit, approximately 5% of the total amount of bile acids reach the large intestine where they are deconjugated and then metabolized by 7α-dehydroxylation by the native microbiota to generate secondary bile acids (38, 39). (**Figure 1.3.**) Upon antibiotic treatment, or during gut dysbiosis, the members of the colonic flora that mediate this metabolism are lost and this results in sufficient taurocholate concentrations (coupled with the increased pH) to germinate the spores (5, 7, 45). It should be noted that certain conditions, like obesity, may significantly affect the severity of CDI by altering the ratio of primary to secondary bile acids present in the gut, with the increased levels of primary bile acids favoring the persistence of *C. difficile* and worsening the clinical outcomes (46). Another way by which diet may influence CDI is by altering colonic pH levels. Recent work suggests that *C. difficile* germination is highly sensitive to even slight pH level variations, with the optimal pH for germination being greater than pH 6.2, and that particular diets, *i.e.*, those high in fiber, may lower the

colonic pH below the optimum, thereby reducing spore germination and outgrowth (45, 47).

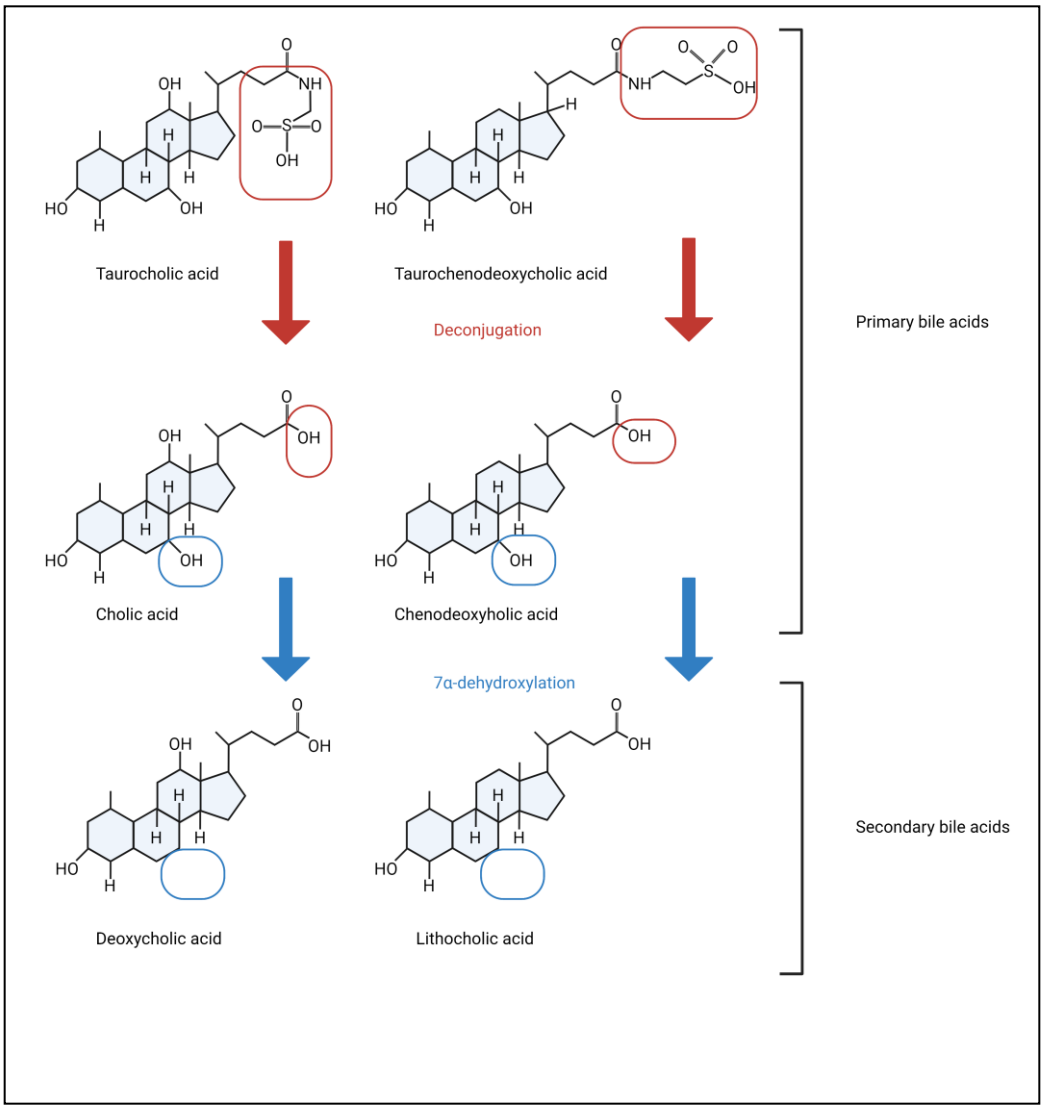

Figure 1.3. Bile acids

Bile acids, synthesized in the liver using cholesterol as a scaffold. In the liver, cholic acid and chenodeoxycholic acids are conjugated with either a taurine (to generate taurocholic acid and taurochenodeoxycholic acid) or glycine (to generate glycocholic acid or glycochenodeoxycholic acid; not shown). During GI transit, the conjugated amino acids is removed (deconjugation, shown in red) by bile salt hydrolases encoded by many members of the host's microbiome. Subsequently, cholic acid and chenodeoxycholic acid are further modified by other bacteria through the removal of the 7α-hydroxyl group (shown in blue) to form secondary bile acids, deoxycholic acid and lithocholic acid.

Though bile acids are necessary to stimulate *C. difficile* spore germination *in vitro*, they are not sufficient, and a co-germinant signal is required (36, 42, 43, 48-50). Several amino acids can function as *C. difficile* spore co-germinants, but glycine is the most efficient amino acid co-germinant (calcium can also function as a co-germinant) (36, 43, 48, 50). Recent work by Leslie and colleagues (51) has shown that pre-colonization with a non-toxigenic *C. difficile* strain depletes glycine in the mouse gut and this prevents subsequent establishment of a super-infection when spores derived from a toxigenic *C. difficile* strain are introduced. Their work suggests that despite the capability of other amino acids to stimulate spore germination *in vitro*, glycine is an important *in vivo* spore co-germinant.

Because spores, unlike vegetative cells, are insensitive to the toxic actions of antibiotics, one strategy to eradicate *C. difficile* in the gut is to initiate germination with the administration of germinants, while simultaneously administering antibiotics to kill the resulting vegetative cell (52). This ‘germinate to eradicate’ strategy could be a potential avenue for the prevention of recurring CDI (53). Alternatively, compounds that block the initiation of spore germination have potential in preventing *C. difficile* infection. By blocking the initiation of spore germination, all subsequent downstream events (*e.g.*, outgrowth, vegetative growth, toxin production and sporulation) are prevented. This strategy has been shown to be effective in animal models of CDI (54-56).

1.4. CspC

In most endospore-forming bacteria, germinants are recognized at the inner spore membrane by Ger-type germinant receptors (*e.g.*, GerAA – GerAB – GerAC) (57). *C. difficile* does not encode the Ger-type germinant receptors and instead

recognizes germinants using the CspA, CspB, and CspC proteins (44, 49, 58-63). Prior to work done in *C. difficile*, the Csp proteins were best studied in *Clostridium perfringens*. In *C. perfringens*, CspA, CspB and CspC are subtilisin-like serine proteases and are hypothesized to remove the inhibitory propeptide from the cortex-degrading enzyme, pro-SleC (64-67). Interestingly, in *C. difficile*, *cspB* and *cspA* are translationally fused, and *cspC* is encoded downstream of the *cspBA* gene. Again, unlike what is found in *C. perfringens*, *C. difficile* CspA and CspC have lost their catalytic triad and are, thus, pseudoproteases (49, 58-63).

In an ethylmethane sulfonate (EMS) screen to identify germination-null strains, single point mutations in *C. difficile cspC* were found to abrogate spore germination in response to bile acids and another ($CspC_{G457R}$) altered germinant specificity by inducing germination in response to chenodeoxycholate, a primary bile acid that is normally an inhibitor of germination (37, 40, 63). These results suggested that despite its loss of catalytic activity, the *C. difficile* CspC pseudoprotease still functioned to regulate germination in response to bile acids, potentially as a regulatory inhibitor of the CspB protease (44, 63). In recent work, Rohlfing and colleagues (59) crystallized the *C. difficile* CspC protein and used the data provided by this structure to probe regions of the protein and test how mutations in these regions altered *C. difficile* spore germination. Interestingly, they found that the $CspC_{G457R}$ mutation was hypersensitive to both bile acid-mediated germination (*i.e.*, taurocholate) and the co-germinant signal (*i.e.*, glycine or arginine) (59). Moreover, the authors found that the a strain harboring a mutation in a neighboring amino acid ($CspC_{R456G}$) was also hypersensitive (59). Despite this, not all *cspC* mutations altered sensitivities to both stimulatory molecules, and the

authors found that $CspC_{D429K}$ led to increased bile acid sensitivity but not to sensitivity to the co-germinant signal (19). Surprisingly, restoration of the catalytic site residues to CspC decreased protein stability and resulted in decreased germination (58). These results suggest that CspC is a signaling point for *C. difficile* spore germination or that, potentially, CspC interacts with the other germinant receptors and these mutations alter the binding to these proteins.

1.5. CspBA

Encoded upstream of *C. difficile cspC* is *cspBA*. CspBA is produced as a translational fusion between the *cspB* and *cspA* genes and undergoes interdomain processing during sporulation separating CspBA into the CspB protease and the CspA pseudoprotease (61, 62). CspA undergoes further processing by the YabG protease (49, 61). Deletion or disruption of *cspB* or cspA prevents spore germination indicating that the CspA pseudoprotease, like the CspC pseudoprotease, is important for *C. difficile* spore germination (49, 60). The role of CspB in *C. difficile* spore germination is clear. It must cleave the inhibitory pro-peptide from the cortex degrading enzyme, pro-SleC, to trigger germination (60, 62).

Mutations in *C. difficile cspA* also prevent spore germination. However, the mechanism by which *C. difficile* CspA functions during germination is complex. Disruption of the *cspA* portion of the *cspBA* gene prevents the incorporation of CspC into the developing spore suggesting that CspA and CspC may interact at some point during spore development, or that CspA is important for CspC stability in the dormant spore, or both (49, 60, 61). Moreover, a *C. difficile yabG* mutant strain resulted in spores that no longer responded to a co-germinant and germinated in response to bile acids

only (49). In this strain, CspBA is no longer efficiently processed into the CspB and CspA forms (the interdomain processing of CspBA was weak in this strain) (49). Moreover, small deletions in *cspA*, near the hypothesized YabG processing site within CspA [*cspBA*$_{\Delta 537\text{-}571}$ or *cspBA*$_{\Delta 581\text{-}584}$ (an SRQS deletion)], resulted in a strain whose spores could germinate in response to taurocholate only. However, unlike the *yabG* mutant, spores derived from a *cspBA*$_{\Delta 537\text{-}571}$ strain could still respond to co-germinants (49). This latter work led to the hypothesis that *C. difficile* CspA functions as the co-germinant receptor for *C. difficile* spore germination (49).

1.6. SleC

The *C. difficile* cortex lytic enzyme, SleC, is essential for spore germination (68). SleC is deposited into the spore as an inactive zymogen (pro-SleC) (62, 65). Upon germinant and co-germinant recognition by CspA and CspC (44, 49, 58-61, 63), CspB is activated (somehow) and CspB cleaves the inhibitory pro-peptide from SleC, thereby activating it (62). To provide specificity for the cortex peptidoglycan (so that the germ cell wall peptidoglycan is not degraded), SleC recognizes the muramic-δ-lactam (MDL) residues that are uniquely found in the cortex layer. SleC then degrades the cortex peptidoglycan layer by cleaving the glycosidic linkages. The degradation of the spore cortex permits the release of DPA from the spore core, in exchange for water (69, 70). Though SleC is the major spore cortex lytic enzyme, its ability to hydrolyze the cortex is dependent on the modification of the cortex peptidoglycan by GerS and CwlD (71, 72). Interestingly, removal of the inhibitory pro-peptide is not required for *in vitro* degradation of muramic-δ-lactam-containing peptidoglycan – CspB activation of SleC may be required in *C. difficile* spores for proper lytic activity (73).

1.7. DPA release

In *C. difficile* and other spore-forming organisms, pyridine-2,6-dicarboxylic acid (dipicolinic acid [DPA]) is chelated in 1:1 ratio with Ca^{2+} (Ca-DPA) and packaged into the spore in large amounts at the expense of water. DPA is largely responsible for spore wet heat resistance, although it is not required for *C. difficile* spore formation and germination (26, 27, 31, 33). For the spore metabolic processes to resume, DPA must be released from the core in exchange for water. During dormancy, the cortex prevents the osmotic expansion of the spore core, thereby preventing the release of DPA (32, 70, 74). In *B. subtilis* the proteins encoded by the *spoVA* operon (SpoVAA-AB-AC-AD-AEa-AEb-AF) play a role in DPA packaging and release*. C. difficile* encodes three orthologues of the *spoVA* operon: SpoVAC, SpoVAD, and SpoVAE. In *B. subtilis,* SpoVAD binds to DPA and is likely important in the packaging of DPA into the developing spore, a *spoVAEa* mutation causes only a slight germination defect, and the role of *spoVAEb* is unclear (75, 76). The mechanosensing protein, SpoVAC, is embedded in the inner spore membrane and, presumably, serves as the channel through which DPA is packaged into the spore core during sporulation and released during germination (32, 77). In work described below, I show that *C. difficile* SpoVAD and SpoVAE interact at inner spore membrane and, along with SpoVAC, likely form a complex required for packaging of DPA. This is perhaps applicable to other spore-forming organisms that encode the *spoVA* operon (78). There is evidence that the DPA packaging into the spore core may be under regulation of other genes besides those in *spoVA* operon in *C. difficile.* Spores from strains lacking CD3298, an AAA+ ATPase, contain <1% of DPA found in spores of wild-type strains, similar to

SpoVAC/SpoVAD/SpoVAE mutants, potentially indicating a role of CD3298 in DPA transport into the forespore during sporulation (50). Upon activation of SleC, degradation of the spore cortex results in the loss of ‘constraint’ on the inner spore membrane resulting in the activation of the mechanosensing SpoVAC protein and release of DPA from the core, in exchange for water (an ‘outside – in germination pathway) (32, 70). The rehydrated core then begins metabolic activity, and the spore eventually develops into a vegetative cell. This order of events is inverted from what is observed during *B. subtilis* spore germination. In *B. subtilis*, germinant recognition by the Ger-type germinant receptor leads to release of DPA and the released DPA can activate degradation of the cortex layer (an ‘inside – out’ germination pathway) (32, 57, 70, 79).

1.8. A model for C. difficile spore germination

There are several hypotheses where the Csp-type germinant receptors are located in *C. difficile* spores. Proposed locations are in the spore coat and outer spore membrane (80), outer spore membrane alone (72), or the inner spore membrane (28), where they exist as either a complex or individually. In a working / potential model for *C. difficile* spore germination, the CspB protease is held in an inactive state by the CspA and CspC pseudoproteases (**Figure 1.4.A.**). In this complex, the interaction of the three proteins regulates spore germination in response to exogenous signals. Upon recognition of the bile acid by CspC and the co-germinant by CspA, these proteins disassociate from CspB. The liberated CspB is free to process pro-SleC into its active form resulting in degradation of the spore cortex layer (**Figure 1.4.B.**). Based on the data provided by Rohlfing and colleagues (59), we hypothesize that $CspC_{D429}$ is near the CspB and CspA binding interfaces and the D429K allele is hypersensitive to the TA germinant and calcium co-germinant due to instability of these surfaces (59). The $CspC_{R456}$ and $CspC_{G457}$ amino acids may be located near the binding interface with CspA and with CspB because the $CspC_{R456G}$ and $CspC_{G457R}$ alleles are hypersensitive to both bile acid germinants and amino acid co-germinants (59, 63). We hypothesize that this leads to destabilization of the CspA/CspC and the CspC/CspB binding interface and thus weakening the overall complex. In a *yabG* mutant strain, CspA is not processed from CspB and thus is not positioned in the complex to regulate spore germination in response to co-germinants (49).

In a dormant spore, the SpoVAC mechanosensing protein is in a closed state and prevents the release of the large depot of CaDPA from the spore core. Upon

activation of germination, SleC degrades the spore cortex layer. This results in an osmotic shift that is perceived at the inner spore membrane and SpoVAC opens to release DPA from the core (**Figure 1.4.B.**).

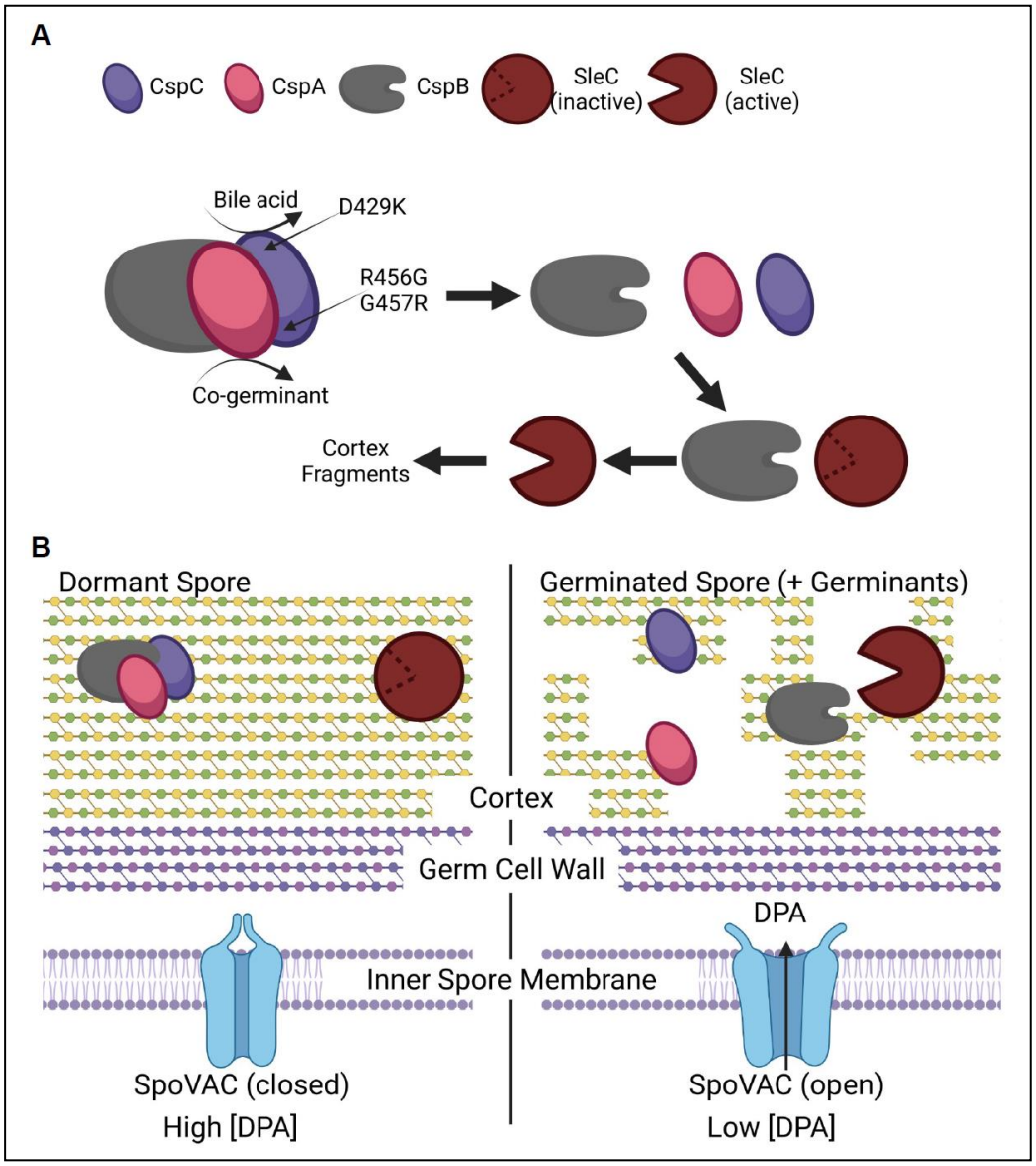

Figure 1.4. A model of *C. difficile* spore germination, from germinant detection to DPA release

The Csp proteins are in a complex, with CspC and CspA repressing CspB protease activity. Sensing of bile acid germinants by CspC, and co-germinants by CspA activates CspB which then cleaves the inhibitory propeptide from pro-SleC, allowing it to degrade the cortex. Cortex degradation, in turn, activates SpoVAC mechanosensing protein, resulting in the release of DPA store from the spore core in exchange for water, core rehydration, and the resumption of metabolic activities.

2. IMAGING CLOSTRIDIOIDES DIFFICILE SPORE GERMINATION AND GERMINATION PROTEINS*

2.1. Introduction

Clostridioides difficile is a Gram-positive, obligately anaerobic, spore-forming bacterium that is opportunistically pathogenic in humans. *C. difficile* vegetative cells are susceptible to oxygen and therefore incapable of surviving outside of the host gastrointestinal (GI) tract (81, 82). The spore form is the metabolically dormant stage in the *C. difficile* lifecycle and persists outside of the host in the oxygen-rich environment. Disruptions to the normally-protective native gut microbiota are commonly the result of broad-spectrum antibiotic use (5-8). While the *C. difficile* vegetative form is susceptible to antibiotics, the spores are not and therefore may remain in the gut to initiate recurring infection (9).

C. difficile spores, like spores from other spore-forming organisms, have a complex structure that conveys resistance to various environmental conditions inside and outside of the body (28, 83). The spore core contains the DNA, RNA, and protein required for resumption of metabolic processes upon germination. It is also rich in pyridine-2,6-dicarboxylic acid (dipicolinic acid [DPA]), chelated with calcium (Ca-DPA). DPA is packaged into the core during sporulation in exchange for water, and the high DPA / low water content of the core conveys the dormant spores with remarkable heat resistance (28-33, 70, 78, 84).

---

* Reprinted with permission from “Imaging *Clostridioides difficile* spore germination and germination proteins” by Marko Baloh, Hailee Nerber, Joseph A. Sorg, *bioRxiv* 2022.05.31.494260; doi: https://doi.org/10.1101/2022.05.31.494260

The core is surrounded by the inner spore membrane with low permeability to water. The inner spore membrane is surrounded by the germ cell wall, a layer of peptidoglycan that becomes the cell wall of a newly germinated cell (26, 27). Surrounding this is the cortex, a thick layer of modified peptidoglycan where much of the muramic acid residues are converted to the muramic-δ-lactam moieties that are the target of the cortex lytic enzymes (25, 71, 85-87). Surrounding the cortex is the outer spore membrane (23, 24), the coat layer (22), and the exosporium (18-20, 88-90).

Upon entry into a susceptible host, *C. difficile* spores germinate in response to small molecule germinants (35). *C. difficile* spores respond to host-derived bile acids, synthesized by the liver using cholesterol as a scaffold, as activators or inhibitors of germination (36, 37). In the liver, the primary bile acids cholate and chenodeoxycholate are modified by conjugation with either taurine or glycine (38, 39). Cholate derivatives, taurocholate in particular, are the most effective *C. difficile* spore germinants, but chenodeoxycholate is a competitive inhibitor of cholic acid-mediated germination (36, 37, 41-44). Though these primary bile acids are required, they are not sufficient to trigger *C. difficile* spore germination. Amino acids and calcium can function as co-germinants, and glycine has been shown to be the most efficient co-germinant, especially *in vivo*, since the depletion of glycine in mouse models prevents the establishment of CDI (36, 43, 48, 50, 51).

In the majority of the studied endospore-forming organisms, spores detect germinants via Ger-type receptors embedded in the inner spore membrane (57). *C. difficile* does not encode Ger-type germinant receptors and, instead, uses the CspA and CspC proteins as germinant receptors (58, 60-62, 91). Prior to the work done in *C.*

difficile, CspA, CspB, and CspC proteins were characterized in *Clostridium perfringens*, and found to be subtilisin-like serine proteases. These proteins contain a catalytic triad that is capable of processing the cortex lytic enzyme SleC from its inactive pro-form into an active enzyme that degrades the cortex and initiates spore germination (65, 67). Unlike what is found in *C. perfringens, C. difficile cspB* and *cspA* are translationally fused (CspBA), and *cspC* is encoded downstream from the *cspBA* gene. Interestingly, both CspA and CspC have lost their catalytic triad and, therefore, are pseudoproteases (58, 91).

Translation of *cspBA* produces CspBA which then undergoes interdomain processing by YabG to generate the CspB protease and the CspA pseudoprotease. When activated, CspB cleaves the inhibitory pro-peptide from pro-SleC to trigger germination (60-62). The disruption of *cspA* prevents incorporation of CspC into the developing spore, suggesting interaction of CspA and CspC and cleavage of CspA from CspBA is important for response to co-germinants, suggesting that CspA functions as the co-germinant receptor (49, 60, 61). Finally, CspC has been identified to be the bile acid germinant receptor or as a hub for germinant processing (37, 40, 41, 91).

There are several hypotheses about where the Csp-type germinant receptors are located in *C. difficile* spores. Prior studies have proposed locations in the spore coat and outer spore membrane (92), outer spore membrane alone (72), or the inner spore membrane (28), where they exist as either a complex or individually. Here, we used TEM imaging and immunogold labeling to show that CspB, CspA, CspC, and SleC are localized to the spore cortex layer. This is consistent with our observation that the cortex thickness decreases dramatically within 5 minutes of the initiation of germination. We

also show by SEM that germination and the transition of a spore into a vegetative cell can proceed entirely while the nascent cell is still enveloped in the coat and exosporium layer, without observable disruption to those layers.

2.2. Materials and Methods

2.2.1. Bacteria and strains

C. difficile R20291, and derived strains, were grown at 37 °C in an anaerobic chamber (Coy Laboratories; model B; >4% H2, 5% CO2, 85% N2) on brain heart infusion agar supplemented with 5 g / L yeast extract and 0.1% L-cysteine (BHIS) or TY agar medium (30 g / L Bacto typtone, 20 g / L yeast extract), as indicated. *Escherichia coli* DH5α (93) was grown on LB medium. Chloramphenicol (20 mg / ml), thiamphenicol (10 mg / ml), kanamycin (50 mg / ml), and ampicillin (100 mg / ml) were added where indicated. Spores were generated on 70:30 agar medium (63 g / L Bacto peptone, 3.5 g / L proteose peptone, 11.1 g / L BHI, 1.5 g / L yeast extract, 1.06 g / L tris base and 0.7 g / L ammonium sulfate [$(NH_4)_2SO_4$].

2.2.2. Construction of R20291 Δ*bac* and FLAG-tag reporter strains

C. difficile R20291 Δ*sleC* strain, a TargeTron *sleC* insertion mutant, was previously constructed by our lab (49). *C. difficile* R20291 Δ*cspBAC* strain, a complete CRISPR-induced deletion of the csp*BAC* operon was constructed, as follows. Plasmid pHN168 was generated by inserting CRISPR_CspB_2 gBlock into PCR 2.1 – TOPO plasmid. pHN168 was digested at the *KpnI* and *MluI* restriction sites to generate a free fragment consisting of the gRNA. This fragment was ligated at 16 °C overnight into pKM126 that had also been digested at the *KpnI* and *MluI* restriction sites. The resulting

plasmid was digested with NotI and XhoI to insert the homology arms for the *cspBAC* deletion. The upstream homology fragment was amplified with primers 5'cspBAC_UP and 3'cspBAC_UP while the downstream homology fragment was amplified with 5'cspBAC_DN and 3'cspBAC_DN. Gibson assembly was used to insert these homology fragments into the above digested plasmid, resulting in pHN23. Due to problems with the *tetR* promoter having leaky expression of *cas9*, this was exchanged for the *xylR* promoter. The *xylR* promoter was amplified from pCE641 with the primers 5'cspBAC_HR_xylR and 3'cas9_Pxyl 2. This fragment was inserted into PacI and XhoI digested pHN23 using Gibson assembly (94), resulting in pHN36. HNN08 (R20291 Δ*cspBAC*) was generated by passaging R20291 pHN36 4 times on TY supplemented with Tm and 1% xylose. The resulting strain was cured of the plasmid by passaging twice in BHIS broth (without antibiotic selection).

FLAG-tagged reporter strains were constructed by FLAG-tag fusions to the C-terminal of *C. difficile cspBA* and *sleC* genes on a plasmid that was transformed into the *C. difficile* R20291 Δ*cspBAC* and Δ*sleC* mutant strains, respectively. For CspBA-FLAG fusion, the wild-type *cspBA* genes (including the 500 bp upstream region) were amplified from the *C. difficile* R20291 using primers 5' CspBA promoter NdeI and 3' CspBA-FLAG and, along with the gBlock containing FLAG tag, and inserted by Gibson assembly (94) into plasmid pMTL 84151 digested with NdeI / XhoI. For the SleC-FLAG fusion, the wild-type *sleC* gene (including the 500 bp upstream region) was amplified from *C. difficile* R20291 genome using primers 5' SleC promoter NdeI and 3' SleC-FLAG, along with with the gBlock containing FLAG tag, and inserted by Gibson assembly into plasmid pMTL 84151 digested with NdeI / XhoI. This yielded plasmids

pMB96 and pMB98, respectively. The plasmids were then transformed into *E. coli* DH5α for storage. These plasmids were subsequently transformed into *E. coli* HB101 / pRK24 and grown on LB medium supplemented with chloramphenicol and ampicillin. The resulting strain was grown overnight and then mixed with the *C. difficile* R20291 Δ*cspBAC* or Δ*sleC* strain grown in BHIS in an anaerobic chamber. The conjugation mixtures were spotted onto BHI plates and allowed to grow for 24 hours. Subsequently, the cells were washed with BHIS, and the slurry was transferred onto BHIS medium supplemented with thiamphenicol (for plasmid maintenance) and kanamycin (to counter select *E. coli* growth) [BHIS(TK)]. Thiamphenicol resistant colonies were tested for the presence of the desired fusion construct on the plasmid by PCR and confirmed by sequencing. All strains and plasmids in this study are listed in **Table 1**. Primers used to construct the strains and plasmids are listed in **Table 2**.

Table 1: List of strains and plasmids used in Chapter 2

Strain or plasmid	Description	Reference No
R20291	Wild type, ribotype 027	(40)
E. coli DH5α	Cloning strain	(95)
E. coli HB101 pRK24	Conjugal donor strain for *C. difficile*	(96)
RS10	R20291 Δ*sleC*	(97)
HNN08	R20291 Δ*cspbac*	This study
pMTL81451	Backbone used to make BA-FLAG and SleC-FLAG plasmids	(98)
pHN168	CRISPR *cspB*-targeting gBlock	This study
pKM126	pyrE-targeted CRISPR-*Cas9* vector; *traJ oriT*	(99)
pHN23	CRISPR *cspB*-targeting gBlock + *cspBAC* homology regions	This study
pCE641	Source of *xylR* promoter	(100)
pHN36	CRISPR *cspB*-targeting gBlock + *cspBAC* homology regions + *xylR* promoter	This study
pMB96	CspBA-FLAG fusion plasmid	This study
pMB98	SleC-FLAG fusion plasmid	This study

Table 2: List of primers used in Chapter 2

Plasmid made	Sequence	Primer name
pHN168	ggtaccgctggaaataatgcagataaGTTTTAGAGCTAGAAATAGCAAGTTAAAATAAGGCT AGTCCGTTATCAACTTGAAAAAGTGGCACCGAGTCGGTGCTTTTTTTCTATGGAG AAATCTAGATCAGCATGATGTCTGACTAGACGCGT	CRISPR_CspB_2 gBlock
pHN23	atttttttatcaggaaacagctatgaccgcggccgctataatttacttccattgtc	5'cspBAC_UP
pHN23	acattaataataattttagaagtcgaggtgctctatagataagaacctatgtaa	3'cspBAC_UP
pHN23	ataattttacataggttcttatctatagagcacctcgacttctaaaattatt	5'cspBAC_DN
pHN23	tctgcgatcgcgcatgtctgcaggcCTCGAGaatctattaatactgaatgga	3'cspBAC_DN
pHN36	TAATCCTATACTATATTTTTTATCCATttaattaaCTCTCCTCTTTACCCTCCTT	3'cas9_Pxyl 2
pHN36	tttttaatatccattcagtattaatagattCTCGAGCTAGCATAAAAATAAGAAGCCT	5'cspBAC_HR_xylR
pMB96	aaacagctatgaccgcggccgctgtatccagtaaatctattaatactgaatgg	5' CspBA promoter NdeI
pMB96	TTTATAATCactaccactaccactaccacttcttaaaacatcaaacattc	3' CspBA-FLAG
pMB96	gatgttagaggaatgtttgatgttttaagaagtggtagtggtagtggtagtGATTATAAAGATGATGATGATA AAGACTATAAAGATGACGATGATAAGGATTATAAGGATGATGATGACAAATAActa gagtcgacgtcacgcgtccatggagatc	CspBA-FLAG gBlock
pMB98	aaacagctatgaccgcggccgctgtatccatcagagcttttacaccttc	5' SleC promoter NdeI
pMB98	TTTATAATCactaccactaccactaccactaattaaaggatttaaagaagctattc	3' SleC-FLAG
pMB98	caactagaatagcttctttaaatcctttaattagtggtagtggtagtggtagtGATTATAAAGATGATGATGAT AAAGACTATAAAGATGACGATGATAAGGATTATAAGGATGATGATGACAAATAAct agagtcgacgtcacgcgtccatggagatc	SleC-FLAG gBlock

2.2.3. Spore purification

Spores were purified as previously described (32, 36, 63, 70). Briefly, strains were grown on 70:30 sporulation medium. After 5 days, growth from 2 plates each was scraped into 1 mL distilled water (dH_2O) in microcentrifuge tubes and left overnight at 4 °C. The cultures were then resuspended in the dH_2O in the same microcentrifuge tubes

and centrifuged at >14,000 × g for 10 min, the top layer containing vegetative cells and cell debris was removed by pipetting, and the rest of the sediment resuspended in fresh dH_2O. The tubes, again, were centrifuged for 1 min at >14,000 × g, the top layer removed, and the sediment resuspended. This was repeated 5 more times, combining the sediment from 2 tubes into one. The spores were then separated from the cell debris by centrifugation through 50% sucrose solution for 20 min at 4 °C and 3,500 × g. The resulting spore pellet was then washed 5 times with dH_2O, resuspended in 1 mL dH_2O, and stored at 4 °C until use.

2.2.4. TEM ultrastructure sample preparation

For ultrastructure imaging of germinating spores, inside the anaerobic chamber, 50 µL of purified spores was incubated in 950 µL of BHIS supplemented with 10 mM TA and 30 mM glycine inside a 2.0 mL microcentrifuge tube. So that the samples were ready for the subsequent critical fixation step at the same time, the first sample incubated was the latest time point (*i.e.,* T=180 minutes) and each subsequent tube was a previous time point (*i.e.,* T=120, T=90, T=60, T=30, T=20, T=10, T=5), with the last tube incubated representing T=0 (ungerminated spores) which contained 950 µL of BHIS without TA or glycine. The tubes were taken out of the anaerobic chamber, centrifuged for 1 min at >14,000 × g, supernatant removed and replaced with 1,950 µL of fixative (5% glutaraldehyde, 2% acrolein in 0.05 M HEPES, pH 7.4). The samples were incubated in the fixative overnight at 4 °C. The following day, the fixed samples were centrifuged for 5 min at >14,000 × g, and post-fixed and stained for 2 hours with 1% osmium tetroxide in 0.05 M HEPES, pH 7.4. The samples were then centrifuged and washed with water 5 times, and dehydrated with acetone, using the following

protocol: 15 minutes in 30%, 50%, 70%, 90% acetone each, then 100% acetone 3 changes, 30 minutes each. At the final wash step, a small amount of acetone, barely covering the pellets, was retained to avoid rehydration of the samples. The samples were then infiltrated with modified Spurr's resin (Quetol ERL 4221 resin, Electron Microscopy Sciences, RT 14300) in a Pelco Biowave processor (Ted Pella, Inc.), as follows: 1:1 acetone:resin for 10 minutes @ 200 W – no vacuum, 1:1 acetone:resin for 5 minutes @ 200 W – vacuum 20'' Hg (vacuum cycles with open sample container caps), 1:2 acetone:resin for 5 minutes @ 200 W – vacuum 20'' Hg, 4 x 100% resin for 5 minutes @ 200 W – vacuum 20'' Hg. The resin was then removed, and the sample fragments transferred to BEEM conical tip capsules prefilled with a small amount of fresh resin, resin added to fill the capsule, and capsules left to stand upright for 30 minutes to ensure that the samples sank to the bottom. The samples were then polymerized at 65 °C for 48 hours in the oven, then at left at RT for 24 hours before sectioning. 70-80 nm samples were sectioned by Leica UC / FC7 ultra-microtome (Leica Microsystems), deposited onto 300 mesh copper grids, stained with uranyl acetate / lead citrate and imaged.

2.2.5. TEM immunogold sample preparation

Spores derived from the *C. difficile* R20291, and *C. difficile* Δ*cspBAC* and *C. difficile* Δ*sleC* strains were embedded in Lowicryl HM20 using HPF. 50 µL of purified spores were lightly fixed in 1 mL of 0.05% glutaraldehyde / 4% formaldehyde in 0.05 M HEPES, pH 7.4 for 30 minutes at RT. The spores were centrifuged and resuspended in 50 µL of 3% low melting point agarose. Approximately 2 µL of the spore suspension per sample was then processed with Leica EM ICE HPF apparatus (Leica Microsystems),

and then freeze substituted and embedded in Lowicryl HM20 (Electron Microscopy Sciences, RT 14340), using Leica EM AFS2 freeze substitution and low temperature embedding system and Leica EM FSP freeze substitution processor. The freeze substitution protocol was adapted from Edelmann et. al. (101), with modifications, as follows: 144 hours 100% acetone at – 90 °C., temperature increase at 5 °C / hour to – 50 °C, 4 hours 100% ethanol, 4 hours 100% ethanol: 100% HM20 in 3:1 ratio, 4 hours 100% ethanol: 100% HM20 in 1:1 ratio, 4 hours 100% ethanol: 100% HM20 in 1:3 ratio, 100% HM20 2x4 hours, 100% HM20 18 hours, 100% HM20 one exchange, UV polymerization 48 hours, temperature increase 5 °C / hour to RT with UV using lamp integral to FSP, UV polymerization 48 hours at RT using dedicated UV lamp. Ultrathin sections (70-80 nm) were deposited on nickel formvar carbon coated grids, immunolabeled, stained with uranyl acetate / lead citrate, and imaged.

Spores derived from the *C. difficile* Δ*cspBAC* and *C. difficile* Δ*sleC* strains, transformed with plasmids harboring BA-FLAG and SleC-FLAG fusions were processed using PLT in Leica EM AFS2 freeze substitution and low temperature embedding system. 50 µL of purified spore samples were lightly fixed in 1 mL of 0.05% glutaraldehyde / 4% formaldehyde in 0.05 M HEPES, pH 7.4 for 30 minutes at RT. The spores were centrifuged and resuspended in 50 µL of 3 % low melting point agarose. About 10 µL of the sample were placed in a cryotubes filled with 30% ethanol prechilled to 0 °C. The protocol was as follows: 30% ethanol 1 hr, replaced with 50% ethanol, lowered the temperature to – 20 °C (5 °C / hr), 50% ethanol 1 hr, replaced with 70% ethanol, lowered the temperature to – 35 °C (5 °C / hr), 70% ethanol overnight, replaced with 90% ethanol for 1 hr, replace with 100% ethanol for 1 hr, twice, K4M 33% for 1 hr,

K4M 50% for 1 hr, K4M 66% for 1 hr, K4M 100% overnight, K4M 100% 1 hr, thrice, samples placed into pre-chilled BEEM conical capsules prefilled with K4M, equilibrate at -35 °C for 1 hr, UV polymerize at -35 °C for 48 hours, UV polymerize while increasing the temperature to 24 °C at 5 °C / hr for a total of 24 hours, UV polymerize at RT for 48 hours. Ultrathin sections (70-80 nm) were deposited on nickel formvar carbon coated grids, immunolabeled, stained with uranyl acetate / lead citrate, and imaged.

2.2.5. Immunolabeling

Immunolabeling of Lowicryl-embedded samples was performed using modified protocol by Dittmann et al. (102). Samples were incubated at RT, section facing down on 30 µL droplets as follows: 2 times 5 minutes 50 mM glycine in PBS, blocking solution (0.5% cold water fish skin gelatin, 0.5% bovine serum albumin, 0.01% Tween 20, in PBS) for 1 min, blocking solution for 1 hr, primary antibody diluted in blocking solution for 1 hr, 6 time blocking solution for 5 minutes, secondary antibody in blocking solution for 1 hour, 6 times blocking solution for 5 minutes, 6 times PBS for 5 minutes, 5 minutes 2% glutaraldehyde in PBS, 6 times dH_2O for 5 minutes. For the detection of FLAG-conjugated proteins we used rabbit anti-DYKDDDDK antibody (Rockland Immunochemicals, Inc., Number 600-401-383). For the detection of CspB, CspA, CspC, and SleC we used rabbit α-CspB, α-CspA, α-CspC, and α-SleC antibodies. Secondary antibodies used were goat-anti-Rabbit IgG conjugated to 10nm gold particles (Electron Microscopy Sciences, Cat. # 25109). We also labeled the samples with secondary gold-conjugated antibody alone to test for the non-specific labeling and found virtually no labeling in each case (data not shown). For each sample immunolabeled in this way (*i.e.,* R20291, Δ*cspBAC,* Δ*sleC,* CspBA-FLAG, and SleC-FLAG tagged samples) we

imaged 100 random spores on the grid and counted the gold labels present. This was repeated at least 3 times, each time on new sections deposited on a new grid, immunolabeled in an independent trial.

2.2.6. SEM sample preparation

Spores for SEM imaging of germination were prepared in the same way as the spores for TEM ultrastructure imaging, described above, up to the dehydration step. At this point the samples were processed as follows: 35 / 50 / 70 / 80% ethanol 10 min each, 1:2 hexamethyldisilazane (HMDS):ethanol for 20 minutes, 1:1 HMDS:ethanol for 20 min, 100% HMDS 2 x 20 min. At the last stage of HMDS drying, a small volume of HMDS was left in the tube, and about 10 µL of sample deposited on the circular glass cover slip. The cover slips were left to dry overnight in the fume hood in a semi-covered glass petri dish. The samples were then sputter coated with 8 nm of Pd / Pt in Cressington 208HR Sputter Coater (Cressington Scientific Instruments Ltd.) and imaged.

2.2.7. TEM/SEM imaging

All ultrathin TEM sections were imaged on JEOL 1200 EX TEM (JEOL, Ltd.) at 100 kV, images were recorded on SIA-15C CCD (Scientific Instruments and Applications) camera at the resolution of 2721 x 3233 pixels using MaxImDL software (Diffraction Limited). Images were subsequently adjusted for brightness / contrast using Fiji (103).

SEM samples were imaged on Quanta 600 FEG (FEI Technologies, Inc.) equipped with a field emission gun at 20 kV, at 1024 x 943 pixels.

All equipment used is located at Texas A and M University Microscopy and Imaging Center Core Facility (RRID:SCR_022128) (104).

2.2.8. Statistical analysis

Data represent results from at least 3 independent experiments, and the error bars represent standard errors of the means. One-way analysis followed by Tukey's or Šídák's multiple-comparison test, as indicated, was performed using GraphPad Prism version 9.0.2 (161) for Windows (GraphPad Software, San Diego, California USA).

2.3. Results

2.3.1. C. difficile cortex degradation is a quick event

C. difficile germination begins with the detection of germinants and co-germinants by the germinant receptors. This results in the initiation of cortex degradation, release of DPA, core rehydration, and the resumption of metabolic activity. In prior work, we found that DPA release is a quick event, with the majority of DPA being released within 20 minutes of germination initiation (32, 70, 78). Because the DPA release from the spore core is dependent on the activation of the SpoVAC mechanosensing protein embedded in the inner spore membrane (32), the cortex degradation must be a quick event; indeed the cortex fragments are quickly detected after initiation of germination (69). In order to observe the structural changes that occur in the germinating spore (from the early stage of germination to the development of vegetative cell), we induced germination in spores derived from the wild-type *C. difficile* R20291 strain by incubating them with taurocholate (TA) and glycine in BHIS liquid medium. We then sampled between T=0 minutes (ungerminated spores) to T=180

minutes, when we expected to see fully developed vegetative cells, based on prior work (70). The samples were fixed and processed for TEM imaging. In order to observe the potential changes to the morphology of the spore surface, samples were also prepared for SEM imaging.

At T=0 all of the spore structures are clearly distinguishable by TEM (i.e., exosporium, coat, outer spore membrane, cortex, germ cell wall, inner spore membrane, and the core) (**Figure 2.1. A-C**). SEM imaging showed no changes in the spore morphology between T=0 and T=60 minutes (**Figure 2.1. D, E**). At T=180, we began to observe vegetative cells exiting spores (**Figure 2.1. F**). For comparison, we also imaged cultures by both TEM and SEM grown overnight in rich media (BHIS) (**Figure 2.1. G-I**).

Compared to dormant spores (T=0), at T=5, we observed a reduction in the thickness of the cortex, as well as the disappearance of a clearly distinguishable germ cell wall layer (**Figure 2.2. A**). Cortex thickness was measured in dormant spores in both horizontally cross-sectioned spores and spores sectioned along the longitudinal axis. These were compared 5 minutes post-germination. The average cortex thickness in both orientations was nearly the same (**Figure 2.2. B**). After 5 minutes of incubation in media containing germinants, the average cortex thickness was reduced by approximately 68% for cross-sectioned spores and by 67% for longitudinally sectioned spores (**Figure 2.2. B**). These results confirm prior observations by TEM that cortex is rapidly degraded upon germinant sensing.

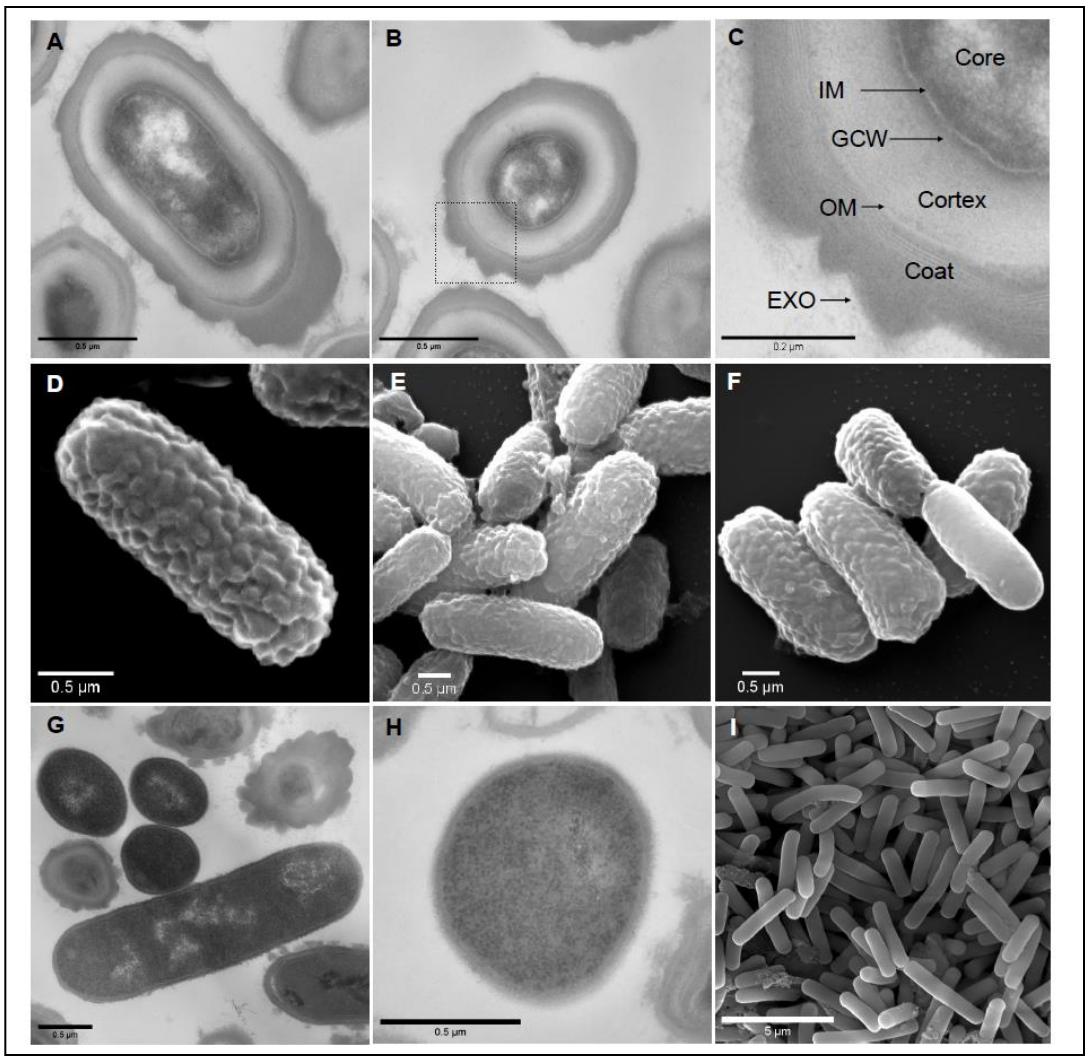

Figure 2.1.: *C. difficile* spore structure and cell morphology visualized by TEM and SEM

Spores (A-F) and vegetative cells (G-I) derived from the *C. difficile* R20291 strain were embedded in epoxy resin, sectioned, and imaged by TEM (A, B, C, G, H) or were chemically dried, sputter coated, and imaged by SEM (D, E, F, I).

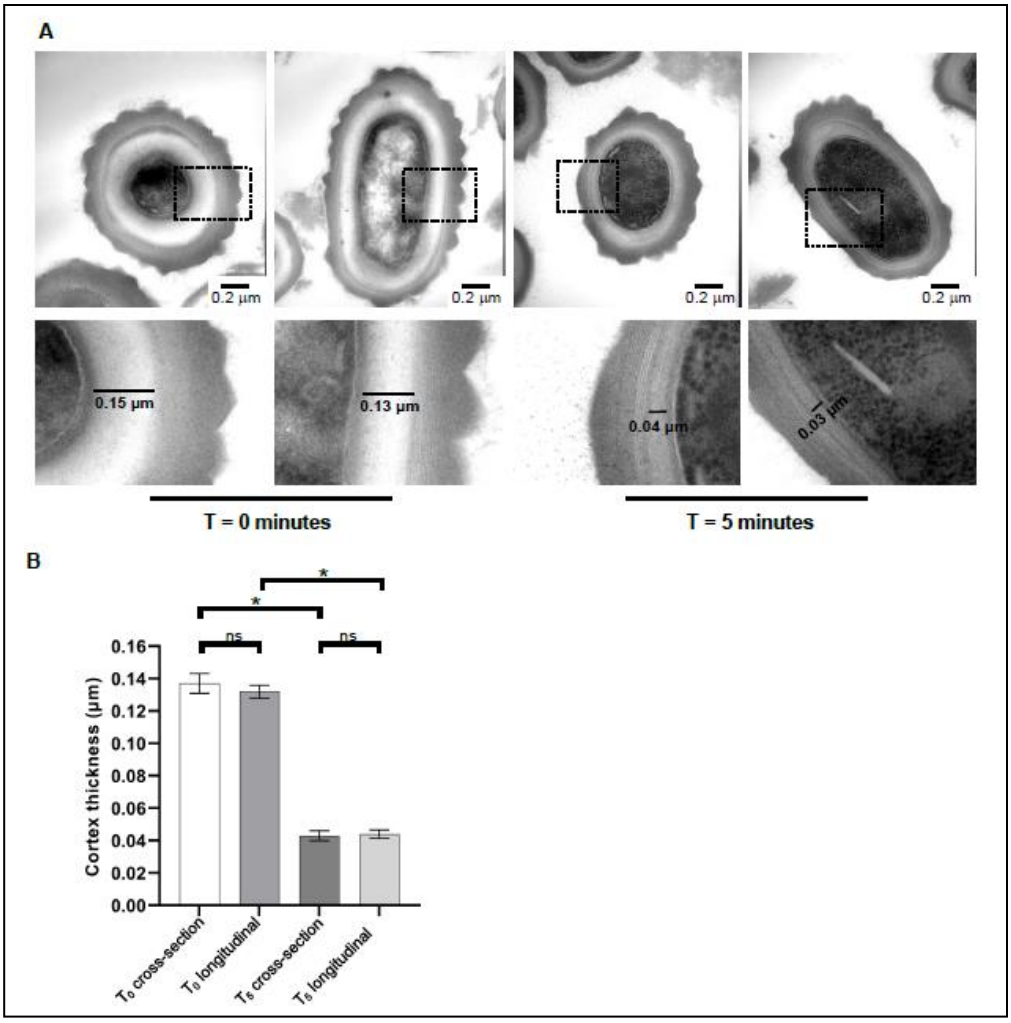

Figure 2.2. *C. difficile* cortex significantly thins within 5 minutes of germinant addition

C. difficile spores were germinated in rich medium supplemented with 10 mM TA and 30 mM glycine. A sample was taken prior to the addition of germinants (T_0) and 5 minutes post-germinant additions (T_5). (A) Representative images of T_0 spores and T_5 spores. Boxes represent areas of cortex thickness measurement, with magnified view with measurement scale bars shown underneath. (B) Average cortex thickness was measured in cross-sectioned and longitudinally-section spores, at T_0 and T_5. N=10 spores of each section orientation counted in both conditions (Total N=20). Cortex thickness was measured using Fiji Scale Bar tool. * indicates $p < 0.0001$ as determined by one-way ANOVA using Tukey's multiple-comparison test. 'ns' indicates no significance.

Starting at T=5 minutes after germination initiation (**Figure 2.3. T=5**), the majority of the spores showed reduced cortex thickness, along with unidentified changes within

the core. At later time points of germination there is a considerable variation in the spore core appearance. At T=60 minutes we began to observe what looked like early vegetative forms, but still encased inside the spore coat (**Figure 2.3. T=60**). At T=90 minutes we observed free cells and cells in the process of exiting the coat / exosporium layer (**Figure 2.4.**). This was more commonly observed event at T=180 (**Figure 2.4.**). At T=180 minutes, we observed vegetative cells without the coat layer, vegetative cells undergoing division, and spores that had not fully germinated. (**Figure 2.4.**). This probably reflects the previously established findings that there is considerable variability in spore development (105, 106). Nevertheless, it seems that cortex degradation observed at T=5 occurs in the majority of the spore population.

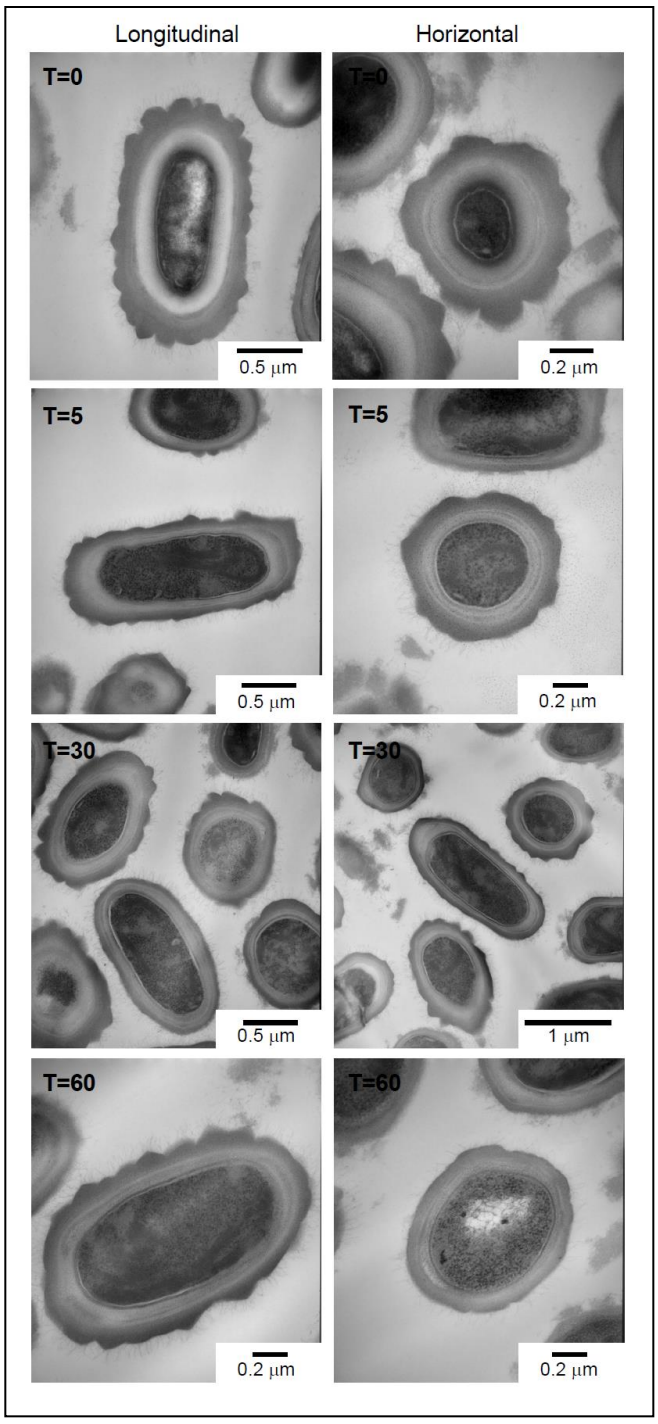

Figure 2.3.: Monitoring *C. difficile* spore germination over time (T_0 – T_{60}).

Dormant (T_0) *C. difficile* R20291 spores, or spores germinated for T_5, T_{30}, and T_{60} minutes were embedded in epoxy resin, sectioned, and imaged by TEM.

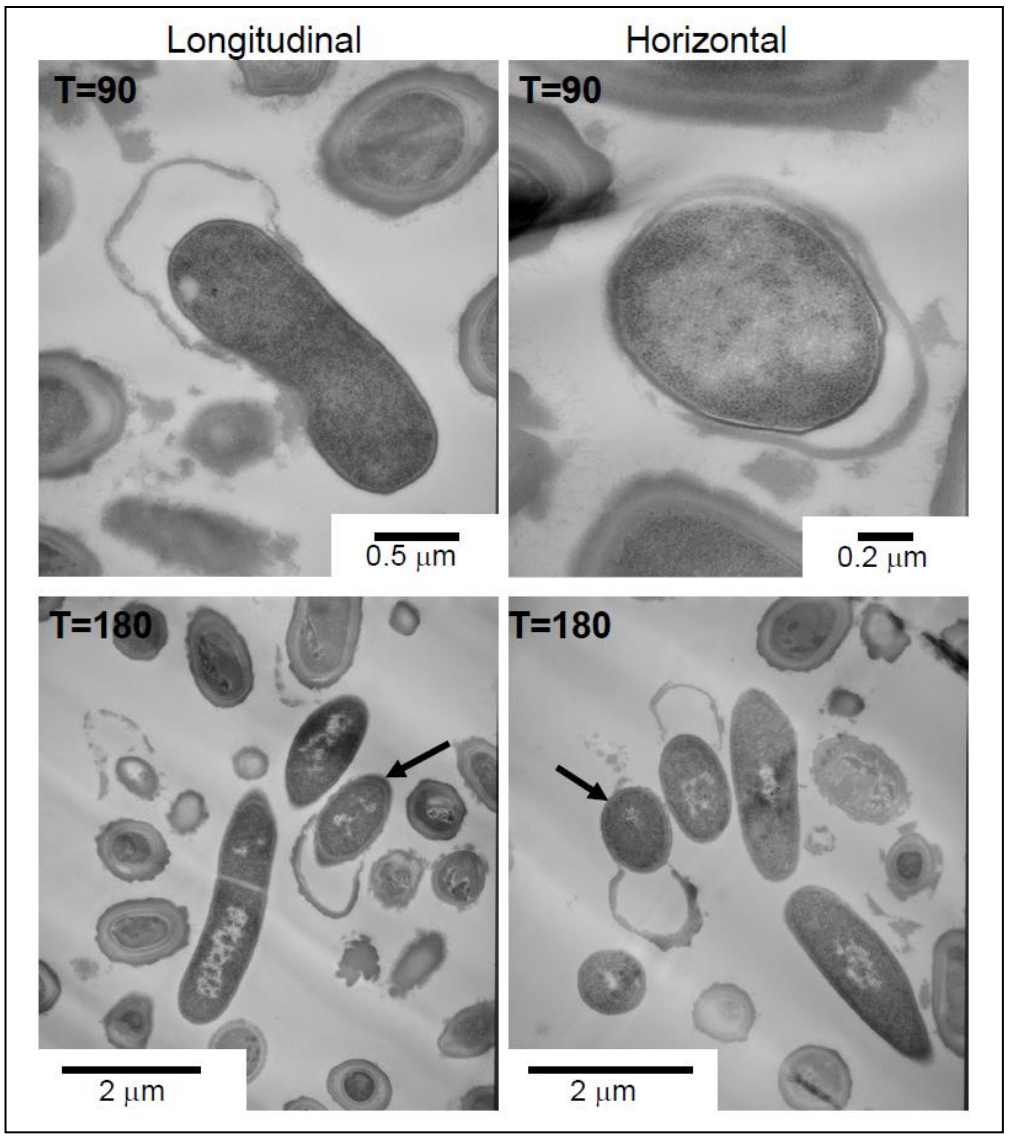

Figure 2.4.: Monitoring *C. difficile* spore germination over time (T_{90} & T_{180}).

C. difficile R20291 spores germinated for T_{90} and T_{180} were embedded in epoxy resin, sectioned, and imaged by TEM. Arrows indicate cells exiting the coat / exosporium layer.

2.3.2. Germinating *C. difficile* spores develop into vegetative cells inside the protective coat and exosporium layers

While there is no observable difference via SEM imaging between ungerminated spores and spores undergoing germination at the time points tested, T=0, T=5, T=20 (data not shown), we observed cells exiting the exosporium at T=180. We note that the newly hatched vegetative cells exit the exosporium at a pole of the spore, and that the exosporium structure remains intact during the entire germination process (**Figure 2.5.**). This is not always the case in TEM images, probably due to the different, considerably longer and harsher, sample preparation steps required for TEM that may damage the exosporium layer. Nevertheless, a similar process can be observed in the T=180 spores imaged by TEM (**Figure 2.5.**).

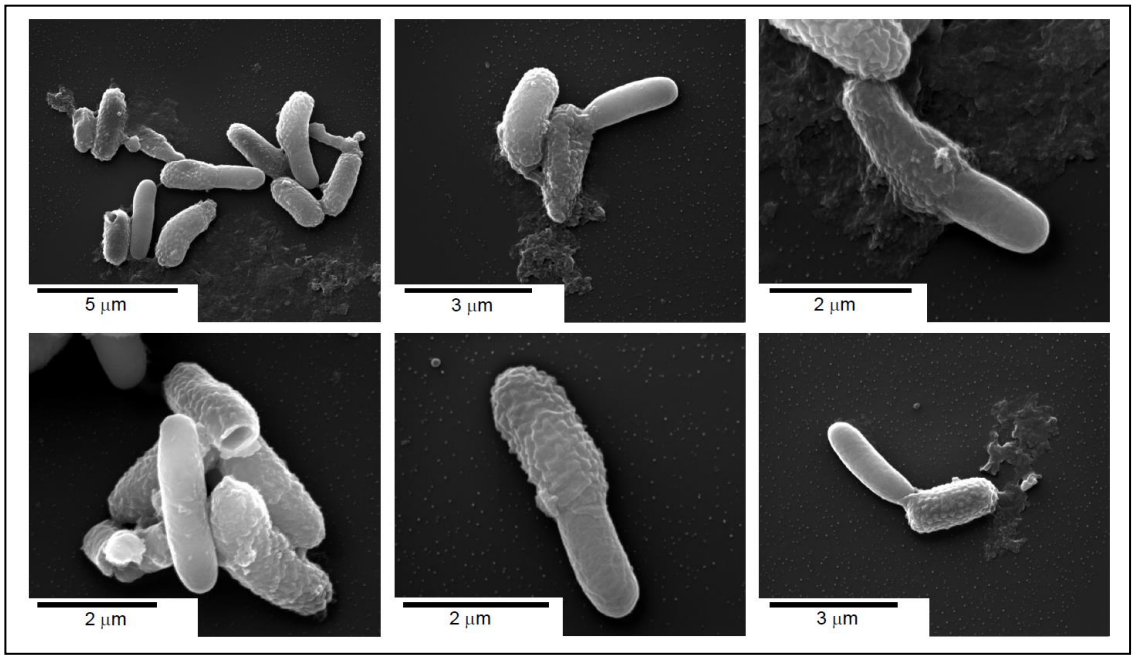

Figure 2.5.: *C. difficile* outgrowth occurs inside the coat / exosporium layer.

Representative images of spores and vegetative cells derived from *C. difficile* R20291 strain, germinated for 180 minutes, fixed, chemically dried, sputter coated, and imaged by SEM.

2.3.4. CspBA, CspC and SleC are localized to the spore cortex

Our TEM imaging showed that the cortex layer undergoes dramatic thinning within 5 minutes of the initiation of germination. This rapid time frame might suggest the proteins responsible for cortex degradation are already present in this layer. We therefore set out to determine the location of the *C. difficile* CspB, CspA, CspC, and SleC proteins in the spore using immunolabeled TEM samples. To accomplish this, we used two approaches. We embedded spores derived from the wild-type *C. difficile* R20291 and (as negative controls) *C. difficile* R20291 Δ*cspBAC* and *C. difficile* Δ*sleC* in Lowicryl HM20 resin, using high pressure freezing (HPF), then sectioned them. The 70-80 nm sections were labeled with primary antibodies raised against *C. difficile* CspB, CspC, CspA, and SleC, followed by the gold-conjugated secondary antibodies. We also constructed plasmids harboring *cspBA*-FLAG and *sleC*–FLAG tag C-terminal fusions that we transformed into *C. difficile* R20291 Δ*cspBAC* and *C. difficile* Δ*sleC* strains, respectively. These transformed strains were then embedded in resin, sectioned, incubated with primary antibodies targeting the FLAG reporter, followed by secondary gold-conjugated antibodies. In this case, the negative control was *C. difficile* R20291 spores. Samples were imaged, gold labels counted and compared to counts obtained from the negative controls.

Our results show that in both cases, either by direct labeling of the *C. difficile* CspB, CspA, CspC, and SleC proteins, or as in CspBA-FLAG and SleC-FLAG-tagged strains, there is a significant increase in labeling in the spore cortex, compared to the negative controls (**Figure 2.6.**). Importantly, we did not observe much labeling in the coat or core layers. We conclude that *C. difficile* CspB, CspA, CspC, and SleC are

localized to the spore cortex, and are responsible for the observed cortex thinning during the early stages of germination.

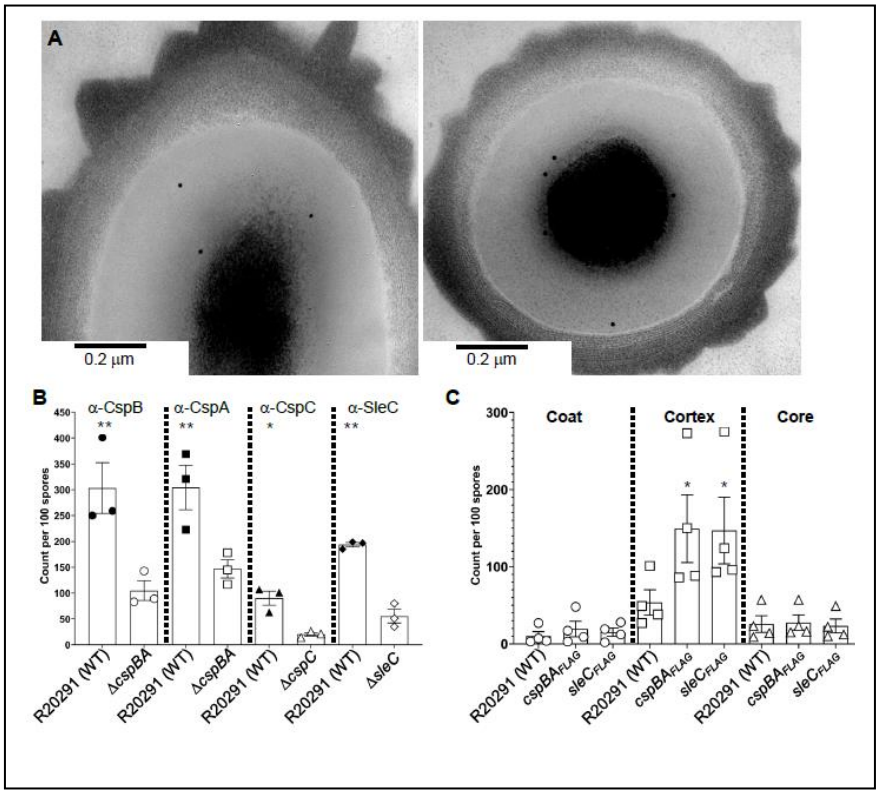

Figure 2.6.: CspB, CspA, CspC, and SleC are located in the spore cortex

Spores derived from *C. difficile* R20291, *C. difficile* Δ*cspBAC, C. difficile* Δ*sleC, C. difficile* Δ*cspBAC* p*cspBA*$_{FLAG}$*, and C. difficile* Δ*sleC* p*sleC*$_{FLAG}$*,* were fixed, embedded in acrylic resins, sectioned, immunolabeled with antibodies specific for the CspB, CspA, CspC, SleC proteins or the FLAG epitope and then imaged by TEM. (A) Representative images of immunolabeled spores. (B) Counts for the spores derived from the *C. difficile* R20291 strain, *C. difficile* Δ*cspBAC* and *C. difficile* Δ*sleC* strains labeled with α-CspB, α-CspA, α-CspC, and α-SleC primary and gold-conjugated secondary antibodies. For clarity, only the counts for the particles located in the cortex are shown since the counts for the coat layer and the core do not reach statistical significance. Counts were compared to the counts observed in the deletion mutant. (C) Count for the spores derived from the *C. difficile* R20291, *C. difficile* Δ*cspBAC* p*cspBA*$_{FLAG}$*,* and *C. difficile* Δ*sleC* p*sleC*$_{FLAG}$*,* labeled with α-FLAG primary and gold-conjugated secondary antibodies. The data represent the average of 3 or 4 biological replicates and the error bars represent the standard errors of the mean. **, $p < 0.0001$, * $p < 0.05$ as determined by one-way ANOVA using Šídák's multiple-comparison test.

2.4. Discussion

C. difficile spore germination is a tightly regulated process evolved to ensure that the vegetative cells emerge in an environment that is conducive to survival. For *C. difficile,* the obligately anaerobic cells do not survive exposure to the oxygen-rich environment (along with other potentially damaging conditions like UV radiation, desiccation, etc.). Another challenge is the inability of the *C. difficile* cells to compete against the native host microbiota in healthy individuals, requiring the ability of the metabolically dormant spores to probe for appropriate conditions when ingested by a host. These evolutionary pressures have led to the development of germination pathways that are triggered only when the proper location (the lower gastrointestinal tract of a host organism), and the proper conditions (the lack of competing microbiota) are detected.

C. difficile utilizes the Csp-type germinant receptors. There has been considerable research done on the role and the location of *C. perfringens* CspB, CspA, and SleC. Several studies have suggested, using immunoblotting and immunoelectron microscopy, that *C. perfringens* SleC is localized to the spore coat (107, 108). Other studies, again using immunoblotting of the spore coat fraction, have reported this while also suggesting the same location for CspB (64, 65, 67). Though it is plausible that the CspB, CspA, CspC, and SleC proteins are located in the same spore layer in both *C. perfringens* and in *C. difficile*, our results suggest that is not the case, at least for *C. difficile*. The studies that used immunoelectron microscopy to determine the location of SleC have drawn their conclusions from the subjective interpretation of the EM images of the spores labeled with anti-SleC antiserum, without using deletion mutants as

negative controls. Here, our approach was to quantify and analyze the labeling differences between the spores derived from *C. difficile* R20291 and the spores derived from the *C. difficile* Δ*cspBAC* and *C. difficile* Δ*slec* strains. Additionally, we constructed CspBA-FLAG and SleC-FLAG fusions for further validation and obtained similar results. In the prior work that used immunoblotting of spore coat fractions (64, 65, 67, 107), it is perhaps inevitable that cortex localized proteins are also extracted, which could then lead to the conclusion that the coat is the location of both SleC and CspB. The data from these studies has led to the proposals that Csp proteins and SleC (in its pro-SleC form) are found in the spore coat and / or the spore outer membrane, in a complex or individually (50, 62, 63, 72). Another proposed model states that CspB, CspA, and CspC are in a 'germinosome' complex, similarly to what is found in *B. subtilis* (49). In this scenario, the CspB protease activity is inhibited by the CspC bile acid receptor and the CspA co-germinant receptor until the detection of germinants, when it is capable of cleaving the proSleC prodomain, ensuring tight control of germination initiation. SleC is unlikely to be a part of this complex, due to its much greater abundance in the spore (44), but it is reasonable to hypothesize that it is located in the spore cortex, as well. Here, using combined TEM ultrastructure imaging of *C. difficile* spores during the early stages of germination, coupled with TEM immunogold labeling, we show that all three members of the *C. difficile* germinosome, and SleC, indeed are located in the spore cortex.

Our combined TEM / SEM images of germinating *C. difficile* spores have led to an interesting observation that spores fully germinate while still encased in the exosporium layer. This leads to an interesting question of how newly developed cells

exit this layer and why it occurs at the spore pole. It has been suggested that the exosporium has a role in adherence of *C. difficile* spores and its experimental removal reduces their adherence to Caco-2 cells, presumably due to the removal of specific proteins that recognize the apical cell surfaces (88). Any other role of the exosporium at this time is unknown, but our finding that it remains undisturbed throughout the germination process *in vitro* tempts us to propose that it may serve a protective role for a newly germinated cell at the earliest stage. We also note that newly hatched cells exiting the exosporium tend to be sickle-shaped, unlike mature vegetative cells (**Figure 2.5.**), perhaps indicative of the physical stress of exiting the exosporium. Future research into this stage of cell development may provide insight into the mechanisms of exosporium / coat shedding.

3. SPOVAD AND *SPOVAE* ARE REQUIRED FOR THE UPTAKE OF DPA INTO THE SPORE*

3.1. Introduction

Clostridioides difficile is a Gram-positive, spore-forming, strictly anaerobic bacterium that is opportunistically pathogenic in humans. According to the most recent report by the Centers for Disease Control and Prevention, issued in 2019, it is estimated that 223,900 cases of *C. difficile* occurred in 2017 (1, 2)**.** Of these, 12,800 deaths can be directly attributed to *C. difficile*, with the majority of deaths occurring among people aged 65 and older. In recent years, there has been an emergence of antibiotic-resistant strains, as well as strains with increased virulence making *C. difficile* a leading cause of hospital-associated infections with an estimated $5 billion in annual treatment-associated cost for *C. difficile* infections (CDI) in US hospitals alone (3, 4).

C. difficile infections are initiated upon disruption to the normally protective microbiota, commonly due to broad spectrum antibiotic use (5-8)**.** Antibiotics are prescribed to treat CDI (*i.e.* vancomycin or fidaxomicin) but patients frequently relapse with recurring CDI due to the continued disruption to the colonic microbiome and the presence of antibiotic-resistant spores that remain in the gastrointestinal tract or in the surrounding environment (9)**.**

---

* Reprinted with permission from Baloh M, Sorg JA. Clostridioides difficile SpoVAD and SpoVAE Interact and Are Required for Dipicolinic Acid Uptake into Spores. J Bacteriol. 2021 Oct 12;203(21):e0039421. doi: 10.1128/JB.00394-21. Epub 2021 Aug 23. PMID: 34424035; PMCID: PMC8508128.

Though the *C. difficile* vegetative form is the disease-causing agent, it is the spore form that is the infective agent due to its ability to survive outside of the host in the aerobic environment. *C. difficile* spores are structurally complex, composed of several distinct layers that are broadly similar to spores produced by other endospore-forming organisms, *e.g., Bacillus subtilis* (28, 83)**.** In the spore core pyridine-2,6-dicarboxylic acid (dipicolinic acid [DPA]), chelated with calcium (Ca-DPA), provides extreme heat resistant properties (26, 70). The core is surrounded by an inner membrane that has low permeability, even to water, and potentially DNA-damaging molecules, from entering the core (84, 109)**.** Surrounding the inner spore membrane is a germ cell wall that will become the cell wall of the vegetative cell, post-germination. Surrounding the germ cell wall is a thick layer of cortex peptidoglycan. In the cortex, a proportion of muramic acid residues is converted to muramic-δ-lactam (71, 85). The muramic-δ-lactam residues are the targets of cortex lytic enzymes during spore germination (87, 110)**.** The cortex is surrounded by the outer spore membrane and by the coat, which provides the spore with protection from environmental insults and decontaminants (22)**.** In some endospore-forming bacteria, the outermost layer of spores is an exosporium layer, which may have a role in adherence to host intestinal epithelial cells and other surfaces (89, 111).

Spores are metabolically dormant until the detection of germinants by germinant receptors. Germinant recognition initiates a cascade of events that irreversibly commits the spore to the germination pathway (36, 112, 113). This event is followed by the release of DPA from the core and degradation of the cortex by spore cortex lytic enzymes (SCLE), either simultaneously or sequentially, depending on the organism (34,

87, 114). In the model spore-forming bacterium, *B. subtilis*, SCLEs can be activated by exogenously added Ca-DPA or the release of Ca-DPA from the core, meaning that DPA release precedes cortex hydrolysis (87). However, in *C. difficile* these two early germination steps are inverted and cortex hydrolysis precedes DPA release (32, 70).

In *C. difficile,* activation of the SleC cortex lytic enzyme leads to the release of DPA stores from the spore core in exchange for water. In *B. subtilis* the proteins encoded by the *spoVA* operon (SpoVAA-AB-AC-AD-AEa-AEb-AF) play a role in DPA uptake and release, but *C. difficile* encodes only 3 orthologues: *spoVAC, spoVAD*, and *spoVAE*. Recent work in *B. subtilis* has demonstrated that SpoVAC, SpoVAD, and SpoVAEb are the minimal set of proteins required for DPA import and that they form a membrane complex (115). In this model, SpoVAC and SpoVAEb form a membrane channel, and SpoVAD functions as a cytoplasmic plug, and the transport of DPA occurs in continuous rounds of unplugging and replugging of the channel, as DPA accumulates in the core(115, 116). Herein, we show that *C. difficile spoVAD* and *spoVAE* are essential for DPA uptake into the spore. Because in *B. subtilis* the proteins of the *spoVA* operon are hypothesized to form a membrane channel enabling the uptake of DPA into the forming spore during sporulation and release of DPA from the spore during germination, we speculated that this also may be the case in *C. difficile* (76, 117). Using a split-luciferase reporter system we find that indeed some of the products of the *spoVA* operon interact. This led us to propose a model of a SpoVAC / SpoVAD / SpoVAE interaction that describes their roles in DPA uptake and release during *C. difficile* spore formation and germination, respectively.

3.2. Materials and methods

3.2.1. Bacteria and strains

C. difficile CRG2359 and its derivative strains were grown at 37 ° C in an anaerobic chamber (Coy Laboratories, model B, >4% H_2, 5% CO_2, 85% N_2), on brain heart infusion agar supplemented by 5 g / liter yeast extract and 0.1% L-cysteine (BHIS). The *C. difficile* CRG2359 strain is derived from the *C. difficile* R20291 strain from the Anaerobe Reference Laboratory (Cardiff, Whales, United Kingdom) (118, 119). *E. coli* DH5α (93) was grown on LB medium. Chloramphenicol (20 µg / mL), thiamphenicol (10 µg / mL), kanamycin (50 µg / mL), ampicillin (100 µg / mL) were added where indicated. Deletion mutants were selected on *C. difficile* minimal medium (CDMM) supplemented with 5 µg / mL 5-fluoroorotic acid (FOA) and 20 µg / mL uracil.

3.2.2. Construction of *spoVAD* and *spoVAE* mutants

Deletion mutations were introduced using the established *pyrE*-mediated allelic exchange technique (118). Briefly, 1kb upstream and downstream DNA regions that surround *spoVAD* and *spoVAE* (including the first 30 bp of the 5' and 3' of the gene) were amplified using primers spoVAD_ndeI_L, spoVAD_ndeI_R, spoVAD_KO_RHA_For, spoVAD_xhoI_R for *spoVAD* and spoVAE_ndeI_L, 250_Downstream_VAE, 250_Upstream_VAE, spoVAE_xhoI_R for *spoVAE*, assembled using PCR stitching, inserted by Gibson assembly (94) into pMTL-YN4 plasmid digested with NdeI and XhoI, yielding plasmids pMB02 and pMB04. The plasmids were then transformed into *E. coli* DH5α. These plasmids were subsequently transformed into *E. coli* HB101 pRK24 and grown on LB medium supplemented with chloramphenicol and

ampicillin. The resulting strain was grown overnight and then mixed with the *C. difficile* CRG2359 strain grown in BHIS in anaerobic chamber. The conjugation mixtures were spotted onto BHI plates and allowed to grow for 24 hours. Subsequently, the cells were washed with BHIS and the slurry was transferred onto BHIS medium supplemented with thiamphenicol (for plasmid maintenance) and kanamycin (to counter-select *E. coli* growth) [BHIS(TK)]. Individual colonies were passaged several times onto BHIS(TK) supplemented with uracil [BHIS(TKU)] to encourage the single crossover events. Growth was then transferred to CDMM medium supplemented with FOA and uracil to select for colonies that have excised the plasmid from the chromosome. Thiamphenicol-sensitive colonies were tested for desired mutation by PCR and confirmed by sequencing. The wild-type *pyrE* allele was restored using the same technique. The resulting *C. difficile* Δ*spoVAD* strain was renamed MB03 and the *C. difficile* Δ*spoVAE* strain MB04. The mutations were complemented by introduction of a wild-type gene under the control of a native promoter on a plasmid.

3.2.3. Construction of split luciferase interaction plasmids

Plasmids for luciferase assays were purchased from Addgene (ID: 105494 – 105497) and plasmids for testing interaction in vegetative cells were constructed following previously established protocols (120, 121). For these plasmids, *spoVAC, spoVAD,* and *spoVAE* was amplified using *C. difficile* R20291 DNA as a template to create fragments with the appropriate overlap for SmBit reporter fragment fusions (5' SpoVAC SmBit Gibson / 3' SpoVAC SmBit Gibson for *spoVAC,* 5' SpoVAD SmBit Gibson / 3' SpoVAD SmBit Gibson for *spoVAD,* 5' SpoVAE SmBit Gibson / 3' SpoVAE SmBit Gibson for *spoVAE*). These fragments were then introduced by Gibson assembly

into plasmid pAP118 digested with SacI / XhoI. Using the same approach, fragments for LgBit reporter fusions were created (5' SpoVAC LgBit Gibson / 3' SpoVAC LgBit Gibson, 5' SpoVAD LgBit Gibson / 3' SpoVAD LgBit Gibson, 5' SpoVAE LgBit Gibson / 3' SpoVAE LgBit Gibson). These fragments were then ligated into the above plasmids, digested with PvuI / NotI, yielding the interaction plasmids. To construct the negative control interaction plasmids, plasmid pAF256 was digested with SacI / XhoI, plasmid pAF257 digested with PvuI / NotI, and the required single fusion fragments were introduced into them by Gibson assembly. To construct the negative control interaction plasmid, with only SmBit and LgBit reporters without the protein fusion, LgBit reporter fragment was amplified from pAF256 using primers 5' LgBit Gibson / 3' LgBit Gibson and inserted by Gibson assembly (94) into plasmid pAF257 digested with PvuI / BamHI. This yielded plasmids pMB45 through pMB62 with all combinations of interacting partners and negative controls needed for vegetative cell expression. Next, we created plasmids with a native *spoVAC* promoter to drive the expression of the requisite constructs from the native promoter. For SpoVAC-SpoVAE we amplified the promotor region fragment from a wild-type template using primers 5' SpoVAC prm / 3' SpoVAC prm-SpoVAC, and the fusion partner sequence from pMB45 using primers 5' SpoVAC RBS / 3' LgBit-pJS116. For SpoVAD-SpoVAC, we amplified the promotor region from a wild-type template using primers 5' SpoVAC prm / 3' spoVAC pr. - spoVAD Gibson, and the fusion partner sequence from pMB46 using primers 5' SpoVAC prm-SpoVAD / 3' LgBit-pJS116. For SpoVAD-SpoVAE we amplified the promoter region from a wild-type template using primers 5' SpoVAC prm / spoVAC pr. - spoVAD Gibson and the fusion partner sequence from pMB48 using primers 5'

SpoVAC prm-SpoVAD / 3' LgBit-pJS116. Fragments were introduced by Gibson assembly into pMTL84151 digested with NotI / HinDIII. This yielded plasmids pMB72 (SpoVAC-SpoVAE), pMB73 (SpoVAD-SpoVAC), and pMB75 (SpoVAD-SpoVAE). We also created the plasmids where the SmBit or LgBit reporter fragment is inserted into an extra cytoplasmic-facing segment of SpoVAC or SpoVAE. For AC_{Sm}AC-AD_{Lg} we amplified fragments from wild-type template using primers 5' SpoVAC downstream (linker-SmBit) / 3' SpoVAC downstream (linker-SmBit) and primers 5' SpoVAC prm / 3' SpoVAC upstream (linker-SmBit), from pMB54 template using primers 5' SpoVAC-SpoVAD / 3' LgBit-pJS116, and from pMB51 template using primers 5' linker-SmBit (SpoVAC) / 3' linker-SmBit (SpoVAC). For AD_{Lg}- AC_{Sm}AC we amplified fragments from the wild-type template using primers 5' SpoVAC prm / 3' spoVAC pr. - spoVAD Gibson, primers 5' SpoVAC LgBit Gibson / 3' SpoVAC upstream (linker-SmBit), primers 5' linker-LgBit (SpoVAC) / 3' Linker-LgBit (SpoVAC), from pMB51 template using primers 5' SpoVAC prm-SpoVAD / 3' SmBit-SpoVAC RBS, and from pMB54 template using primers 5' linker-SmBit (SpoVAC) / 3' Linker-LgBit. For AC_{Sm}AC- AE_{Lg} we amplified fragments from the wild-type template using primers 5' SpoVAC prm / 3' SpoVAC upstream (linker-SmBit), primers 5' SpoVAC downstream (linker-SmBit) / 3' SpoVAC downstream (linker-SmBit) – SpoVAE, from pMB51 template using primers 5' linker-SmBit (SpoVAC) / 3' linker-SmBit (SpoVAC), and from pMB54 template using primers 5' SpoVAC-SpoVAE / 3' Linker-LgBit. For AE_{Sm}- AC_{Lg}AC we amplified fragments from the wild-type template using primers 5' SpoVAC prm / 3' spoVAC pr. - spoVAE Gibson, primers 5' SpoVAC LgBit Gibson / 3' SpoVAC upstream (linker-SmBit), primers 5' linker-LgBit (SpoVAC) / 3' Linker-LgBit (SpoVAC), from pMB52 template using primers 5'

spoVAC pr. - spoVAE Gibson / 3' SmBit-SpoVAC RBS, and from pMB54 template using primers 5' linker-SmBit (SpoVAC) / 3' Linker-LgBit (SpoVAC). For AD_{Sm}- $AE_{Lg}AE$ we amplified fragments from the wild-type template using primers 5' SpoVAC prm / 3' spoVAC pr. - spoVAD Gibson, primers 5' SpoVAE LgBit Gibson / 3' spoVAE-SpoVADSm, primers 5' SpoVAE-plasmid LgBit Mid / 3' SpoVAE-plasmid LgBit Mid, from pMB75 template using primers 5' SpoVAC prm-SpoVAD / 3' spoVAD-SmBit, and from pAP118 template using primers 5' SpoVAE LgBit Mid / 3'SpoVAE LgBit Mid. For $AE_{S/m}AE$- AD_{Lg} we amplified fragments from the wild-type template using primers 5' SpoVAC prm / 3' spoVAC pr. - spoVAE Gibson, primers 5' spoVAC pr. - spoVAE Gibson / 3' SpoVAESm-SpoVADLg, primers 5' SpoVAE Smbit Mid / 3' SpoVAE Smbit Mid, from pMB50 template using primers 5' SpoVAE-SmBit / 3' SpoVAE-SmBit, and from pMB56 template using primers 5' SpoVAE SmBit mid - SpoVAD LgBit / 3' LgBit-pJS116. The fragments were introduced by Gibson assembly (94) into the pMTL84151 plasmid digested with NotI / HinDII, yielding plasmids pMB82 – pMB85, and pMB88 – pMB89. All strains and plasmids in this study are listed in Table 3. Primers used to construct the strains and plasmids are listed in Table 4.

3.2.4. Spore purification

Spores were purified as previously described (32, 36, 63, 70). Briefly, strains were grown on 70:30 sporulation medium. After 5 days, growth from 2 plates each was scraped into 1 mL dH_2O in microcentrifuge tubes and left overnight at 4 °C. The cultures were then resuspended in the dH_20 in the same microcentrifuge tubes, centrifuged at >14,000 x g for 10 minutes, the top layer containing vegetative cells and cell debris was removed by pipetting, and the rest of the sediment resuspended in fresh dH_20. The

tubes, again, were centrifuged for 1 minute at >14,000 x g, the top layer removed, and the sediment resuspended. This was repeated 5 more times, combining the sediment from 2 tubes into one. The spores were then separated from the cell debris by centrifugation through a 50% sucrose gradient for 20 minutes at 4 °C and 3,500 x g. The resulting spore pellet was then washed 5 times with dH_20, resuspended in 1 mL dH_20, and stored at 4 °C until use.

Table 3 – List of strains and plasmids used in Chapter 3

***C. difficile* strains**	**Description**	**Reference**
R20291	Wild type, ribotype 027	(40)
CRG2359	R20291 Δ*pyrE*	(118)
RS19	CRG2359 restored *pyrE*	(49)
MB03	Δ*spoVAD* strain	This study
MB04	Δ*spoVAE* strain	This study
Other strains		
E. coli DH5α	Cloning strain	(93)
E. coli HB101 pRK24	Conjugal donor strain for *C. difficile*	(122)
Plasmid	**Description**	**Reference**
pMTL-YN4	Backbone used to make deletions in R20291 by allelic exchange	(118)
pMTL84151	Backbone used to make complementing plasmids and spore luciferase interaction plasmids	(123)
pMB02	To create Δ*spoVAD* deletion	This study
pMB04	To create Δ*spoVAE* deletion	This study
pMB34	*spoVAD* complementing plasmid	This study
pMB35	*spoVAE* complementing plasmid	This study
pAP118	Plasmid encoding an aTC inducible HupA-SmBiT and HupA-LgBiT fusions	(120)
pAF256	Plasmid encoding an aTC inducible HupA-SmBiT and LgBiT	(120)
pAF257	Plasmid encoding an aTC inducible SmBiT and HupA-LgBiT	(120)
pAF259	Plasmid encoding an aTC inducible BitlucOpt	(120)
pMB50	Luciferase spoVAC / Smbit-LgBit	This study
pMB51	Luciferase spoVAD / Smbit-LgBit	This study
pMB52	Luciferase spoVAE / Smbit-LgBit	This study
pMB53	Luciferase Smbit-spoVAC / LgBit	This study
pMB54	Luciferase Smbit-spoVAD / LgBit	This study
pMB55	Luciferase Smbit-spoVAE / LgBit	This study
pMB62	Luciferase spoVAC / Smbit-SpoVAC / LgBit	This study

Table 3 continued

C. difficile strains	Description	Reference
pMB45	Luciferase spoVAC / Smbit-SpoVAE / LgBit	This study
pMB46	Luciferase spoVAD / Smbit-SpoVAC / LgBit	This study
pMB47	Luciferase spoVAD / Smbit-SpoVAD / LgBit	This study
pMB48	Luciferase spoVAD / Smbit-SpoVAE / LgBit	This study
pMB49	Luciferase spoVAE / Smbit-SpoVAC / LgBit	This study
pMB57	Luciferase spoVAE / Smbit-SpoVAE / LgBit	This study
pMB60	Luciferase spoVAC / Smbit-SpoVAD / LgBit	This study
pMB61	Luciferase Smbit-LgBit	This study
pMB72	spoVAC-SmBit / spoVAE-LgBit luciferase spore complementation	This study
pMB73	spoVAD-SmBit / spoVAC-LgBit luciferase spore complementation	This study
pMB75	spoVAD-SmBit / spoVAE-LgBit luciferase spore complementation	This study
pMB79	HupA-SmBit / HupA-LgBit luciferase spore complementation	This study
pMB81	BitLuc luciferase spore complementation	This study
pMB82	SpoVAC-SmBit-SpoVAC / SpoVAD-LgBit; small luciferase reporter inserted mid-AC gene, ADLg partner	This study
pMB83	SpoVAD-SmBit / SpoVAC-LgBit-SpoVAC; large luciferase reporter inserted mid-AC gene, ADSm partner	This study
pMB84	SpoVAC-SmBit-SpoVAC / SpoVAE-LgBit; small luciferase reporter inserted mid-AC gene, AELg partner	This study
pMB85	SpoVE-SmBit / SpoVAC-LgBit-SpoVAC; large luciferase reporter inserted mid-AC gene, AESm partner	This study
pMB87	Sm-Lg luciferase spore interaction plasmid, negative control.	This study
pMB88	SpoVAD-Sm / SpoVAE-Lg-SpoVAE; large luciferase reporter inserted mid-AE gene, ADSm partner	This study
pMB89	SpoVAE-Sm-SpoVAE / SpoVAD-Lg; small luciferase reporter inserted mid-AE gene, ADLg partner	This study

Table 4 – List of primers used in Chapter 3

Plasmids	No.	Name	Sequence
Δ*spoVAD*	648	spoVAD_ndeI_L	agctatgaccgcggccgctgtatccatatggactcaaagtgaaataggagagatgctcaa
	649	spoVAD_ndeI_R	ctactcatttactattactactgcatgtgctgttctttttccaattctttttatttttcatattttc
	618	spoVAD_KO_RHA_For	atgaaaaataaaagaattggaaaaagaacagcacatgcagtagtaatagtaaatgag
	650	spoVAD_xhoI_R	tgccaagcttgcatgtctgcaggcctcgagaaaaatcatactcttctttttttattgatt
Δ*spoVAE*	651	spoVAE_ndeI_L	agctatgaccgcggccgctgtatccatatgatatcaactggaactatagtgggtcctaag
	759	250_Downstream_VAE	tttaagcacctagaaacagttgaataactgata
	758	250_Upstream_VAE	tatactgactgtggtatagagatgtttaacc
	652	spoVAE_xhoI_R	tgccaagcttgcatgtctgcaggcctcgaggtagtttttaactcttgtattatagaaatcgcagg
Cell interaction plasmids	1792	5' SpoVAC LgBit Gibson	ACTTTTTGAAGAAATTCTATAGCTCGATCGATACTTTAGAGAGGTGTTTAGTATG
	1793	3' SpoVAC LgBit Gibson	ACCACCACCACCACTAGAACCTGCGGCCGCAAACATCTTAAAAATATAATAAATAATTC

Table 4 continued

Plasmids	No.	Name	Sequence
	1794	5' SpoVAC SmBit Gibson	CTTGATCGTAGCGTTAACAGATCTGAGCTCATACTTTAGAGAGGTGTTTAGTATG
	1795	3' SpoVAC SmBit Gibson	ACCACCACCACCACTAGAACCCCCTCGAGAAAACATCTTAAAAATATAATAAATAATTC
	1796	5' SpoVAD LgBit Gibson	ACTTTTTGAAGAAATTCTATAGCTCGATCGAAAATTAAAAAGGTGTGAAAATATG
	1797	3' SpoVAD LgBit Gibson	ACCACCACCACCACTAGAACCTGCGGCCGCCTCATTTACTATTACTACTGCATG
	1798	5' SpoVAD SmBit Gibson	CTTGATCGTAGCGTTAACAGATCTGAGCTCAAAATTAAAAAGGTGTGAAAATATG
	1799	3' SpoVAD SmBit Gibson	ACCACCACCACCACTAGAACCCCCTCGAGACTCATTTACTATTACTACTGCATGTG
	1800	5' SpoVAE LgBit Gibson	ACTTTTTGAAGAAATTCTATAGCTCGATCGAATGAGTAGGAAGTGATATAATATG
	1801	3' SpoVAE LgBit Gibson	ACCACCACCACCACTAGAACCTGCGGCCGCTGGTTTTGCTTTTGGAG
	1802	5' SpoVAE SmBit Gibson	CTTGATCGTAGCGTTAACAGATCTGAGCTCAATGAGTAGGAAGTGATATAATATG
	1803	3' SpoVAE SmBit Gibson	ACCACCACCACCACTAGAACCCCCTCGAGATGGTTTTGCTTTTGGAG
	1932	5' LgBit Gibson	agacttttgaagaaattctatagctcgatcgctgcagtaaaggagaaaattttg
	1933	3' LgBit Gibson	aaagttttattaaaacttataggatccagcctaactgtttatagttactctaaacaac
Spore interaction plasmids	1991	5' SpoVAC prm	atttttttatcaggaaacagctatgaccgctaagcatgaaaggagaaagtg
	1992	3' SpoVAC prm-SpoVAC	gtctacatatttttttataatttttatccatactaaacacctctctaaagtattatttg
	1993	5' SpoVAC RBS	ataggtttatttttttaaaattaacaaataatactttagagaggtgtttag
	1994	3' LgBit-pJS116	acgttgtaaaacgacggccagtgccaagctctaactgtttatagttactctaaacaac
	1469	3' spoVAC pr. - spoVAD Gibson	tgttctttttccaattctttttatttttcatactaaacacctctctaaagtattatttg
	1995	5' SpoVAC prm-SpoVAD	aacaaataatactttagagaggtgtttagtatgaaaaataaaagaattggaaaaag
Mid-gene reporter insertion spore interaction plasmids	2090	5' SpoVAC downstream (linker-SmBit)	acaggttatagacttttgaagaaattctactaggtgctagttctgc
	2091	3' SpoVAC downstream (linker-SmBit)	tttcacacctttttaattttcgatcgagctaaaacatcttaaaaatataataaataattc
	2087	3' SpoVAC upstream (linker-SmBit)	accaccagaaccaccaccaccactagaacctttatcaagacctccaactttcatatac
	2092	5' SpoVAC-SpoVAD	ttatatttttaagatgttttagctcgatcgaaaattaaaaaggtgtgaaaatatg
	2088	5' linker-SmBit (SpoVAC)	ttgtatatgaaagttggaggtcttgataaaggttctagtggtggtggtg
	2089	3' linker-SmBit (SpoVAC)	tgttattgatgttgcagaactagcacctagtagaatttcttcaaaaagtctataacctg

Table 4 continued

Plasmids	No.	Name	Sequence
	2095	5' linker-LgBit (SpoVAC)	tctatgttgtttagagtaactataaacagtctaggtgctagttctgcaac
	2096	3' Linker-LgBit (SpoVAC)	gtaaaacgacggccagtgccaagctgcctaaaacatcttaaaaatataataaataattcc
	2093	3' SmBit-SpoVAC RBS	aaacacctctctaaagtatcgatcgagctatagaatttcttcaaaaagtctataacctg
	2094	3' Linker-LgBit	tgttattgatgttgcagaactagcacctagactgtttatagttactctaaacaacatag
	2097	3' SpoVAC downstream (linker-SmBit) - SpoVAE	atatcacttcctactcattcgatcgagctaaaacatcttaaaaatataataaataattcc
	2098	5' SpoVAC-SpoVAE	ttatatttttaagatgttttagctcgatcgaatgagtaggaagtgatataatatg
	1471	3' spoVAC pr. - spoVAE Gibson	aataaatactcttacatagtccattaacatactaaacacctctctaaagtattatttg
	1472	5' spoVAC pr. - spoVAE Gibson	aacaaataatactttagagaggtgtttagtatgttaatggactatgtaagagtatt
	1469	3' spoVAC pr. - spoVAD Gibson	tgttctttttccaattcttttatttttcatactaaacacctctctaaagtattatttg
	2165	3' spoVAD-SmBit	atatcacttcctactcattcgatcgagctatagaatttcttcaaaaagtctataacctg
	1800	5' SpoVAE LgBit Gibson	ACTTTTTGAAGAAATTCTATAGCTCGATCGAATGAGTAGGAAGTGATATAATATG
	2166	3' spoVAE-SpoVADSm	accaccagaaccaccaccaccactagaaccatatccaaatcctattataggaac
	2169	5' SpoVAE-plasmid LgBit Mid	tctatgttgtttagagtaactataaacagttcacttgctacaggagtaataaaatc
	2170	3' SpoVAE-plasmid LgBit Mid	gttgtaaaacgacggccagtgccaagctgcttatggttttgcttttggagtaaatac
	2167	5' SpoVAE LgBit Mid	ggttctagtggtggtggtggttctggtggtggtggttctagtggtgtttttac
	2168	3'SpoVAE LgBit Mid	aattgattttattactcctgtagcaagtgaactgtttatagttactctaaacaacatag
	2171	3' SpoVAESm-SpoVADLg	accaccagaaccaccaccaccactagaaccatatccaaatcctattataggaactg
	2172	5' SpoVAE-SmBit	gcaacagttcctataataggatttggatatggttctagtggtggtgg
	2173	3' SpoVAE-SmBit	ttgattttattactcctgtagcaagtgatagaatttcttcaaaaagtctataacctg
	2174	5' SpoVAE Smbit Mid	acaggttatagacttttgaagaaattctatcacttgctacaggagtaataaaatc
	2175	3' SpoVAE Smbit Mid	attttcacacctttttaattttcgatcgagttatggttttgcttttggagtaaatac
	2176	5' SpoVAE SmBit mid - SpoVAD LgBit	tactccaaaagcaaaaccataactcgatcgaaaattaaaaaggtgtgaaaatatg

3.2.5. DPA and OD germination assays

Ca-DPA release was measured using a SpectraMax M3 plate reader for 1 hr at 37 °C with excitation at 270 nM and emission at 545 nM and with a 420 nM cutoff. Spores were heat activated at 65 °C for 30 minutes and suspended in water at an OD_{600}

= 50. The spores were then added to final OD of 0.5 in 100 µL final volume of HEPES buffer pH 7.5, containing 100 mM NaCl, 10 mM TA, 30 mM glycine, and 250 µM Tb^{3+} in a 96 well plate. OD_{600} was monitored using the same plate reader at 37 °C for 1 hr. The heat-activated spores were added to a final OD of 0.5 in in the same HEPES buffer composition as in Ca-DPA release assay, omitting Tb^{3+} (49, 124).

3.2.6. Luciferase assays

Assays involving vegetative cells were performed using the previously published protocols (120). Briefly, strains were grown overnight in liquid BHIS supplemented with thiamphenicol. The following day the liquid cultures were diluted to an OD_{600} = 0.05 and allowed to grow to an OD_{600} = 0.3 – 0.4. Next, 100 µL was removed and placed into wells of a transparent 96 well plate, suitable for OD_{600} and another 100 µL placed into white flat-bottom 96-well plate for the luminescence assay. The rest of the cultures were induced with 200 ng / mL of aTc for 1 hour. 20 µL of NanoGlo luciferase (Promega N1110) was added to each sample well to measure luciferase activity using SpectraMax M3 plate reader in the luminescence mode, using all channels, and 0.1 second sampling time. After 1 hour, the induced cultures were assayed for OD and luciferase activity in the same way. The luciferase activity was normalized to culture optical density at OD_{600}.

3.2.7. Western blot

Solutions of $1x10^8$ spores of *C. difficile* R20291, *C. difficile* Δ*spoVAD,* and *C. difficile* Δ*spoVAE* were prepared and 100 µL of each was incubated in HEPES buffer pH 7.5, containing 100 mM NaCl, 10 mM TA, 30 mM glycine for 15 minutes to induce germination. These samples and equal amounts of non-germinated control spore

solutions were boiled for 20 minutes in 2x NuPage buffer at 95 °C. Then, 10 µL of each sample was separated on 10% SDS-PAGE gel. The protein was transferred to PVDF membrane and then blocked overnight at 4 °C with 5% milk powder dissolved in TBST. The membrane was washed thrice for 20 minutes at room temperature with TBST and then probed for 1 hour in 5% milk dissolved in TBST with anti-SleC antibodies at room temperature. The membrane was then washed thrice for 20 minutes at room temperature with TBST before labeling with anti-rabbit IgG secondary antibody. The membrane was again washed and then incubated for 5 minutes with Pierce ECL Western Blotting Substrate (ThermoScientific), overlaid with X-ray film, exposed and developed.

3.2.8. Statistical analysis

Data represents results from at least 3 independent and the error bars represent standard errors of the means. One-way ANOVA followed by Tukey's or Dunnett's multiple comparisons test, as indicated, was performed using GraphPad Prism version 9.0.2 (161) for Windows, (GraphPad Software, San Diego, California USA).

3.3. Results

3.3.1. *spoVAD* and *spoVAE* are responsible for DPA uptake into the developing spore

Prior research on *C. difficile spoVAC* found that a *spoVAC* deletion resulted in spores that contain only 1% of the wild-type level of DPA (31, 32, 125). To understand the contribution of *spoVAD* and *spoVAE* to sporulation and DPA uptake, we used an established p*yrE*-based allelic exchange system (118) to create *spoVAD* or *spoVAE*

deletion strains in the *C. difficile* CRG2359 strain, restored the *pyrE* deletion, and then analyzed spores derived from the resulting strains for their DPA content using terbium fluorescence (63). Spores derived from *C. difficile spoVAD* and *spoVAE* mutant strains contained approximately 1% of the wild-type levels of DPA (**Figure 3.1.A**). The amount of spore DPA content could be restored to wild type levels by expressing *spoVAD* or *spoVAE*, *in trans,* from a plasmid. These results suggest that *spoVAD* and *spoVAE*, like *spoVAC*, are required for DPA uptake into the *C. difficile* spore, similar to their roles in *B. subtilis* (75, 76).

Next, we tested if the absence of DPA led to a loss of heat resistance to spores derived from the mutant strains. When spores derived from the *C. difficile* Δ*spoVAD* and Δ*spoVAE* strains were heated at 65 ° C for 30 minutes and plated on BHIS medium supplemented with taurocholic acid (a potent spore germinant), we observed a >90% decrease in the number of colony forming units compared to the unheated samples or to the samples containing complementation plasmids (**Figure 3.1.B**). These results show that spores derived from the *C. difficile* Δ*spoVAD* and Δ*spoVAE* mutant strains are heat sensitive due to the lack of DPA or that heat treatment blocks an early germination event.

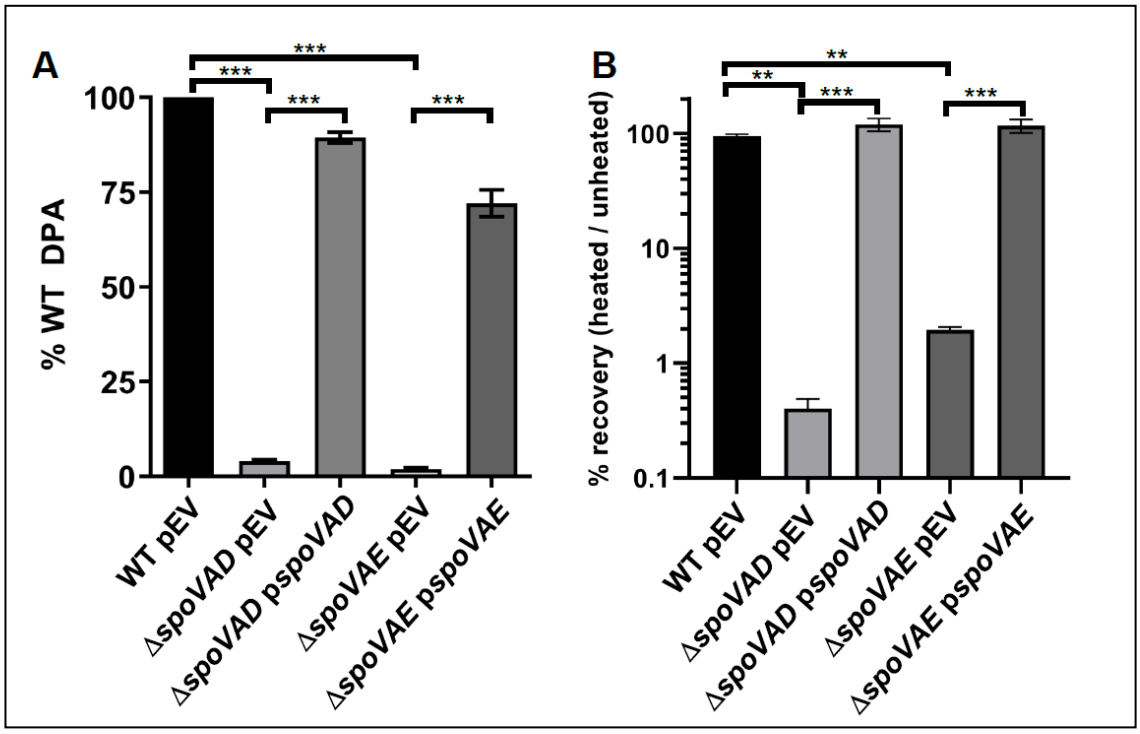

Figure 3.1. *spoVAD* and s*poVAE* are required for DPA uptake into the spore.

(A) Equal amounts of spores purified from *C. difficile* strains RS19 (WT), MB03 (Δ*spoVAD*), and MB04 (Δ*spoVAE*), containing an empty vector (pEV) or a complementing plasmid, were boiled for 20 minutes and DPA amounts quantified by Tb^{3+} fluorescence. Values are reported as percentage of the WT DPA content. (B) $1x10^8$ spores were serially diluted and plated on BHIS plates supplemented with TA, before and after heating at 65 °C for 30 minutes. The values are reported as percentage of heated spores that formed colonies, compared to unheated spores. The data represents results from 3 independent assays and the error bars represents the standard error of the mean. ** indicates p<0.001, *** indicates p<0.0001 as determined by one-way ANOVA using Tukey's multiple comparisons test.

3.3.2. spoVAE may contribute to *C. difficile* spore germination

C. difficile spore germination is activated upon binding of certain bile acid and certain amino acid germinants to receptors (36, 43, 48, 49, 63). This results in the irreversible initiation of germination and the release of the majority of DPA from the spore core. Another indicator of germination is the change of optical density of the spore solution. This assay takes advantage of the transition of dormant spores from a phase-bright, dormant, state to a phase-dark, germinated, state. In both assays, equal

numbers of spores derived from *C. difficile* RS19 [*C. difficile* CRG2359 with a restored *pyrE* (49)], *C. difficile* Δ*spoVAD*, or *C. difficile* Δ*spoVAE* strains containing empty vectors or the complementation constructs, were suspended in buffer alone or buffer supplemented with the germinants taurocholate and glycine. Subsequently, the release of DPA and the change in OD_{600} values were measured over a period of 1 hour.

Due to the reduced abundance of DPA in the spores, *C. difficile* Δ*spoVAD* spores release very little DPA (**Figure 3.2.A**). This phenotype can be complemented by the expression of the wild type copy of the gene *in trans.* In the optical density-based germination assay we observed only a small, ~10%, reduction in OD_{600} values for *C. difficile* Δ*spoVAD*-derived spores. Moreover, due to the lack of DPA in the spores, these mutants are difficult to purify as they do not migrate through density gradients well. To circumvent this issue, nearly 100 plates were required to purify spores from the mutant strains. The spores derived from the wild type and the complemented strain germinated normally (**Figure 3.2.B**). Spores derived from the *C. difficile* Δ*spoVAE* strain also released very little DPA, and this phenotype was only partially complemented to wildtype levels (**Figure 3.2.C**). In the optical density germination assay, *C. difficile* Δ*spoVAE*-derived spores showed an intermediate phenotype, with an ~30% reduction in OD_{600} values, which can again only be partially complemented to wild-type levels (**Figure 3.2.D**). Despite the lack of DPA, spores derived from the *C. difficile* Δ*spoVAD* and Δ*spoVAE* strains are capable of initiating germination. Western blot analysis showed that the cortex lytic enzyme SleC, required for the initiation of *C. difficile* spore germination, was activated to similar levels in the spores derived from the mutant and the wild type strains (**Figure 3.2.E**). These results suggest that spores derived from *C.*

difficile Δ*spoVAD* and Δ*spoVAE* strains activate SleC normally but that the *C. difficile* Δ*spoVAE* mutant strain has a small defect in germination.

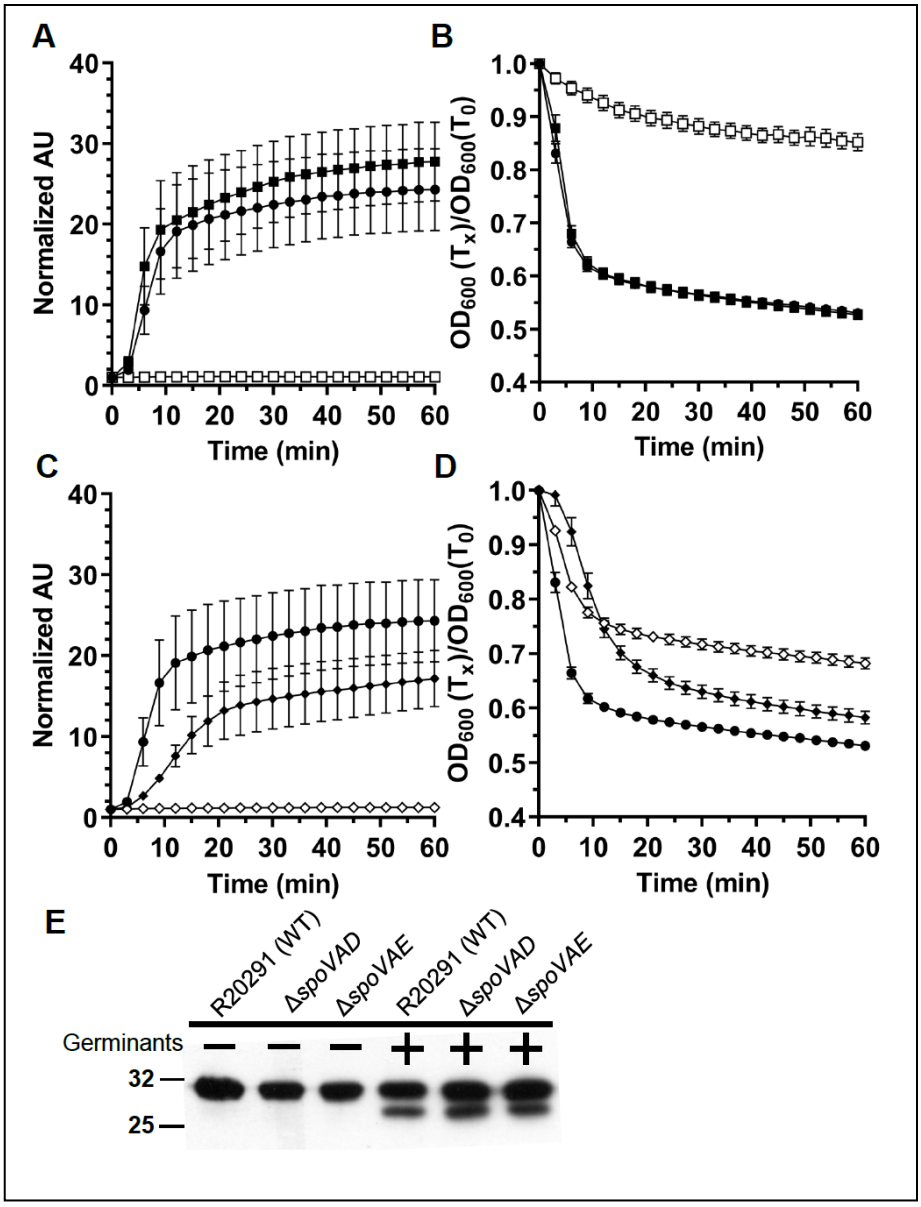

Figure 3.2. *C. difficile spoVAD* and s*poVAE* mutant spores initiate germination normally.

Spores derived from *C. difficile* RS19 pEV (●), MB03 pEV (Δ*spoVAD*; □), MB03 p*spoVAD* (■), MB04 (Δ*spoVAE*; ◊) and MB04 p*spoVAE* (♦) were purified and germination was quantified by (A and C) Tb^{3+} or (B and D) OD_{600}. For clarity, every fifth data point is plotted. The data represents results from 3 independent biological replicates and the error bars represent standard error of the mean. (E) 10^8 spores derived from *C. difficile* CRG2359 (WT), MB03 (Δ*spoVAD*), and MB04 (Δ*spoVAE*) were incubated in buffer alone or in buffer supplemented with the germinants taurocholate and glycine and then boiled in sample buffer, the proteins resolved by SDS-PAGE, and probed with anti-SleC antibody. Inactive pro-SleC corresponds to the ~32 kDa band while activated SleC is the ~29 kDa.

3.3.3. Testing the interaction of the *C. difficile* SpoVAC, SpoVAD, and SpoVAE proteins

Our findings of *C. difficile spoVAD* and s*poVAE* mutant phenotypes indicate that deletion of either gene results in the absence of DPA in the spore core. Prior research has shown a similar phenotype in a *C. difficile spoVAC* mutant (31, 32). In both *B. subtilis* and *C. difficile* the SpoVAC protein is a transmembrane protein, hypothesized to be embedded in the inner spore membrane, and acts in a mechanosensing fashion to release DPA from the spore core during germination (70, 77). While SpoVAD is not predicted to have transmembrane domains, we analyzed the *C. difficile* SpoVAE protein sequence with Constrained Consensus TOPology prediction server (CCTOPS) that predicts protein topology as a consensus of 10 different methods, and the results indicated that SpoVAE has several transmembrane domains (126). Thus, the location of the *C. difficile* SpoVA proteins are consistent with those found *B. subtilis* (76, 77, 117, 127, 128). The similar phenotype of single mutants and their predicted topology led us to hypothesize that SpoVAC, SpoVAD, and SpoVAE interact and form a complex at the inner spore membrane. To test the potential interaction of these proteins, we used the luciferase protein interaction assay, developed for use in *C. difficile* (120). Briefly, the codon-optimized luciferase reporter was split into two parts, SmBit and LgBit. Each reporter gene fragment was translationally fused to the 3' end of *C. difficile spoVAC*, *spoVAD*, and *spoVAE*, and each fusion pair was expressed under the control of an anhydrotetracycline (aTc) inducible promoter. The plasmids were introduced into the wildtype *C. difficile* R20291 strain and luciferase activity was measured before induction and 1 hour after induction with aTc. As positive controls, we used the full-length

luciferase reporter BitLuc, and the HupA-HupA fusions that were originally used to validate the assay (120). As negative controls, we used single s*poVAC* or *spoVAD* or *spoVAE* fusions (to one reporter fragment) while the second reporter fragment remained unfused. We detected a greater than 2-$\log_{10}$ increase in luminescence signal after 1 hour of induction for the positive controls BitLuc and HupA-HupA. Interestingly, we observed an increase in luciferase signal for SpoVAC-SpoVAE, SpoVAD-SpoVAC, and SpoVAD-SpoVAE interaction pairs (**Figure 3.3.**). Though the signal for other interaction pairs after induction was increased, it did not reach statistical significance. In our negative controls the signal did not increase significantly after induction except, notably, in SpoVAD-SmBit fusion where the signal significantly increased for unknown reasons. Nevertheless, the other negative control, SpoVAD-LgBit does not exhibit a significant luciferase signal increase after induction.

Because the uptake of DPA into the spore occurs in the late stages of sporulation (129, 130), we wanted to test for the potential SpoVA protein interactions in cultures that are actively undergoing sporulation. The full length BitLuc control, the negative SmBit-LgBit control, and the interaction partners that showed a significant luciferase signal in induced vegetative cultures (SpoVAC-SpoVAE, SpoVAD-SpoVAC, and SpoVAD-SpoVAE) were cloned into a plasmid and placed under the control of a native *C. difficile spoVAC* promoter (a region of 500 bp upstream of *spoVAC*) and conjugated into the wild-type *C. difficile* R20291 strain. Additionally, we cloned either a SmBit or LgBit luciferase reporter fragment into a segment of the SpoVAC and SpoVAE that is predicted to face outside of the core and, therefore, SpoVAD(based on the CCTOPs prediction) (117, 126, 128).

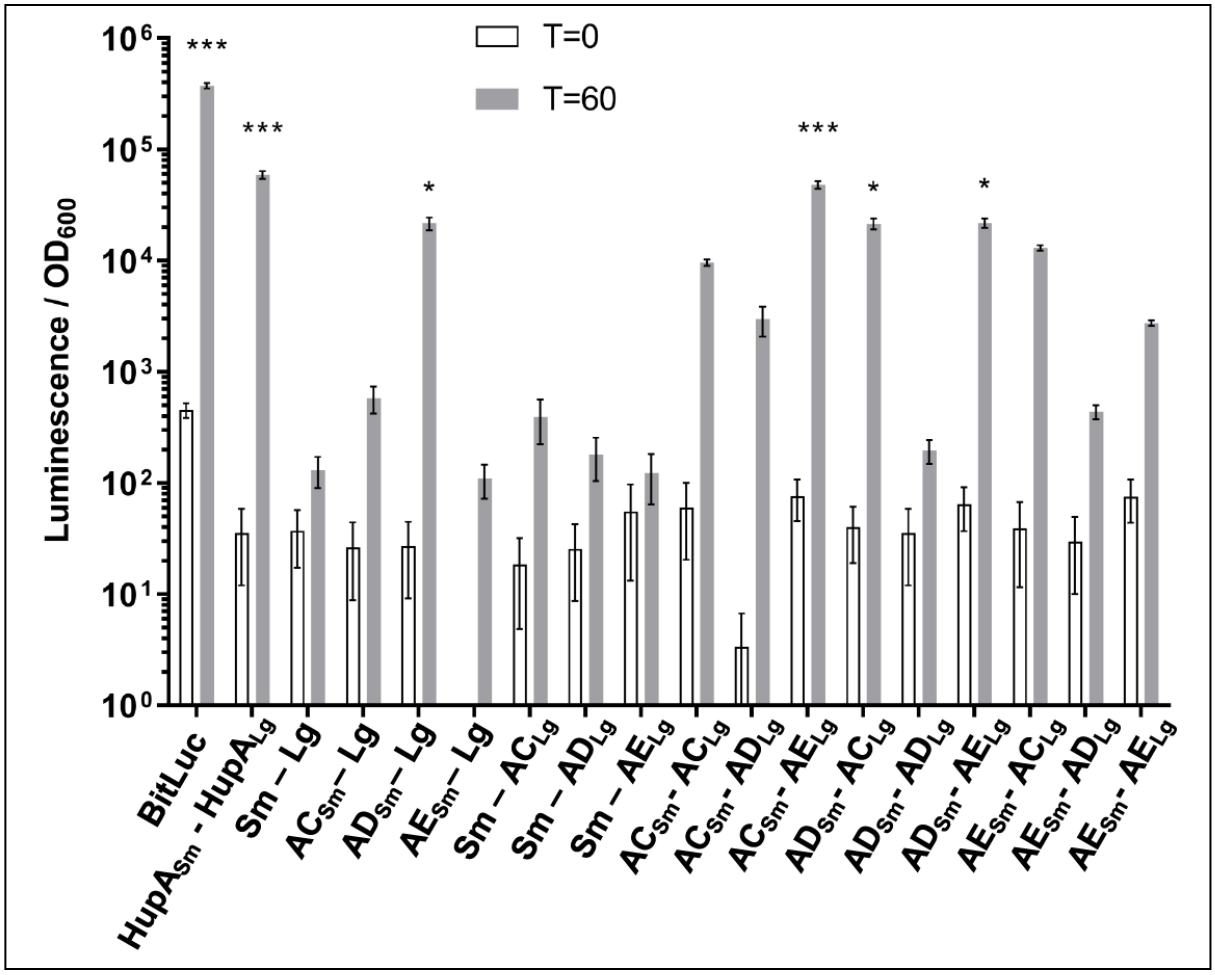

Figure 3.3. SpoVAC, SpoVAD, and SpoVAE interact *in* vivo

C. difficile vegetative cells transformed with the indicated plasmids were induced with 200 ng / mL of aTc for 60 minutes. Averages of 3 biological replicates shown. Optical density-normalized luciferase activity (LU / OD) is shown before induction (white bars) and after 60 minutes (grey bars). Positive interaction was determined by comparison of LU / OD at T = 60 of transformed strains with the negative control (SmBit-LgBit). No significant difference was detected at T=0. * $p < 0.05$, *** $p < 0.0001$ as determined by one-way ANOVA using Dunnett's multiple comparisons test.

The strains were streaked onto sporulation medium and left to grow for 2 days, the period of time that would ensure that the sporulation has commenced, but not fully completed, for the majority of cells in the sample. The cell mass was scraped and

resuspended in water, and equal number of cells for each strain were incubated with luciferase substrate and luminescence signal measured (**Figure 3.4.**). Under these conditions, we observed that SpoVAD and SpoVAE yielded the greatest signal, indicating that during sporulation these two proteins come into close proximity. The other constructs showed a smaller luminescence signal but did not reach statistical significance.

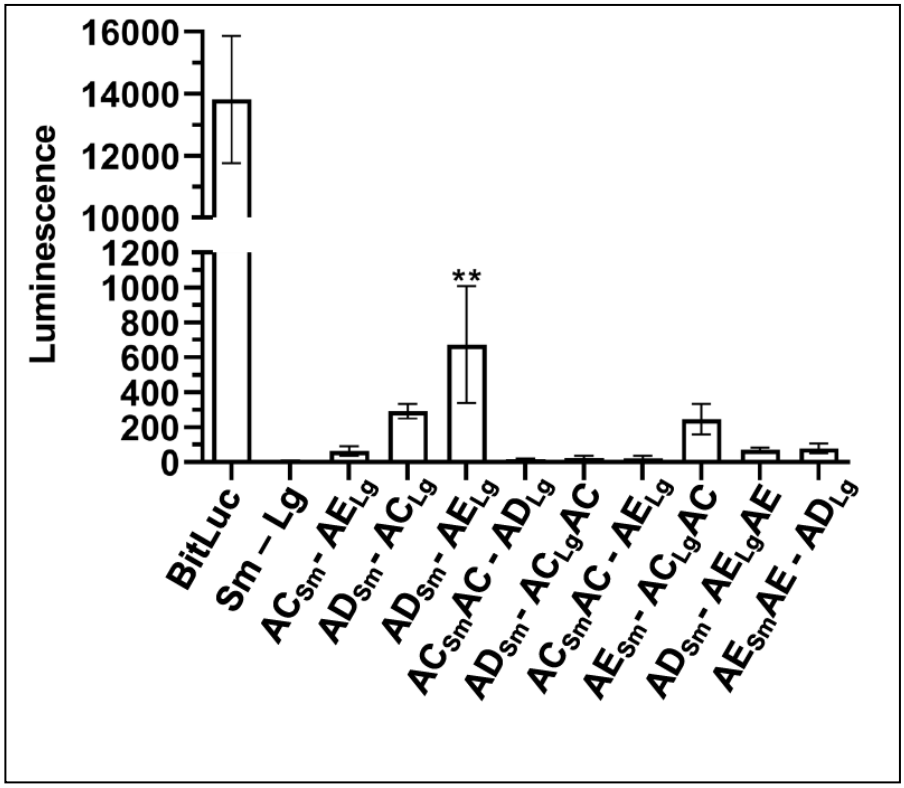

Figure 3.4 SpoVAD and SpoVAE interact in sporulating cultures

C. difficile cells transformed with the indicated plasmids were grown on sporulation medium. Luminescence of the sporulating culture was assayed after 2 days of growth. Averages of 4 biological replicates are shown. ** $p < 0.001$ as determined by one-way ANOVA using Dunnett's multiple comparisons test.

Because our data indicate that SpoVAD and SpoVAE interact during sporulation, it is plausible that these proteins would remain in close proximity in the metabolically dormant spore. We therefore tested the same protein interaction pairs in fully formed dormant spores. The strains were sporulated on sporulation medium, and spores purified as previously described. Next, $1x10^8$ spores of each strain were assayed for luciferase activity (**Figure 3.5.**). Similar to what we observed for a sporulating culture, the SpoVAD-SpoVAE interacting pair showed the highest level of interaction, while SpoVAC-SpoVAD, SpoVAD-SpoVAC, and SpoVAE-SpoVAClgAC showed a small but non-significant signal. Taken together, our results suggest that SpoVAD-SpoVAE interact when expressed in vegetative cell or in sporulating / dormant spores, while the other SpoVA proteins may weakly and / or transiently interact.

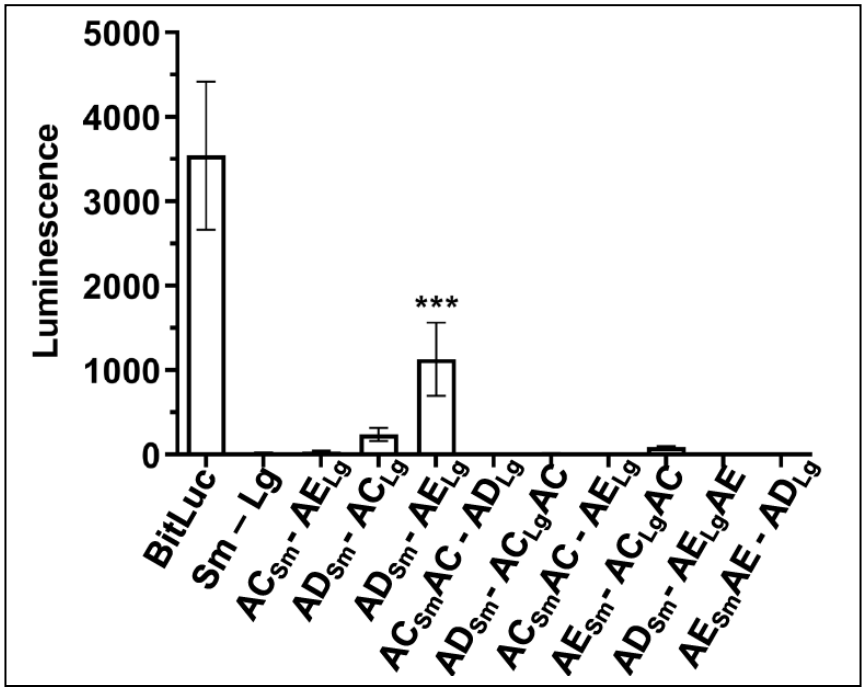

Figure 3.5. SpoVAD and SpoVAE demonstrate interaction in dormant spores

C. difficile cells transformed with the indicated plasmids were grown on sporulation medium and the resulting spores were purified and assayed for luminescence. Averages of 3 biological triplicates shown. *** $p < 0.0001$ as determined by one-way ANOVA using Dunnett's multiple comparisons test.

We hypothesized that the SpoVA proteins that interact during DPA uptake would still interact upon spore germination. To test this, we exposed $1x10^8$ spores derived from the indicated strains to the germinants taurocholate and glycine in buffer and measured the luminescence signal over the period of 30 minutes. Similar to our observation in the sporulating culture and dormant spores, the SpoVAD-SpoVAE seems to interact the most strongly and gives the highest luminescence signal (**Figure 3.6.**). The other interacting pairs, the C-terminal fusions and mid-protein fusions, also had an increase in signal. However, these signals did not reach statistical significance. But this and the similar signal increase in the previous assays using sporulating cultures and dormant spores suggests either a weak or transient interaction. We therefore conclude that SpoVAD and SpoVAE interact during all stages of *C. difficile* development cycle; in vegetative cells, sporulating cells, spores, and germinating spores.

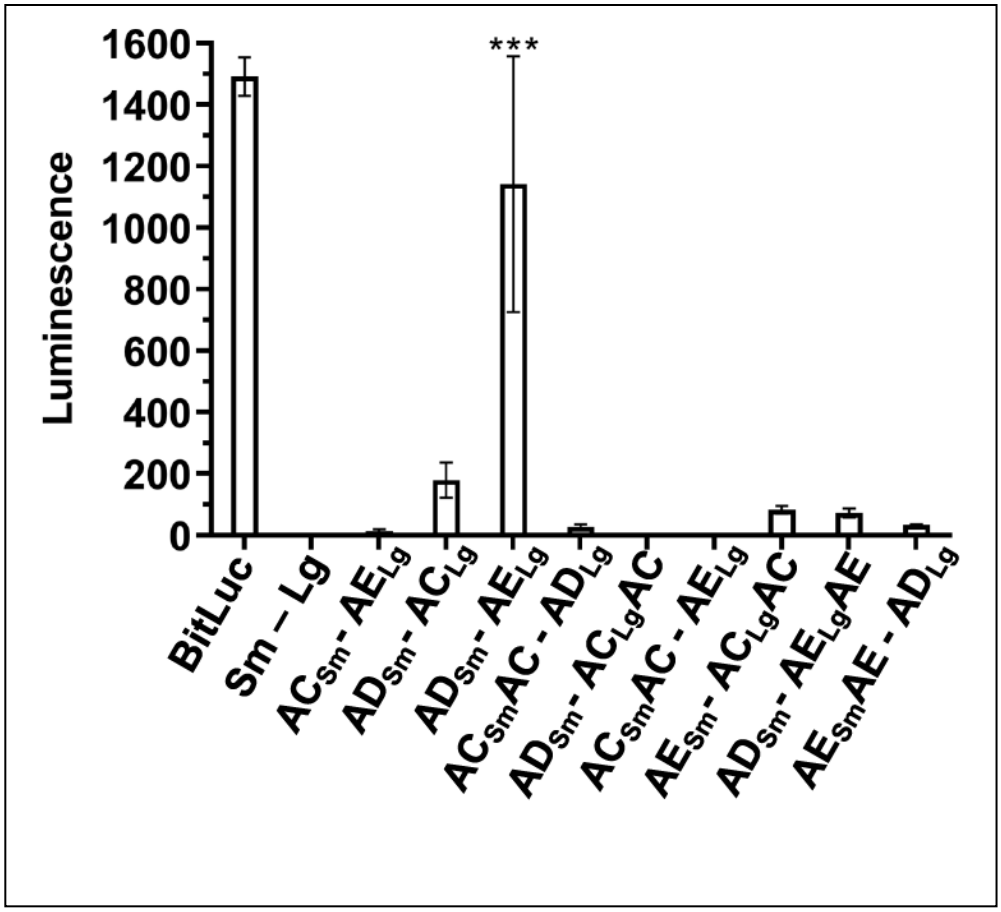

Figure 3.6. SpoVAD and SpoVAE interact during spore germination

Spores derived from the strains containing the indicated plasmids were germinated in the presence of TA and glycine. Luminescence was measured over the period of 30 minutes, but only T = 15 minutes shown for clarity. Averages of 3 biological triplicates shown. *** $p < 0.0001$ as determined by one-way ANOVA using Dunnett's multiple comparisons test.

3.4. Discussion

C. difficile spores, like most spores from endospore-forming organisms, are notable for their resilience to wet heat. Peak natural environment temperatures and even temperatures that are commonly recommended for heat treatment of foodstuffs are often insufficient to destroy the spores or render them incapable of germination (131). This heat resistance, along with other characteristics of spores that provide

resistance to UV radiation, desiccation, and resistance to common disinfectants, makes *C. difficile* (or other spore-forming organisms) difficult to eradicate (132). The spore resistance to heat is largely the consequence of large amounts of DPA in the spore core that replaces the majority of water and comprises 5-15% of dry weight of the spore (57). Since spores are metabolically dormant, in order for metabolic processes to initiate, this DPA must be released from the spore core in exchange for water during the initial stages of spore germination.

The initiation of germination is a non-reversible process and the release of DPA, in exchange for water, is tightly regulated by the germinant receptors. To initiate *C. difficile* spore germination, the Csp-type germinant receptors, composed of a hypothesized CspB, CspA, and CspC protein complex, become activated by bile acid and co-germinants (*i.e.*, certain amino acids or Ca^{2+}). Germinant activation of the germinant receptors leads to the processing of the inhibitory pro-peptide from the cortex lytic enzyme SleC (49, 61). Activated SleC degrades the spore cortex layer resulting in the activation of the SpoVAC mechanosensing protein and DPA release from the core (32, 70). Though, the importance of *spoVAC* is known in both *B. subtilis* and *C. difficile*, the roles of *spoVAD* and *spoVAE* have not been tested in *C. difficile*. Here, we find that the mutations in *C. difficile spoVAD* and *spoVAE* prevent DPA uptake into the spore core. This is similar to prior observations with *C. difficile spoVAC* mutants and *B. subtilis spoVAD* mutants (31, 32, 75).

Because a mutation in any member of the *C. difficile spoVA* operon resulted in a similar phenotype, we hypothesized that the products of this operon form a complex and interact during DPA uptake. Because SpoVAC is a transmembrane protein that is

embedded in the inner spore membrane, and SpoVAE is predicted to have transmembrane domains, this complex should be located at, or near, the inner spore membrane. Even though SpoVAD is not predicted to have a transmembrane domain, consistent with its hypothesized role as a DPA binding protein (75), it should be located near the inner spore membrane during DPA uptake in order to transfer DPA via SpoVAC into the spore core. Using the recently developed split luciferase system for studying protein-protein interactions in *C. difficile* (120), we detected a large increase in luminescence for SpoVAD and SpoVAE and smaller, but non-significant increases in other interaction pairs, in vegetative cells, sporulating cells, dormant spores, and germinating spores. We therefore propose a model in which the DPA, synthesized in the mother cell in the late stage of sporulation, is taken up into the spore by the interaction between all 3 SpoVA proteins. In this model, SpoVAD acts as a DPA-binding protein, SpoVAC as a channel through which DPA passes into the spore core, and SpoVAE acting as an accessory protein (**Figure 3.7.**). Consistent with the predictions arising from this model, we first observed interaction between all 3 protein pairs in vegetative cells (i.e., SpoVAC-SpoVAE, SpoVAD-SpoVAC, and SpoVAD-SpoVAE). In our assay, the protein pair expression was driven by an aTc-induced pTet promoter which likely induces protein expression above the level of baseline expression in vegetative *C. difficile* cells, but this served to show that the interaction partners could interact, and to discover any interactions that may be transient, temporary, or at low incidence rate in the uninduced culture. However, this was dependent upon the fusions being located on the region of the proteins predicted to be on the outer surface of the inner membrane, where the proteins are likely to interact. We also discovered such

interactions in sporulating cultures, in the dormant spores, and in the germinating spores. We found that in all 3 stages of spore development the strongest interacting partners were SpoVAD and SpoVAE. This has given us confidence in our model because SpoVAE has predicted transmembrane domains and is found in the inner spore membrane of *B. subtilis* spores (75, 76). Though SpoVAD has no predicted transmembrane domains, our data suggests it is situated on the inner spore membrane with SpoVAE, similar to its location in *B. subtilis* (127).

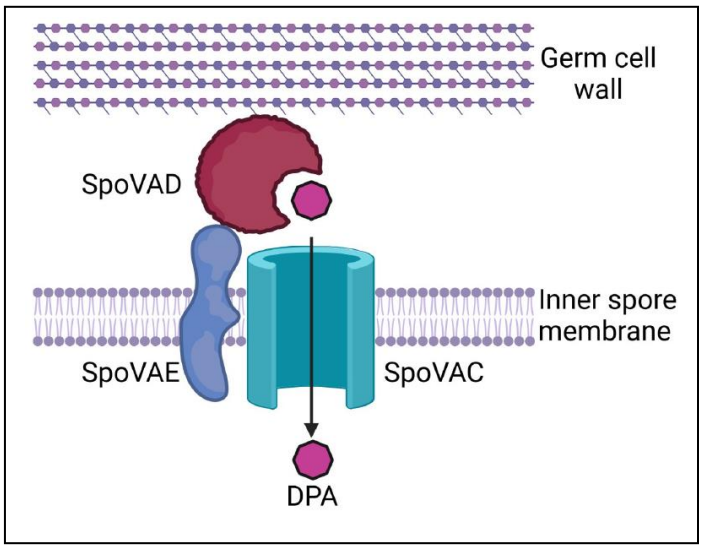

Figure 3.7. Proposed model of SpoVA protein interaction

SpoVA proteins interaction at the inner spore membrane by which DPA produced by the mother cell is taken up into the spore during sporulation and released in the initial stages of germination. Created with BioRender.com

Because the expression of the fusions was driven by an inducible promoter, the data likely represent the signal at the maximum expression levels, which may be why the SpoVAC-SpoVAD interaction signal is quite high. Because the mother cell produces large amounts of DPA during the late stages of sporulation, the trafficking of DPA by SpoVAD to SpoVAC, and their interaction, must be a high-incidence event, if perhaps

temporary. After sporulation is completed, the assays showed the highest interaction signal for SpoVAE-SpoVAD, suggesting that this pair forms a more stable interaction.

In the model spore-forming organism *B. subtilis*, the *spoVA* operon is composed of 8 genes, while the *C. difficile spoVA* operon is considerably less complex and encodes only 3 orthologues, making it a convenient system for study. Since our data suggests that all of the *C. difficile* SpoVA proteins may interact, we hypothesize that the protein products of a more complex *B. subtilis spoVA* operon form a complex, as well.

4. CONCLUSIONS

Secretion of the *C. difficile* from the vegetative cells damage the host colonic epithelium resulting in the disruption of the cytoskeletal structure and the tight junctions of the cells, cell rounding, and cell death (133). Though the cell is the toxin-secreting, and disease-causing, stage of the *C. difficile* lifecycle, it is the spore that is the infective stage due to cells' sensitivity to oxygen and the inability to compete against the native healthy host microbiota. Spores need to germinate in an environment conducive to the establishment of CDI; in the proper location in the GI tract, and in conditions when the competition from the native host microbiota is reduced or non-existent. Spore germination, therefore, must be a tightly regulated mechanism because the commitment to germination is an irreversible process and germination within a inhospitable environment would result in the death of the cell. In *C. difficile*, this is regulated by the Csp-type germinant receptor complex, a protein complex responsible for the sensing of germinants indicating the appropriate environmental conditions for germination, leading to the activation of the cortex lytic enzyme SleC, cortex degradation, and in exchange of water for DPA within the spore core. The spore is remarkably resistant to the various environmental conditions due to its complex structure. Resistance to antibiotics, oxygen, UV, alcohols, ROS, detergents, and heat all contribute to the spore survival in the environment outside the host, but also within the host, particularly during the antibiotic treatment targeting CDI, often resulting in recurrent infection. Materials and equipment contaminated with *C. difficile* spores from patients with CDI (i.e., feces as a consequence of diarrhea, the most common CDI symptom) are, obviously, disinfected but the spore resistance to various disinfectants may prevent their total eradication. The

heat treatment by autoclaving is effective, but not all contaminated material can be treated in that way. In laboratory settings, spores are commonly heated to 65 °C for a period of 30 minutes to destroy any vegetative cells, with no effect on the efficiency of the remaining spores' germination. The heat resistance is largely due to the presence of DPA in the spore core, replacing the water. In hospital environments, the most common source of *C. difficile,* this heat resistance contributes to its spread. DPA is produced by the mother cell during sporulation and its packaging into the spore core is regulated by *spoVA* operon in most endospore-forming organisms. There is intriguing evidence that the *B. subtilis* strains (and some other *Bacillus* species) that carry additional copies of the *spoVA* operon on a TN*1546* transposon exhibit increased wet heat resistance due to an increase in the DPA content of the spore (30), as well as increased pressure resistance (134). It would be interesting to test whether this phenotype could be replicated in *C. difficile* by overexpression of *spoVA* operon either on a plasmid or a transposable element. One of the potential avenues of future research could be tied to the finding that *B. subtilis* SpoVAD, the DPA-binding protein, exhibits high affinity to the particular DPA isomer ($DPA_{2,6}$) and significantly lower affinity to other DPA isomers (116). Nevertheless, even this affinity for $DPA_{2,6}$ is relatively low and large amounts of DPA are released into the medium by sporulating mother cell (135), presumably as consequence of this low affinity. Overexpression of SpoVAD may result in not only increased DPA content of the spore, but lower amounts of detected DPA in the sporulation medium.

If the germination mechanisms were to be disrupted, by affecting the Csp germinosome, spores could either prevented from germinating, or germinated in

conditions unsuitable for the establishment of CDI (i.e., ‘germinate to exterminate’), reducing or eliminating the need for antibiotic treatment (136, 137). If the packaging of DPA into the developing spore core could be disrupted by affecting SpoVA proteins while the spore is still in the forespore of the mother cell, resulting spores would be extremely heat-sensitive. As shown before, incubating DPA-less spores at 65 °C for a period of 30 minutes (temperatures easily reached by commercial washing machines) results in virtually no spores surviving (**Figure 3.1**). Disruption of either of these protein complexes could be another weapon in the arsenal used to deal with this important human pathogen.

In these chapters, I presented the results of the investigation into elucidating the mechanisms behind the interaction of the proteins responsible for germinant sensing, and the proteins responsible for the packaging of DPA into the spore core, the release of which, in exchange for water, is the first step in the resumption of metabolic activity in *C. difficile* spore.

Temporally speaking, the DPA **packaging** is one of the last events during sporulation in the mother cell, while DPA **release** is the last step of exiting from spore dormancy, before the resumption of metabolic activities (28, 31) (**Figure 4.1.**). The packaging of the large amounts of DPA synthesized by the mother cell into the developing spore is under the control of *spoVA* operon in most spore-forming organisms (32, 77, 116), and *C. difficile* encodes 3 orthologues, *spoVAC, spoVAD,* and *spoVAE.* Interestingly, in *B. subtilis,* the proteins encoded by *spoVAC, spoVAD,* and *spoVAEb* have been determined to form the minimal set of proteins required for DPA packaging and release (115). Using *pyrE* allelic exchange, I constructed the Δ*spoVAD* and

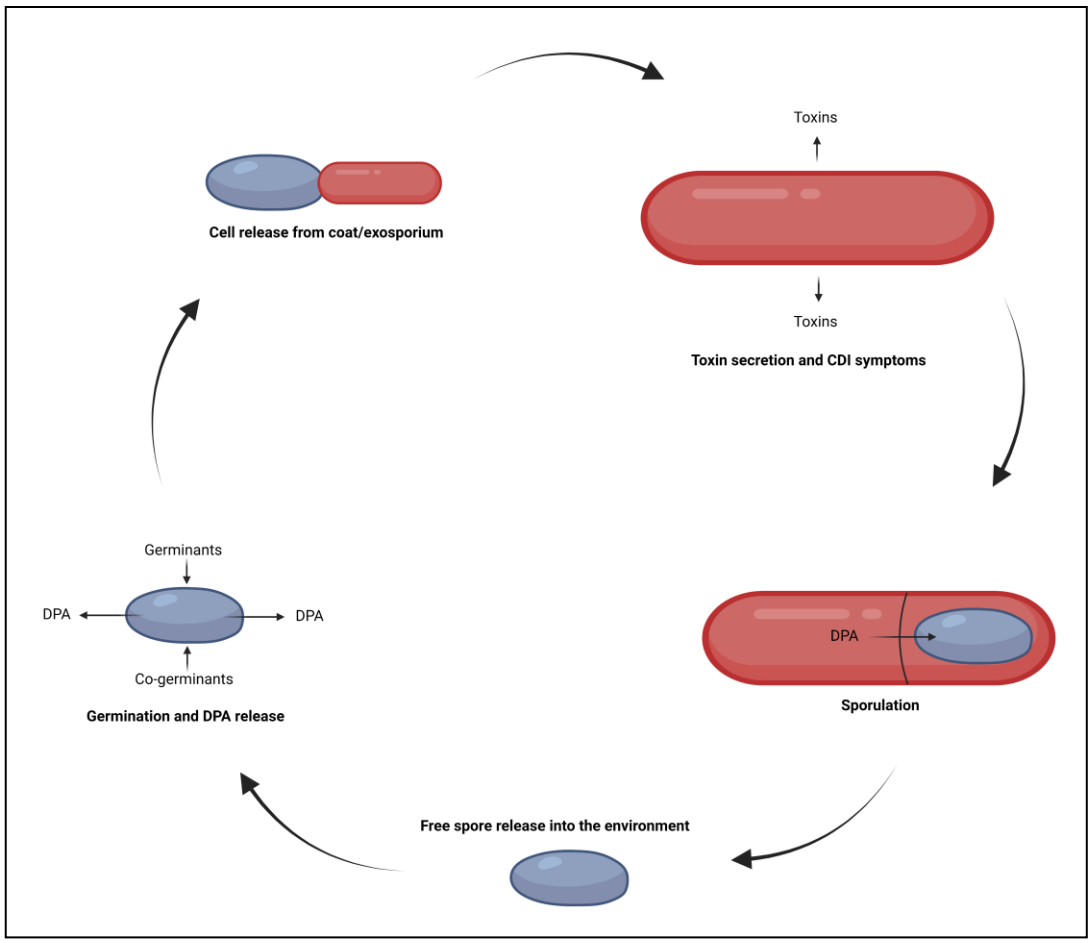

Figure 4.1. *C. difficile* lifecycle

If a spore is ingested into a host and detects germinants and co-germinants, signaling that the conditions for germination are appropriate, it releases its store of DPA in exchange for water, the cell develops and exits the coat/exosporium layer, secreting toxins causing CDI. Eventually, the cell begins to sporulate, and DPA is packaged into the spore core. The spore is released, and cycle can recommence.

Δ*spoVAE* strains and by characterizing them established that the spores derived from these strains, just like the previously characterized Δ*spoVAC* strain, contain very low amounts of DPA. The finding that individual disruption of any of the 3 members of the *spoVA* operon results in the same phenotype led me to propose that SpoVAC, SpoVAD, and SpoVAE form a complex, where each member is required for DPA uptake into the developing spore. Using split-luciferase protein interaction assay I showed that this is

indeed the case, in vegetative cells, sporulating cells, dormant spores, and germinating spores (78). Based on the predicted locations and structure of *spoVA* proteins in *B. subtilis* and *C. difficile*, we proposed that the *C. difficile* SpoVA complex is found at the inner spore membrane (78, 115). The inner spore membrane is largely impermeable to damaging chemicals, as well as water (84, 109). There is evidence that the reason for the inner spore membrane impermeability is not due to its lipid composition, which is largely similar to the vegetative cell membrane in *B. subtilis* and *B. megaterium* (138, 139), but rather due to the immobility of these lipids due to the inner spore membrane compression by the spore cortex (140). Presumably, various proteins that are embedded in the inner spore membrane are also under this constraint, like SpoVAC, a mechanosensing protein serving as a DPA channel, and SpoVAE, an accessory protein required for DPA uptake that also has predicted transmembrane domains. We detected SpoVAD and SpoVAE protein interaction in all stages of *C. difficile* lifecycle, and SpoVAC and other two proteins only in vegetative cells when the BitLuc reporter-fused protein synthesis was induced by a pTet promoter. It would be interesting to solve the crystal structure of SpoVAE and SpoVAC (SpoVAD structure is already solved), to verify whether there is a possibility of interaction of all 3 proteins as suggested by the interaction signal in induced vegetative cultures. If so, then perhaps SpoVAE and SpoVAC interact during DPA packaging while embedded in the inner spore membrane, however weakly or transiently, despite the inner membrane constraint imposed by the cortex.

The large amount of DPA in the spore core seems to also have a role in regulating UV radiation damage of the spore core DNA, in synergy with small acid-

soluble spore proteins (SASP). SASP binding the spore DNA, along with the low spore core water content due to its replacement with DPA, and potentially binding of DPA itself to the DNA (141, 142), photosensitize DNA and increase the formation of DNA lesions. But this synergistic effect of SASP and DPA favors the formation of TT DNA lesions (5-thyminyl-5,6-dihydrothymine) that is efficiently removed in a process with redundant mechanisms, in the early stages of germination (143). Interestingly, *B. subtilis* strains that are unable to synthesize DPA or SASP exhibit lower levels of total photoproducts, but a larger proportion of cyclobutane dimers (CPD) and 6-4 photoproducts (6-4PP) that are not as efficiently repaired as TT lesions. It would be interesting to see whether the DPA-less mutants we created also exhibit a similar pattern in spore UV resistance, and whether strains outgrowing from such spores accumulate more detrimental or lethal mutations than the wild type strains.

The role of the *C. difficile* germination proteins, CspB, CspA, and CspC, have been established. CspB as a protease, CspC as a bile acid receptor, and CspA as a co-germinant receptor. Their location, and the location of the cortex lytic enzyme SleC has been only hypothesized. Using TEM imaging of the germinating spores I established that the cortex degradation, observed as a thinning of the cortex, is consistent for the majority of the spore population within the first 5 minutes of germination initiation. This is consistent with the predicted location of SleC, in the cortex. Using immunolabeled thin-section spore samples, I established that CspB, CspC, and CspA are also located in the cortex, consistent with the predictions and the changes observed by TEM in the spore cortex.

Previous work has established the roles of CspB, CspC, CspA, leading to the hypothesis that they form a germinosome complex. The role of SleC as cortex lysis enzyme suggests that it should be located in the spore cortex. The immunolabeling study I performed suggest that the location of all these proteins is inside the spore cortex, supporting the germinosome hypothesis. But it should be noted that colocation does not imply interaction. Therefore, to provide stronger evidence for the germinosome hypothesis, future work should focus on showing that CspB, CspC, and CspA indeed interact with each other. One such approach could be using protein interaction assay, perhaps similar to the split-luciferase assays I performed to show SpoVA protein interaction.

Another potential avenue of future research would be determining the nature of potential interaction between CspC, CspA, and CspB. One hypothesis is that CspB is already bound by CspC and CspA and repressed in such a way until the germinants are detected, changing the conformation of CspC and CspA, releasing CspB to cleave the pro-domain from SleC. An alternative hypothesis is that CspC and CspA are activated by binding the germinants and co-germinants, and then bind CspB to activate its protease activity.

The studies described in the above chapters provide new insight into two mechanisms were provide *C. difficile* spores with their remarkable heat resistance and that ensure that the germination is a tightly regulated process resulting in the establishment of CDI. While there are still plenty of open questions that remain in these topics, these studies provide a foundation for the development of treatments aimed at disruption of the establishment of CDI that are not dependent on antibiotics. Ultimately,

the best treatment for CDI and, indeed, any disease is prevention, and these studies may aid in the development of such preventative treatments.

REFERENCES

1. Lessa FC, Mu Y, Bamberg WM, Beldavs ZG, Dumyati GK, Dunn JR, Farley MM, Holzbauer SM, Meek JI, Phipps EC, Wilson LE, Winston LG, Cohen JA, Limbago BM, Fridkin SK, Gerding DN, McDonald LC. 2015. Burden of *Clostridium difficile* infection in the United States. N Engl J Med 372:825-34.
2. CDC. 2019. Antibiotic Resistance Threats in the United States, 2019. U.S. Department of Health and Human Services, CDC,
3. McDonald LC, Killgore GE, Thompson A, Owens RC, Jr., Kazakova SV, Sambol SP, Johnson S, Gerding DN. 2005. An epidemic, toxin gene-variant strain of *Clostridium difficile*. N Engl J Med 353:2433-2441.
4. Abdrabou AMM, Ul Habib Bajwa Z, Halfmann A, Mellmann A, Nimmesgern A, Margardt L, Bischoff M, von Muller L, Gartner B, Berger FK. 2021. Molecular epidemiology and antimicrobial resistance of *Clostridioides difficile* in Germany, 2014-2019. Int J Med Microbiol 311:151507.
5. Buffie CG, Bucci V, Stein RR, McKenney PT, Ling L, Gobourne A, No D, Liu H, Kinnebrew M, Viale A, Littmann E, van den Brink MR, Jenq RR, Taur Y, Sander C, Cross JR, Toussaint NC, Xavier JB, Pamer EG. 2015. Precision microbiome reconstitution restores bile acid mediated resistance to *Clostridium difficile*. Nature 517:205-8.
6. Theriot CM, Bowman AA, Young VB. 2016. Antibiotic-induced alterations of the gut microbiota alter secondary bile acid production and allow for *Clostridium difficile* spore germination and outgrowth in the large intestine. mSphere 1.
7. Theriot CM, Koenigsknecht MJ, Carlson PE, Jr., Hatton GE, Nelson AM, Li B, Huffnagle GB, J ZL, Young VB. 2014. Antibiotic-induced shifts in the mouse gut microbiome and metabolome increase susceptibility to *Clostridium difficile* infection. Nat Commun 5:3114.

8. Wilson KH, Perini F. 1988. Role of competition for nutrients in suppression of *Clostridium difficile* by the colonic microflora. Infect Immun 56:2610-2614.

9. Smits WK, Lyras D, Lacy DB, Wilcox MH, Kuijper EJ. 2016. *Clostridium difficile* infection. Nat Rev Dis Primers 2:16020.

10. Voth DE, Ballard JD. 2005. Clostridium difficile toxins: mechanism of action and role in disease. Clin Microbiol Rev 18:247-63.

11. Kuehne SA, Cartman ST, Minton NP. 2011. Both, toxin A and toxin B, are important in Clostridium difficile infection. Gut Microbes 2:252-255.

12. Lyras D, O'Connor JR, Howarth PM, Sambol SP, Carter GP, Phumoonna T, Poon R, Adams V, Vedantam G, Johnson S, Gerding DN, Rood JI. 2009. Toxin B is essential for virulence of Clostridium difficile. Nature 458:1176-1179.

13. Young MK, Leslie JL, Madden GR, Lyerly DM, Carman RJ, Lyerly MW, Stewart DB, Abhyankar MM, Petri WA, Jr. 2022. Binary Toxin Expression by Clostridioides difficile Is Associated With Worse Disease. Open Forum Infectious Diseases 9.

14. Pruitt R, Lacy DB. 2012. Toward a structural understanding of Clostridium difficile toxins A and B. Frontiers in Cellular and Infection Microbiology 2.

15. Edwards AN, Karim ST, Pascual RA, Jowhar LM, Anderson SE, McBride SM. 2016. Chemical and stress resistances of *Clostridium difficile* spores and vegetative cells. Front Microbiol 7:1698.

16. Joshi LT, Welsch A, Hawkins J, Baillie L. 2017. The effect of hospital biocide sodium dichloroisocyanurate on the viability and properties of *Clostridium difficile* spores. Lett Appl Microbiol 65:199-205.

17. Dyer C, Hutt LP, Burky R, Joshi LT. 2019. Biocide resistance and transmission of *Clostridium difficile* spores spiked onto clinical surfaces from an American health care facility. Appl Environ Microbiol 85.

18. Romero-Rodríguez A, Troncoso-Cotal S, Guerrero-Araya E, Paredes-Sabja D, Ellermeier CD. 2020. The *Clostridioides difficile* cysteine-rich exosporium morphogenetic protein, CdeC, exhibits self-assembly properties that lead to organized inclusion bodies in *Escherichia coli*. mSphere 5:e01065-20.

19. Pizarro-Guajardo M, Calderón-Romero P, Romero-Rodríguez A, Paredes-Sabja D. 2020. Characterization of exosporium layer variability of *Clostridioides difficile* spores in the epidemically relevant strain R20291. Frontiers in Microbiology 11.

20. Diaz-Gonzalez F, Milano M, Olguin-Araneda V, Pizarro-Cerda J, Castro-Cordova P, Tzeng SC, Maier CS, Sarker MR, Paredes-Sabja D. 2015. Protein composition of the outermost exosporium-like layer of *Clostridium difficile* 630 spores. J Proteomics 123:1-13.

21. Castro-Córdova P, Mora-Uribe P, Reyes-Ramírez R, Cofré-Araneda G, Orozco-Aguilar J, Brito-Silva C, Mendoza-León MJ, Kuehne SA, Minton NP, Pizarro-Guajardo M, Paredes-Sabja D. 2020. *Clostridioides difficile* spore-entry into intestinal epithelial cells contributes to recurrence of the disease. bioRxiv:2020.09.11.291104.

22. Driks A, Eichenberger P. 2016. The spore coat, The Bacterial Spore: from Molecules to Systems. American Society of Microbiology.

23. Freer JH, Levinson HS. 1967. Fine structure of *Bacillus megaterium* during microcycle sporogenesis. J Bacteriol 94:441-57.

24. Crafts-Lighty A, Ellar DJ. 1980. The structure and function of the spore outer membrane in dormant and germinating spores of *Bacillus megaterium*. J Appl Bacteriol 48:135-45.

25. Popham DL, Helin J, Costello CE, Setlow P. 1996. Analysis of the peptidoglycan structure of *Bacillus subtilis* endospores. J Bacteriol 178:6451-8.

26. Cowan AE, Koppel DE, Setlow B, Setlow P. 2003. A soluble protein is immobile in dormant spores of *Bacillus subtilis* but is mobile in germinated spores: implications for spore dormancy. Proc Natl Acad Sci U S A 100:4209-14.

27. Sunde EP, Setlow P, Hederstedt L, Halle B. 2009. The physical state of water in bacterial spores. Proc Natl Acad Sci U S A 106:19334-9.

28. Paredes-Sabja D, Shen A, Sorg JA. 2014. Clostridium difficile spore biology: sporulation, germination, and spore structural proteins. Trends Microbiol 22:406-16.

29. Jamroskovic J, Chromikova Z, List C, Bartova B, Barak I, Bernier-Latmani R. 2016. Variability in DPA and calcium content in the spores of *Clostridium* species. Frontiers in Microbiology 7.

30. Berendsen EM, Boekhorst J, Kuipers OP, Wells-Bennik MH. 2016. A mobile genetic element profoundly increases heat resistance of bacterial spores. ISME J 10:2633-2642.

31. Donnelly ML, Fimlaid KA, Shen A. 2016. Characterization of *Clostridium difficile* spores lacking either SpoVAC or dipicolinic acid synthetase. J Bacteriol 198:1694-707.

32. Francis MB, Sorg JA. 2016. Dipicolinic acid release by germinating *Clostridium difficile* spores occurs through a mechanosensing mechanism. mSphere 1.

33. Setlow P. 2014. Spore resistance properties. Microbiol Spectr 2.

34. Shen A. 2020. *Clostridioides difficile* spore formation and germination: New insights and opportunities for intervention. Annu Rev Microbiol 74:545-566.

35. Shen A. 2020. *Clostridioides difficile* spore formation and germination: new insights and opportunities for intervention. Annual Review of Microbiology 74:545-566.

36. Sorg JA, Sonenshein AL. 2008. Bile salts and glycine as cogerminants for *Clostridium difficile* spores. J Bacteriol 190:2505-12.

37. Sorg JA, Sonenshein AL. 2009. Chenodeoxycholate is an inhibitor of *Clostridium difficile* spore germination. J Bacteriol 191:1115-7.

38. Ridlon JM, Kang DJ, Hylemon PB. 2006. Bile salt biotransformations by human intestinal bacteria. J Lipid Res 47:241-59.

39. Ridlon JM, Kang DJ, Hylemon PB, Bajaj JS. 2014. Bile acids and the gut microbiome. Curr Opin Gastroenterol 30:332-8.

40. Sorg JA, Sonenshein AL. 2010. Inhibiting the initiation of *Clostridium difficile* spore germination using analogs of chenodeoxycholic acid, a bile acid. J Bacteriol 192:4983-90.

41. Francis MB, Allen CA, Sorg JA. 2013. Muricholic acids inhibit *Clostridium difficile* spore germination and growth. PLoS One 8:e73653.

42. Ramirez N, Liggins M, Abel-Santos E. 2010. Kinetic evidence for the presence of putative germination receptors in *Clostridium difficile* spores. J Bacteriol 192:4215-22.

43. Howerton A, Ramirez N, Abel-Santos E. 2011. Mapping interactions between germinants and *Clostridium difficile* spores. J Bacteriol 193:274-82.

44. Bhattacharjee D, Francis MB, Ding X, McAllister KN, Shrestha R, Sorg JA. 2016. Reexamining the germination phenotypes of several *Clostridium difficile* strains suggests another role for the CspC germinant receptor. Journal of Bacteriology 198:777-786.

45. Kochan TJ, Shoshiev MS, Hastie JL, Somers MJ, Plotnick YM, Gutierrez-Munoz DF, Foss ED, Schubert AM, Smith AD, Zimmerman SK, Carlson PE, Jr., Hanna PC. 2018. Germinant synergy facilitates *Clostridium difficile* spore germination under physiological conditions. mSphere 3.

46. Jose S, Mukherjee A, Horrigan O, Setchell KDR, Zhang W, Moreno-Fernandez ME, Andersen H, Sharma D, Haslam DB, Divanovic S, Madan R. 2021. Obeticholic acid ameliorates severity of *Clostridioides difficile* infection in high fat diet-induced obese mice. Mucosal Immunology 14:500-510.

47. Yuille S, Mackay WG, Morrison DJ, Tedford MC. 2020. Drivers of *Clostridioides difficile* hypervirulent ribotype 027 spore germination, vegetative cell growth and toxin production *in vitro*. Clinical Microbiology and Infection 26:941.e1-941.e7.

48. Shrestha R, Sorg JA. 2018. Hierarchical recognition of amino acid co-germinants during *Clostridioides difficile* spore germination. Anaerobe 49:41-47.

49. Shrestha R, Cochran AM, Sorg JA. 2019. The requirement for co-germinants during *Clostridium difficile* spore germination is influenced by mutations in *yabG* and *cspA*. PLoS Pathog 15:e1007681.

50. Kochan TJ, Somers MJ, Kaiser AM, Shoshiev MS, Hagan AK, Hastie JL, Giordano NP, Smith AD, Schubert AM, Carlson PE, Jr., Hanna PC. 2017. Intestinal calcium and bile salts facilitate germination of *Clostridium difficile* spores. PLoS Pathog 13:e1006443.

51. Leslie JL, Jenior ML, Vendrov KC, Standke AK, Barron MR, O'Brien TJ, Unverdorben L, Thaprawat P, Bergin IL, Schloss PD, Young VB. 2021. Protection from lethal *Clostridioides difficile* infection via intraspecies competition for cogerminant. mBio 12.

52. Kohler LJ, Quirk AV, Welkos SL, Cote CK. 2018. Incorporating germination-induction into decontamination strategies for bacterial spores. Journal of Applied Microbiology 124:2-14.

53. Budi N, Godfrey JJ, Safdar N, Shukla SK, Rose WE. 2021. Omadacycline compared to vancomycin when combined with germinants to disrupt the life cycle of *Clostridioides difficile*. Antimicrobial Agents and Chemotherapy 65:e01431-20.

54. Howerton A, Patra M, Abel-Santos E. 2013. A new strategy for the prevention of *Clostridium difficile* infection. J Infect Dis 207:1498-504.

55. Howerton A, Seymour CO, Murugapiran SK, Liao Z, Phan JR, Estrada A, Wagner AJ, Mefferd CC, Hedlund BP, Abel-Santos E. 2018. Effect of the synthetic bile salt analog CamSA on the hamster model of *Clostridium difficile* infection. Antimicrob Agents Chemother.

56. Yip C, Okada NC, Howerton A, Amei A, Abel-Santos E. 2021. Pharmacokinetics of CamSA, a potential prophylactic compound against *Clostridioides difficile* infections. Biochem Pharmacol 183:114314.

57. Setlow P, Wang S, Li YQ. 2017. Germination of spores of the orders Bacillales and Clostridiales. Annu Rev Microbiol 71:459-477.

58. Donnelly ML, Forster ER, Rohlfing AE, Shen A. 2020. Differential effects of 'resurrecting' Csp pseudoproteases during *Clostridioides difficile* spore germination. Biochemical Journal 477:1459-1478.

59. Rohlfing AE, Eckenroth BE, Forster ER, Kevorkian Y, Donnelly ML, Benito de la Puebla H, Doublié S, Shen A. 2019. The CspC pseudoprotease regulates germination of *Clostridioides difficile* spores in response to multiple environmental signals. PLOS Genetics 15:e1008224.

60. Kevorkian Y, Shen A. 2017. Revisiting the role of Csp family proteins in regulating *Clostridium difficile* spore germination. J Bacteriol 199.

61. Kevorkian Y, Shirley DJ, Shen A. 2016. Regulation of *Clostridium difficile* spore germination by the CspA pseudoprotease domain. Biochimie 122:243-54.

62. Adams CM, Eckenroth BE, Putnam EE, Doublie S, Shen A. 2013. Structural and functional analysis of the CspB protease required for *Clostridium* spore germination. PLoS Pathog 9:e1003165.

63. Francis MB, Allen CA, Shrestha R, Sorg JA. 2013. Bile acid recognition by the *Clostridium difficile* germinant receptor, CspC, is important for establishing infection. PLoS Pathog 9:e1003356.

64. Banawas S, Korza G, Paredes-Sabja D, Li Y, Hao B, Setlow P, Sarker MR. 2015. Location and stoichiometry of the protease CspB and the cortex-lytic enzyme SleC in *Clostridium perfringens* spores. Food Microbiol 50:83-7.

65. Paredes-Sabja D, Setlow P, Sarker MR. 2009. The protease CspB is essential for initiation of cortex hydrolysis and dipicolinic acid (DPA) release during germination of spores of *Clostridium perfringens* type A food poisoning isolates. Microbiology 155:3464-72.

66. Paredes-Sabja D, Setlow P, Sarker MR. 2009. SleC is essential for cortex peptidoglycan hydrolysis during germination of spores of the pathogenic bacterium *Clostridium perfringens*. J Bacteriol 191:2711-20.

67. Shimamoto S, Moriyama R, Sugimoto K, Miyata S, Makino S. 2001. Partial characterization of an enzyme fraction with protease activity which converts the spore peptidoglycan hydrolase (SleC) precursor to an active enzyme during germination of *Clostridium perfringens* S40 spores and analysis of a gene cluster involved in the activity. J Bacteriol 183:3742-51.

68. Burns DA, Heap JT, Minton NP. 2010. SleC is essential for germination of *Clostridium difficile* spores in nutrient-rich medium supplemented with the bile salt taurocholate. J Bacteriol 192:657-664.

69. Francis MB, Sorg JA. 2016. Detecting cortex fragments during bacterial spore germination. J Vis Exp.

70. Francis MB, Allen CA, Sorg JA. 2015. Spore cortex hydrolysis precedes dipicolinic acid release during *Clostridium difficile* spore germination. J Bacteriol 197:2276-83.

71. Diaz OR, Sayer CV, Popham DL, Shen A. 2018. *Clostridium difficile* lipoprotein GerS is required for cortex modification and thus spore germination. mSphere 3.

72. Fimlaid KA, Jensen O, Donnelly ML, Francis MB, Sorg JA, Shen A. 2015. Identification of a novel lipoprotein regulator of *Clostridium difficile* spore germination. PLoS Pathog 11:e1005239.

73. Gutelius D, Hokeness K, Logan SM, Reid CW. 2014. Functional analysis of SleC from *Clostridium difficile*: an essential lytic transglycosylase involved in spore germination. Microbiology 160:209-16.

74. Bhattacharjee D, Sorg JA. 2018. Conservation of the “outside-in” germination pathway in *Paraclostridium bifermentans*. Frontiers in Microbiology 9.

75. Li Y, Davis A, Korza G, Zhang P, Li YQ, Setlow B, Setlow P, Hao B. 2012. Role of a SpoVA protein in dipicolinic acid uptake into developing spores of *Bacillus subtilis*. J Bacteriol 194:1875-84.

76. Perez-Valdespino A, Li Y, Setlow B, Ghosh S, Pan D, Korza G, Feeherry FE, Doona CJ, Li YQ, Hao B, Setlow P. 2014. Function of the SpoVAEa and SpoVAF proteins of *Bacillus subtilis* spores. J Bacteriol 196:2077-88.

77. Velasquez J, Schuurman-Wolters G, Birkner JP, Abee T, Poolman B. 2014. *Bacillus subtilis* spore protein SpoVAC functions as a mechanosensitive channel. Mol Microbiol 92:813-23.

78. Baloh M, Sorg JA. 2021. *Clostridioides difficile* SpoVAD and SpoVAE interact and are required for dipicolinic acid uptake into spores. J Bacteriol 203:e0039421.

79. Paidhungat M, Ragkousi K, Setlow P. 2001. Genetic requirements for induction of germination of spores of *Bacillus subtilis* by Ca(2+)-dipicolinate. J Bacteriol 183:4886-93.

80. Kochan TJ, Foley MH, Shoshiev MS, Somers MJ, Carlson PE, Hanna PC. 2018. Updates to Clostridium difficile Spore Germination. Journal of Bacteriology.

81. Buggy BP, Wilson KH, Fekety R. 1983. Comparison of methods for recovery of *Clostridium difficile* from an environmental surface. Journal of Clinical Microbiology 18:348-352.

82. Jump RL, Pultz MJ, Donskey CJ. 2007. Vegetative *Clostridium difficile* survives in room air on moist surfaces and in gastric contents with reduced acidity: a potential mechanism to explain the association between proton pump inhibitors and *C. difficile*-associated diarrhea? Antimicrob Agents Chemother 51:2883-7.

83. Permpoonpattana P, Tolls EH, Nadem R, Tan S, Brisson A, Cutting SM. 2011. Surface layers of *Clostridium difficile* endospores. J Bacteriol 193:6461-70.

84. Setlow P. 2007. I will survive: DNA protection in bacterial spores. Trends Microbiol 15:172-80.

85. Coullon H, Rifflet A, Wheeler R, Janoir C, Boneca IG, Candela T. 2018. N-Deacetylases required for muramic-delta-lactam production are involved in *Clostridium difficile* sporulation, germination, and heat resistance. J Biol Chem 293:18040-18054.

86. Makino S, Moriyama R. 2002. Hydrolysis of cortex peptidoglycan during bacterial spore germination. Med Sci Monit:119.

87. Paredes-Sabja D, Setlow P, Sarker MR. 2011. Germination of spores of Bacillales and Clostridiales species: mechanisms and proteins involved. Trends Microbiol 19:85-94.

88. Paredes-Sabja D, Sarker MR. 2012. Adherence of Clostridium difficile spores to Caco-2 cells in culture. Journal of Medical Microbiology 61:1208-1218.

89. Castro-Cordova P, Mora-Uribe P, Reyes-Ramirez R, Cofre-Araneda G, Orozco-Aguilar J, Brito-Silva C, Mendoza-Leon MJ, Kuehne SA, Minton NP, Pizarro-Guajardo M, Paredes-Sabja D. 2021. Entry of spores into intestinal epithelial cells contributes to recurrence of *Clostridioides difficile* infection. Nat Commun 12:1140.

90. Castro-Córdova P, Mendoza-León MJ, Paredes-Sabja D. 2021. Using a ligate intestinal loop mouse model to investigate *Clostridioides difficile* adherence to the intestinal mucosa in aged mice. PLOS ONE 16:e0261081.

91. Rohlfing AE, Eckenroth BE, Forster ER, Kevorkian Y, Donnelly ML, Benito de la Puebla H, Doublie S, Shen A. 2019. The CspC pseudoprotease regulates germination of *Clostridioides difficile* spores in response to multiple environmental signals. PLoS Genet 15:e1008224.

92. Kochan TJ, Foley MH, Shoshiev MS, Somers MJ, Carlson PE, Hanna PC. 2018. Updates to *Clostridium difficile* spore germination. J Bacteriol 200.

93. Hanahan D. 1983. Studies on transformation of *Escherichia coli* with plasmids. J Mol Biol 166:557-80.

94. Gibson DG, Young L, Chuang RY, Venter JC, Hutchison CA, 3rd, Smith HO. 2009. Enzymatic assembly of DNA molecules up to several hundred kilobases. Nat Methods 6:343-5.

95. Hanahan D. 1983. Studies on transformation of Escherichia coli with plasmids. Journal of Molecular Biology 166:557-580.

96. Ma NJ, Moonan DW, Isaacs FJ. 2014. Precise manipulation of bacterial chromosomes by conjugative assembly genome engineering. Nature Protocols 9:2285-2300.

97. Shrestha R, Cochran AM, Sorg J. 2019. The requirement for co-germinants during Clostridium difficile spore germination is influenced by mutations in yabG and cspA. PLoS Pathog 15:1553-7374.

98. Heap JT, Pennington OJ, Cartman ST, Minton NP. 2009. A modular system for Clostridium shuttle plasmids. Journal of Microbiological Methods 78:79-85.

99. McAllister KN, Bouillaut L, Kahn JN, Self WT, Sorg JA. 2017. Using CRISPR-Cas9-mediated genome editing to generate C. difficile mutants defective in selenoproteins synthesis. Scientific Reports 7:14672.

100. Kaus GM, Snyder LF, Müh U, Flores MJ, Popham DL, Ellermeier CD. 2020. Lysozyme Resistance in Clostridioides difficile Is Dependent on Two Peptidoglycan Deacetylases. Journal of bacteriology 202:e00421-20.

101. Edelmann L. 1991. Freeze-substitution and the preservation of diffusible ions. Journal of Microscopy 161:217-228.

102. Dittmann C, Han H-M, Grabenbauer M, Laue M. 2015. Dormant *Bacillus* spores protect their DNA in crystalline nucleoids against environmental stress. Journal of Structural Biology 191:156-164.

103. Schindelin J, Arganda-Carreras I, Frise E, Kaynig V, Longair M, Pietzsch T, Preibisch S, Rueden C, Saalfeld S, Schmid B, Tinevez J-Y, White DJ, Hartenstein V, Eliceiri K, Tomancak P, Cardona A. 2012. Fiji: an open-source platform for biological-image analysis. Nature Methods 9:676-682.

104. Resource. Texas A and M University Microscopy and Imaging Center Core Facility (RRID:SCR_022128).

105. Heeg D, Burns DA, Cartman ST, Minton NP. 2012. Spores of *Clostridium difficile* clinical isolates display a diverse germination response to bile salts. PLoS One 7:e32381.

106. Wang S, Shen A, Setlow P, Li Y-q, Boer Pd. 2015. Characterization of the Dynamic Germination of Individual Clostridium difficile Spores Using Raman Spectroscopy and Differential Interference Contrast Microscopy. Journal of Bacteriology 197:2361-2373.

107. Miyata S, Moriyama R, Miyahara N, Makino S. 1995. A gene (*sleC*) encoding a spore-cortex-lytic enzyme from *Clostridium perfringens* S40 spores; cloning, sequence analysis and molecular characterization. Microbiology 141 (Pt 10):2643-50.

108. Miyata S, Kozuka S, Yasuda Y, Chen Y, Moriyama R, Tochikubo K, Makino S. 1997. Localization of germination-specific spore-lytic enzymes in *Clostridium perfringens* S40 spores detected by immunoelectron microscopy. FEMS Microbiol Lett 152:243-7.

109. Cortezzo DE, Setlow P. 2005. Analysis of factors that influence the sensitivity of spores of *Bacillus subtilis* to DNA damaging chemicals. J Appl Microbiol 98:606-17.

110. Makino S, Moriyama R. 2002. Hydrolysis of cortex peptidoglycan during bacterial spore germination. Med Sci Monit 8:RA119-27.

111. Paredes-Sabja D, Sarker MR. 2012. Adherence of *Clostridium difficile* spores to Caco-2 cells in culture. J Med Microbiol 61:1208-1218.

112. Gibbs PA. 1967. The activation of spores of *Clostridium bifermentans*. J Gen Microbiol 46:285-91.

113. Paredes-Sabja D, Udompijitkul P, Sarker MR. 2009. Inorganic phosphate and sodium ions are cogerminants for spores of *Clostridium perfringens* type A food poisoning-related isolates. Appl Environ Microbiol 75:6299-305.

114. Moir A. 2006. How do spores germinate? J Appl Microbiol 101:526-30.

115. Gao Y, Barajas-Ornelas RDC, Amon JD, Ramírez-Guadiana FH, Alon A, Brock KP, Marks DS, Kruse AC, Rudner DZ. 2022. The SpoVA membrane complex is required for dipicolinic acid import during sporulation and export during germination. Genes Dev 36:634-646.

116. Li Y, Davis A, Korza G, Zhang P, Li Y-q, Setlow B, Setlow P, Hao B. 2012. Role of a SpoVA Protein in Dipicolinic Acid Uptake into Developing Spores of Bacillus subtilis. Journal of Bacteriology 194:1875-1884.

117. Korza G, Setlow P. 2013. Topology and accessibility of germination proteins in the *Bacillus subtilis* spore inner membrane. J Bacteriol 195:1484-91.

118. Ng YK, Ehsaan M, Philip S, Collery MM, Janoir C, Collignon A, Cartman ST, Minton NP. 2013. Expanding the repertoire of gene tools for precise manipulation of the *Clostridium difficile* genome: allelic exchange using *pyrE* alleles. PLoS One 8:e56051.

119. Monteford J, Bilverstone TW, Ingle P, Philip S, Kuehne SA, Minton NP. 2021. What's a SNP between friends: The lineage of *Clostridioides difficile* R20291 can effect research outcomes. Anaerobe 71:102422.

120. Paiva AMO, Friggen AH, Qin L, Douwes R, Dame RT, Smits WK. 2019. The bacterial chromatin protein HupA can remodel DNA and associates with the nucleoid in *Clostridium difficile*. Journal of Molecular Biology 431:653-672.

121. Paiva AMO, Friggen AH, Hossein-Javaheri S, Smits WK. 2016. The signal sequence of the abundant extracellular metalloprotease PPEP-1 can be used to secrete synthetic reporter proteins in *Clostridium difficile*. Acs Synthetic Biology 5:1376-1382.

122. Ma NJ, Moonan DW, Isaacs FJ. 2014. Precise manipulation of bacterial chromosomes by conjugative assembly genome engineering. Nat Protoc 9:2285-300.

123. Heap JT, Pennington OJ, Cartman ST, Minton NP. 2009. A modular system for *Clostridium* shuttle plasmids. J Microbiol Methods 78:79-85.

124. Shrestha R, Sorg JA. 2019. Terbium chloride influences *Clostridium difficile* spore germination. Anaerobe.

125. Vepachedu VR, Setlow P. 2004. Analysis of the germination of spores of *Bacillus subtilis* with temperature sensitive *spo* mutations in the *spoVA* operon. FEMS Microbiol Lett 239:71-7.

126. Dobson L, Remenyi I, Tusnady GE. 2015. CCTOP: a Consensus Constrained TOPology prediction web server. Nucleic Acids Res 43:W408-12.

127. Griffiths KK, Zhang J, Cowan AE, Yu J, Setlow P. 2011. Germination proteins in the inner membrane of dormant *Bacillus subtilis* spores colocalize in a discrete cluster. Mol Microbiol 81:1061-77.

128. Vepachedu VR, Setlow P. 2005. Localization of SpoVAD to the inner membrane of spores of *Bacillus subtilis*. J Bacteriol 187:5677-82.

129. Daniel RA, Errington J. 1993. Cloning, DNA sequence, functional analysis and transcriptional regulation of the genes encoding dipicolinic acid synthetase required for sporulation in *Bacillus subtilis*. J Mol Biol 232:468-83.

130. Fimlaid KA, Bond JP, Schutz KC, Putnam EE, Leung JM, Lawley TD, Shen A. 2013. Global analysis of the sporulation pathway of *Clostridium difficile*. PLoS Genet 9:e1003660.

131. Rodriguez-Palacios A, Lejeune JT. 2011. Moist-heat resistance, spore aging, and superdormancy in *Clostridium difficile*. Appl Environ Microbiol 77:3085-91.

132. Lawley TD, Clare S, Deakin LJ, Goulding D, Yen JL, Raisen C, Brandt C, Lovell J, Cooke F, Clark TG, Dougan G. 2010. Use of purified *Clostridium difficile* spores to facilitate evaluation of health care disinfection regimens. Applied and Environmental Microbiology 76:6895-6900.

133. Di Bella S, Ascenzi P, Siarakas S, Petrosillo N, Di Masi A. 2016. Clostridium difficile Toxins A and B: Insights into Pathogenic Properties and Extraintestinal Effects. Toxins 8:134.

134. Li Z, Schottroff F, Simpson DJ, Gänzle MG, Schaffner DW. 2019. The Copy Number of the spoVA^{2mob} Operon Determines Pressure Resistance of Bacillus Endospores. Applied and Environmental Microbiology 85:e01596-19.

135. Errington J, Cutting SM, Mandelstam J. 1988. Branched pattern of regulatory interactions between late sporulation genes in Bacillus subtilis. Journal of Bacteriology 170:796-801.

136. Howerton A, Ramirez N, Abel-Santos E. 2011. Mapping Interactions between Germinants and *Clostridium difficile* Spores. Journal of Bacteriology 193:274-282.

137. Sharma SK, Yip C, Esposito EX, Sharma PV, Simon MP, Abel-Santos E, Firestine SM. 2018. The Design, Synthesis, and Characterizations of Spore Germination Inhibitors Effective against an Epidemic Strain of Clostridium difficile. Journal of Medicinal Chemistry 61:6759-6778.

138. Racine FM, Vary JC. 1980. Isolation and properties of membranes from Bacillus megaterium spores. Journal of Bacteriology 143:1208-1214.

139. Griffiths KK, Setlow P. 2009. Effects of modification of membrane lipid composition on Bacillus subtilis sporulation and spore properties. Journal of Applied Microbiology 106:2064-2078.

140. Cowan AE, Olivastro EM, Koppel DE, Loshon CA, Setlow B, Setlow P. 2004. Lipids in the inner membrane of dormant spores of Bacillus species are largely immobile. Proc Natl Acad Sci U S A 101:7733-8.

141. Lindsay JA, Murrell WG. 1985. Changes in density of DNA after interaction with dipicolinic acid and its possible role in spore heat resistance. Current Microbiology 12:329-333.

142. Lindsay JA, Murrell WG. 1986. Solution spectroscopy of dipicolinic acid interaction with nucleic acids: Role in spore heat resistance. Current Microbiology 13:255-259.

143. Douki T, Setlow B, Setlow P. 2005. Photosensitization of DNA by dipicolinic acid, a major component of spores of Bacillus species. Photochemical & Photobiological Sciences 4:591-597.

144. Dupuy B, Govind R, Antunes A, Matamouros S. 2008. Clostridium difficile toxin synthesis is negatively regulated by TcdC. J Med Microbiol 57:685-689.

145. Karimova G, Ullmann A, Ladant D. 2000. A bacterial two-hybrid system that exploits a cAMP signaling cascade in Escherichia coli, p 59-73. *In* Thorner J, Emr SD, Abelson JN (ed), Methods in Enzymology, vol 328. Academic Press.

146. Karimova G, Dautin N, Ladant D. 2005. Interaction Network among Escherichia coli Membrane Proteins Involved in Cell Division as Revealed by Bacterial Two-Hybrid Analysis. Journal of Bacteriology 187:2233-2243.

147. Chien C-T, Bartel PL, Sternglanz R, Fields S. 1991. The two-hybrid system: a method to identify and clone genes for proteins that interact with a protein of interest. Proceedings of the National Academy of Sciences 88:9578-9582.

148. Louvet O, Doignon F, Crouzet M. 1997. Stable DNA-binding yeast vector allowing high-bait expression for use in the two-hybrid system. Biotechniques 23:816-820.

149. Li B, Fields S. 1993. Identification of mutations in p53 that affect its binding to SV40 large T antigen by using the yeast two-hybrid system. Faseb j 7:957-63.

150. Iwabuchi K, Li B, Bartel P, Fields S. 1993. Use of the two-hybrid system to identify the domain of p53 involved in oligomerization. Oncogene 8:1693-6.

APPENDIX A

In our investigation of the potential SpoVA protein interactions, we investigated the bacterial two-hybrid system assay [Bacterial Adenylate Cyclase-based Two-Hybrid (BACTH)] and the yeast two-hybrid assay (Y2A), before settling for the split-luciferase protein assay. Below is the brief description of BACTH and Y2A systems we used.

1. Bacterial two-hybrid system

BACTH protein-protein interaction assay is based on the principle of reconstitution of adenylate cyclase (CyA), which can be split into two fragments: T25 and T18. Translation fusions of these T25 and T18 fragments to proteins who are hypothesized to interact are then engineered. Interaction (heterodimerization) between proteins of interest results in functional complementation between T25 and T18 CyA fragments, resulting in cyclic adenosine monophosphate (cAMP) synthesis. cAMP is a secondary messenger used for intracellular signal induction, and, relevant to this assay, it binds the catabolite activator protein (CAP). cAMP/CAP complex is a regulator of gene expression in *E. coli*, turning on the expression of the *lac* and *mal* operons, allowing catabolism of lactose and maltose. The utilization of these sources of carbon can be distinguished on indicator media supplemented with X-gal, as colonies exhibiting blue coloration and, therefore, indicating the interaction of the proteins of interest.

We used the BACTH System Kit from Euromedex (Euromedex, 24 rue des tuileries, 67460 Souffelweyersheim, France) and all the strains, plasmids, reagents, and protocols refer to those found in that kit. The kit was a kind donation by Dr. Beiyan Nan.

For the construction of interaction plasmids, we used pKT25, pKNT25, pUT18, and pUT18C plasmids from the BACTH assay kit. pKT25 is a plasmid that encodes the T25 fragment with the multicloning site sequence (MCS) at the 3' end of T25, allowing construction of in-frame fusions at the C-terminal of T25, and expresses a kanamycin resistance. pKNT25 is like pKT25, except that T25 fragment is downstream from the MCS, allowing construction of N-terminal fusions. pUT18C encodes the T18 fragment with the MCS at 3' end of T18, also allowing the construction of C-terminal fusions, and expresses ampicillin resistance. pUT18 is like pUT18C, except that it permits construction of N-terminal fusions.

We amplified *spoVAC, spoVAD,* and *spoVAE*, using *C. difficile* R20291 DNA as template, to create fragments with the appropriate overlap for either pKT25, pKNT25, pUT18, or pUT18C plasmid MCS insertion. Those plasmids were digested and linearized with XbaI, and the fragments inserted using Gibson assembly, resulting in a library of plasmids harboring both N-and-C-terminal fusion of *spoVAC, spoVAD, spoVAE* to T18 and T25 fragments. Plasmids were transformed into *E. coli* DH5α for storage. As positive controls we used *E. coli* DHM1 reporter strain already transformed with the plasmids pKT25-zip and pUT18C-zip, that came with the assay kit, and we additionally created plasmids harboring *C. difficile tcdR* and *tcdC*, encoding proteins that interact to negatively regulate *C. difficile* toxin synthesis, fused to T18 and T25 fragment at both N and C terminal (144). All strains and plasmids in this study are listed in Table 5. Primers used to construct the strains and plasmids are listed in Table 6.

Table 5 – List of strains and plasmids used in BACTH

Strain or plasmid	Description	Reference No
E.coli DHM1	F-, cya-854, recA1, endA1, gyrA96 (Nal r), thi1, hsdR17, spoT1, rfbD1, glnV44(AS) Reporter strain for BACTH.	(145, 146)
pKT25	Encodes T25 CyaA fragment with MCS at 3’	(145, 146)
pUT18	Encodes T18 CyaA fragment with MCS at 5’	(145, 146)
pKNT25	Encodes T25 CyaA fragment with MCS at 5’	(145, 146)
pUT18C	Encodes T18 CyaA fragment with MCS at 3’	(145, 146)
pMB14	*spoVAC* in pKNT25; N-terminal fusion	This study
pMB15	*spoVAC* in pKT25; C-terminal fusion	This study
pMB16	*spoVAD* in pKNT25; N-terminal fusion	This study
pMB17	*spoVAD* in pKT25; C-terminal fusion	This study
pMB18	*spoVAE* in pKNT25; N-terminal fusion	This study
pMB19	*spoVAE* in pKT25; C-terminal fusion	This study
pMB20	*tcdR* in pKNT25; N-terminal fusion	This study
pMB21	*tcdR* in pKT25; C-terminal fusion	This study
pMB22	*tcdC* in pKNT25; N-terminal fusion	This study
pMB23	*tcdC* in pKT25; C-terminal fusion	This study
pMB24	*spoVAC* in pUT18; N-terminal fusion	This study
pMB25	*spoVAC* in pUT18C; C-terminal fusion	This study
pMB26	*spoVAD* in pUT18; N-terminal fusion	This study
pMB27	*spoVAD* in pUT18C; C-terminal fusion	This study
pMB28	*spoVAE* in pUT18; N-terminal fusion	This study
pMB29	*spoVAE* in pUT18C; C-terminal fusion	This study
pMB30	*tcdR* in pUT18; N-terminal fusion	This study
pMB31	*tcdR* in pUT18C; C-terminal fusion	This study
pMB32	*tcdC* in pUT18; N-terminal fusion	This study
pMB33	*tcdC* in pUT18C; C-terminal fusion	This study

Table 6: List of primers used in BACTH

Plasmid made	Sequence	Primer name
pMB15	GCGCGCACGCGGCGGGCTGCAGGGTCGACTATGGATAAAAATTATAAAAAATATGTAG	5' T25 spoVAC Gibson
	TAGTTACTTAGGTACCCGGGGATCCTCTAGCTAAAACATCTTAAAAATATAATAAATAATTC	3' T25 spoVAC Gibson
pMB17	GCGCGCACGCGGCGGGCTGCAGGGTCGACTATGAAAAATAAAAGAATTGGAAAAAG	5' T25 spoVAD Gibson
	TAGTTACTTAGGTACCCGGGGATCCTCTAGCTACTCATTTACTATTACTACTGCATG	3' T25 spoVAD Gibson
pMB27	GGCGCAGTGGAACGCCACTGCAGGTCGACTATGAAAAATAAAAGAATTGGAAAAAG	5' T18 spoVAD Gibson
	ATTCGAGCTCGGTACCCGGGGATCCTCTAGCTACTCATTTACTATTACTACTGCATG	3' T18 spoVAD Gibson
pMB29	GGCGCAGTGGAACGCCACTGCAGGTCGACTATGTTAATGGACTATGTAAGAGTATTTATTG	5' T18 spoVAE Gibson
	ATTCGAGCTCGGTACCCGGGGATCCTCTAGTTATGGTTTTGCTTTTGGAG	3' T18 spoVAE Gibson
pMB31	GGCGCAGTGGAACGCCACTGCAGGTCGACTATGCAAAAGTCTTTTTATG	5' T18 TcdR Gibson
	ATTCGAGCTCGGTACCCGGGGATCCTCTAGTTACAAGTTAAAATAATTTTCATAGTC	3' T18 TcdR Gibson
pMB19	GCGCGCACGCGGCGGGCTGCAGGGTCGACTatgttaatggactatgtaagagtatttattg	5' T25C spoVAE Gibson
	tagTTACTTAGGTACCCGGGGATCCTCTAGttatggttttgcttttggag	3' T25C spoVAE Gibson

Table 6 continued

Plasmid made	Sequence	Primer name
pMB25	GGCGCAGTGGAACGCCACTGCAGGTCGACTatggataaaaattataaaaaatatgtag	5' T18C spoVAC Gibson
	ATTCGAGCTCGGTACCCGGGGATCCTCTAGctaaaacatcttaaaaatataataaataattc	3' T18C spoVAC Gibson
pMB21	GCGCGCACGCGGCGGGCTGCAGGGTCGACTatgcaaaagtctttttatg	5' T25C TcdR Gibson
	tagTTACTTAGGTACCCGGGGATCCTCTAGttacaagttaaaataattttcatagtc	3' T25C TcdR Gibson
pMB14	ACGCCAAGCTTGCATGCCTGCAGGTCGACTatggataaaaattataaaaaatatgtag	5' T25N spoVAC Gibson
	ATTCGAGCTCGGTACCCGGGGATCCTCTAGctaaaacatcttaaaaatataataaataattc	3' T25N spoVAC Gibson
pMB16	ACGCCAAGCTTGCATGCCTGCAGGTCGACTatgaaaaataaaagaattggaaaaag	5' T25N spoVAD Gibson
	ATTCGAGCTCGGTACCCGGGGATCCTCTAGctactcatttactattactactgcatg	3' T25N spoVAD Gibson
pMB18	ACGCCAAGCTTGCATGCCTGCAGGTCGACTatgttaatggactatgtaagagtatttattg	5' T25N spoVAE Gibson
	ATTCGAGCTCGGTACCCGGGGATCCTCTAGttatggttttgcttttggag	3' T25N spoVAE Gibson
pMB20	ACGCCAAGCTTGCATGCCTGCAGGTCGACTatgcaaaagtctttttatg	5' T25N TcdR Gibson
	ATTCGAGCTCGGTACCCGGGGATCCTCTAGttacaagttaaaataattttcatagtc	3' T25N TcdR Gibson
pMB24	ACGCCAAGCTTGCATGCCTGCAGGTCGACTatggataaaaattataaaaaatatgtag	5' T18N spoVAC Gibson
	ATTCGAGCTCGGTACCCGGGGATCCTCTAGctaaaacatcttaaaaatataataaataattc	3' T18N spoVAC Gibson
pMB28	ACGCCAAGCTTGCATGCCTGCAGGTCGACTatgttaatggactatgtaagagtatttattg	5' T18N spoVAE Gibson
	ATTCGAGCTCGGTACCCGGGGATCCTCTAGttatggttttgcttttggag	3' T18N spoVAE Gibson
pMB30	ACGCCAAGCTTGCATGCCTGCAGGTCGACTatgcaaaagtctttttatg	5' T18N TcdR Gibson
	ATTCGAGCTCGGTACCCGGGGATCCTCTAGttacaagttaaaataattttcatagtc	3' T18N TcdR Gibson
pMB23	GCGCGCACGCGGCGGGCTGCAGGGTCGACTATGTTTTCTAAAAAAAATGATGG	5' T25C TcdC Gibson
	tagTTACTTAGGTACCCGGGGATCCTCTAGTTAATTAATTTTCTCTACAGCTATCC	3' T25C TcdC Gibson
pMB33	GGCGCAGTGGAACGCCACTGCAGGTCGACTATGTTTTCTAAAAAAAATGATGG	5' T18C TcdC Gibson
	ATTCGAGCTCGGTACCCGGGGATCCTCTAGTTAATTAATTTTCTCTACAGCTATCC	3' T18C TcdC Gibson
pMB22	ACGCCAAGCTTGCATGCCTGCAGGTCGACTATGTTTTCTAAAAAAAATGATGG	5' T25N TcdC Gibson
	ATTCGAGCTCGGTACCCGGGGATCCTCTAGTTAATTAATTTTCTCTACAGCTATCC	3' T25N TcdC Gibson
pMB32	ACGCCAAGCTTGCATGCCTGCAGGTCGACTATGTTTTCTAAAAAAAATGATGG	5' T18N TcdC Gibson
	ATTCGAGCTCGGTACCCGGGGATCCTCTAGTTAATTAATTTTCTCTACAGCTATCC	3' T18N Tcdc Gibson
pMB26	ACGCCAAGCTTGCATGCCTGCAGGTCGACTatgaaaaataaaagaattggaaaaag	5' T18N spoVAD Gibson
	ATTCGAGCTCGGTACCCGGGGATCCTCTAGctactcatttactattactactgcatg	3' T18N spoVAD Gibson

To screen for the presence of Lac^+ or Mal^+ revertants, *E. coli* DHM1 reporter strain was grown on LB/IPTG/X-gal plates overnight at 37 °C and white colonies picked for starting the overnight cultures. DHM1 was made chemically competent using the standard lab procedure. The competent DHM1 cells were then co-transformed with plasmid pairs containing the fusion constructs of interest and grown on LB/IPTG/X-gal plates at 30 °C, also using standard lab procedure. Blue colonies indicated interaction, while white colonies indicated no interaction between the proteins (**Figure 5.1.**).

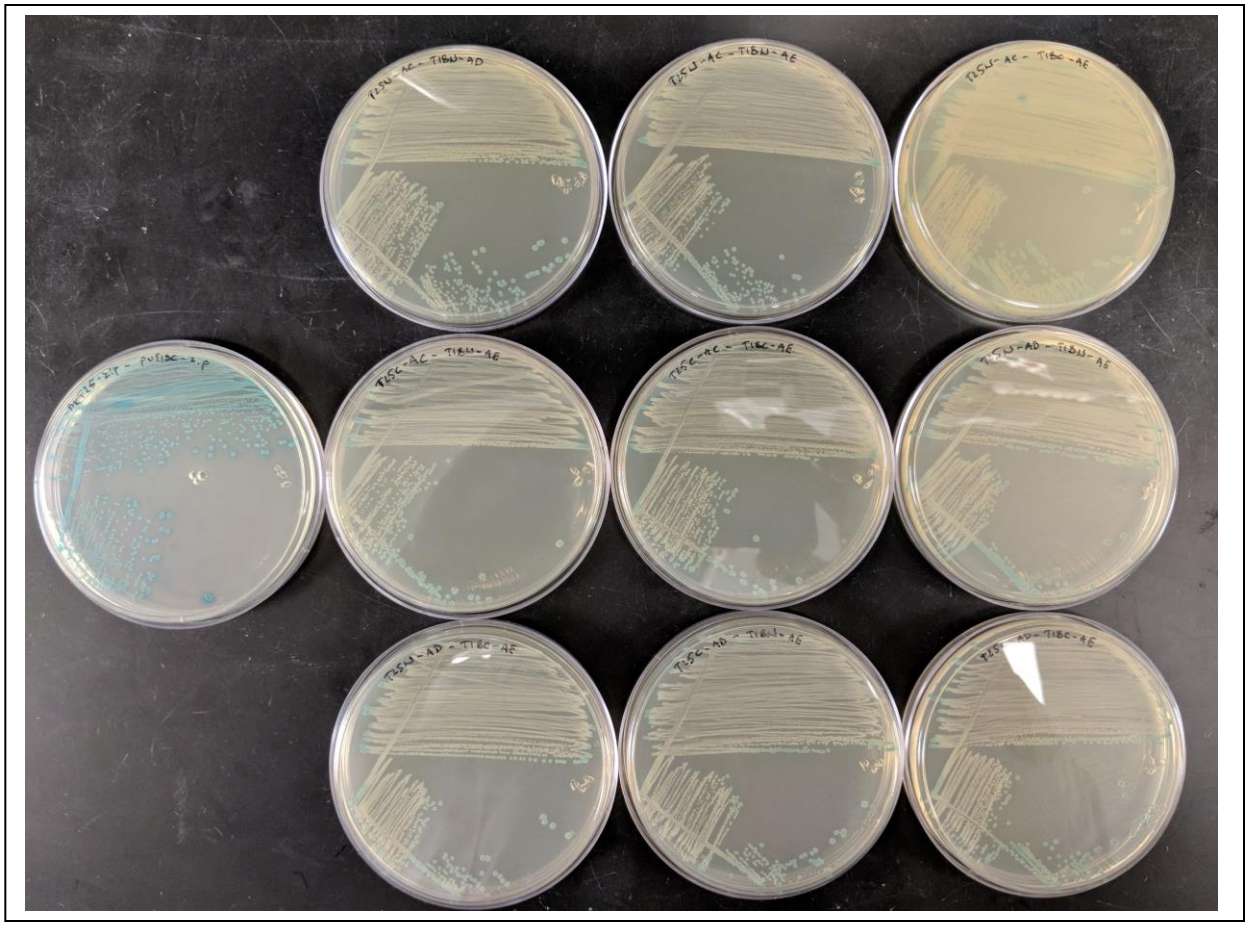

Figure 5.1. BACTH

DHM1 reporter strains was co-transformed with plasmid pairs containing the fusion constructs of interest and grown on LB/IPTG/X-gal. For clarity, not all the interacting pairs tested are shown. Leftmost plate shows the positive control plasmid pair interaction (pKT25-zip and pUT18C-zip).

Our BACTH interaction assay showed no interaction between the tested interaction plasmids harboring either N-and-C-terminal fusion of *spoVAC, spoVAD, spoVAE* to T18 and T25 fragments. Interaction, as indicated by blue colonies, was observed only for the positive control. Notably, our additional positive controls, the N-and-C-terminal fusions of *C. difficile* TcdC and TcdR, also showed no interaction signal. We therefore concluded that *C. difficile* proteins are not well-expressed in *E. coli*, preventing their interaction in this assay.

1. *Yeast two-hybrid system*

In yeast two-hybrid systems (Y2H) an interaction between bait and prey proteins activates the Gal4 transcription factor and reporter genes that enable growth on specific media or provide a color reaction. In a yeast two-hybrid assay we used, one of the interaction proteins, the bait protein, is expressed as a fusion to the Gal4 DNA-binding domain, and the other interaction protein, the prey protein is expressed as a fusion to the Gal4 activation domain. If the bait and prey proteins interact, they bring the Gal4 DNA-binding domain and activation domain into proximity, which then activates the transcription of downstream reporter genes, indicating the interaction.

The system we used for our assay was Matchmaker Gold Yeast Two-Hybrid System by Takara Bio USA (Takara Bio USA, Inc., 1290 Terra Bella Avenue, Mountain View, CA 94043, USA), a kind donation by Dr. Deborah Bell-Pedersen.

The yeast reporter strain was Y2HGold strain, with 4 reporter genes under the control of 3 distinct Gal4-responsive promoters. The reporter genes are *aur1-C*, providing resistance to the fungicide Aureobasidin A, *his3*, the expression of which permits histidine synthesis and growth on -His minimal medium, *ade2*, permitting growth on -Ade medium, and *mel1*, enocoding a-galactosidase, turning yeast cells blue when expressed. For our assays we used *his3, ade2,* and *mel1* as indicators of protein interaction.

The plasmids used were for creation of protein fusions were pGBKT7 and pGADT7. pGBKT7 encodes the Gal4 DNA binding domain (DNA-BD), with the MCS region at the C-terminal, as well as tryptophan (*trp1*) and kanamycin markers for yeast

and bacterial selection, respectively. pGADT7 encodes the Gal4 activation domain (AD), with the MCS region at the C-terminal and leucine (*leu1*) and ampicillin markers for yeast and bacterial selection, respectively. pGBKT7 was digested with NdeI and NotI, and pGADT7 with NdeI and XhoI. We amplified *spoVAC, spoVAD,* and *spoVAE* using *C. difficile* R20291 DNA as template to create fragments with the appropriate overlap for both pGADT7 and pGBKT7 plasmids for MCS insertion, and the fragments inserted using Gibson assembly. This resulted in a library of plasmids harboring C-terminal fusions of *spoVAC, spoVAD, spoVAE* to Gal4 DNA-BD and AD. As positive controls we used pGBKT7-53 plasmid (encoding fusion between the Gal4 DNA-BD and murine p53 antigen) and pGADT7-T (encoding fusion between Gal4 AD and SV40 antigen). p53 and SV40 interact in yeast two-hybrid assays. As negative controls we used pGBKT7 and pGADT7 with no fusions at the C-terminal. Plasmids were transformed into *E. coli* DH5α for storage. All strains and plasmids in this study are listed in **Table 7**. Primers used to construct the strains and plasmids are listed in **Table 8**.

Table 7 – List of strains and plasmids used in Y2H

Strain or plasmid	Description	Reference No
Y2HGold	MATa, trp1-901, leu2-3,112, ura3-52, his3-200, gal4Δ, gal80Δ, LYS2 : : GAL1UAS–Gal1TATA–His3, GAL2UAS–Gal2TATA–Ade2, URA3 : : MEL1UAS–Mel1TATA, AUR1-C MEL1	Nguyen, unpublished
pGADT7	Yeast 2-hybrid empty vector	(147)
pGBKT7	Yeast 2-hybrid empty vector	(148)
pGADT7-T	Yeast 2-hybrid positive control plasmid with SV40	(149, 150)
pGBKT7-53	Yeast 2-hybrid positive control plasmid with p53	(149, 150)
pMB36	Yeast 2-hybrid pGBKT7 plasmid with GAL4 DNA-BD-spoVAE fusion	This study
pMB37	Yeast 2-hybrid pGADT7 plasmid with GAL4 DNA-AD-spoVAC fusion	This study
pMB38	Yeast 2-hybrid pGADT7 plasmid with GAL4 DNA-AD-spoVAD fusion	This study
pMB39	Yeast 2-hybrid pGADT7 plasmid with GAL4 DNA-AD-spoVAE fusion	This study
pMB40	Yeast 2-hybrid pGBKT7 plasmid with GAL4 DNA-BD-spoVAC fusion	This study
pMB41	Yeast 2-hybrid pGBKT7 plasmid with GAL4 DNA-BD-spoVAD fusion	This study

Table 8: List of primers used in Y2H

Plasmid made	Sequence	Primer name
pMB37	GTACCCATACGACGTACCAGATTACGCTCAatggataaaaattataaaaaatatg	5' pGADT7 spoVAC Gibson
	TTCAGTATCTACGATTCATCTGCAGCTCGActaaaacatcttaaaaatataataaata	3' pGADT7 spoVAC Gibson
pMB38	GTACCCATACGACGTACCAGATTACGCTCAatgaaaaataaaagaattgga	5' pGADT7 spoVAD Gibson
	TTCAGTATCTACGATTCATCTGCAGCTCGActactcatttactattactactgca	3' pGADT7 spoVAD Gibson
pMB39	GTACCCATACGACGTACCAGATTACGCTCAatgttaatggactatgtaagagtattta	5' pGADT7 spoVAE Gibson
	TTCAGTATCTACGATTCATCTGCAGCTCGAttatggttttgcttttgg	3' pGADT7 spoVAE Gibson
pMB40	GCAGAAGCTGATCTCAGAGGAGGACCTGCAatggataaaaattataaaaaatatg	5' pGBKT7 spoVAC Gibson
	GCCCCAAGGGGTTATGCTAGTTATGCGGCCctaaaacatcttaaaaatataataaata	3' pGBKT7 spoVAC Gibson
pMB41	GCAGAAGCTGATCTCAGAGGAGGACCTGCAatgaaaaataaaagaattgga	5' pGBKT7 spoVAD Gibson
	GCCCCAAGGGGTTATGCTAGTTATGCGGCCctactcatttactattactactgca	3' pGBKT7 spoVAD Gibson
pMB36	GCAGAAGCTGATCTCAGAGGAGGACCTGCAatgttaatggactatgtaagagtattta	5' pGBKT7 spoVAE Gibson
	GCCCCAAGGGGTTATGCTAGTTATGCGGCCttatggttttgcttttgg	3' pGBKT7 spoVAE Gibson

All media and solutions used wer made according to the to the media recipes found in TakaraBio Yeast Protocols Handbook, and standard lab protocols.

Briefly, YH2Gold strain was grown on YPDA media overnight at 30 °C. The next day it was made chemically competent using lithium acetate (LiAc) and transformed with a single interaction plasmid. The transformed yeast was grown on synthetic minimal medium (SD) without amino acids, supplemented with appropriate amino acids, making it single dropout media (SDO), i.e., pGADT7-transformed yeast was grown on SD -Leu media, and pGBKT7-transformed yeast was grown on SD -Trp medium. The next day the single transformed yeast was grown overnight at 30 °C again. It was made chemically competent using LiAc and transformed with the second plasmid. Double-transformed yeast was grown on SD -Leu -Trp double dropout medium (DDO), to select for yeast harboring both plasmids. To test for protein interaction, double transformed yeast colonies were picked and streaked onto SD -Ade – His – Leu – Trp quadruple

dropout medium (QDO) supplemented with X-α-Gal. Blue colonies indicated protein interaction (**Figure 5.2.**).

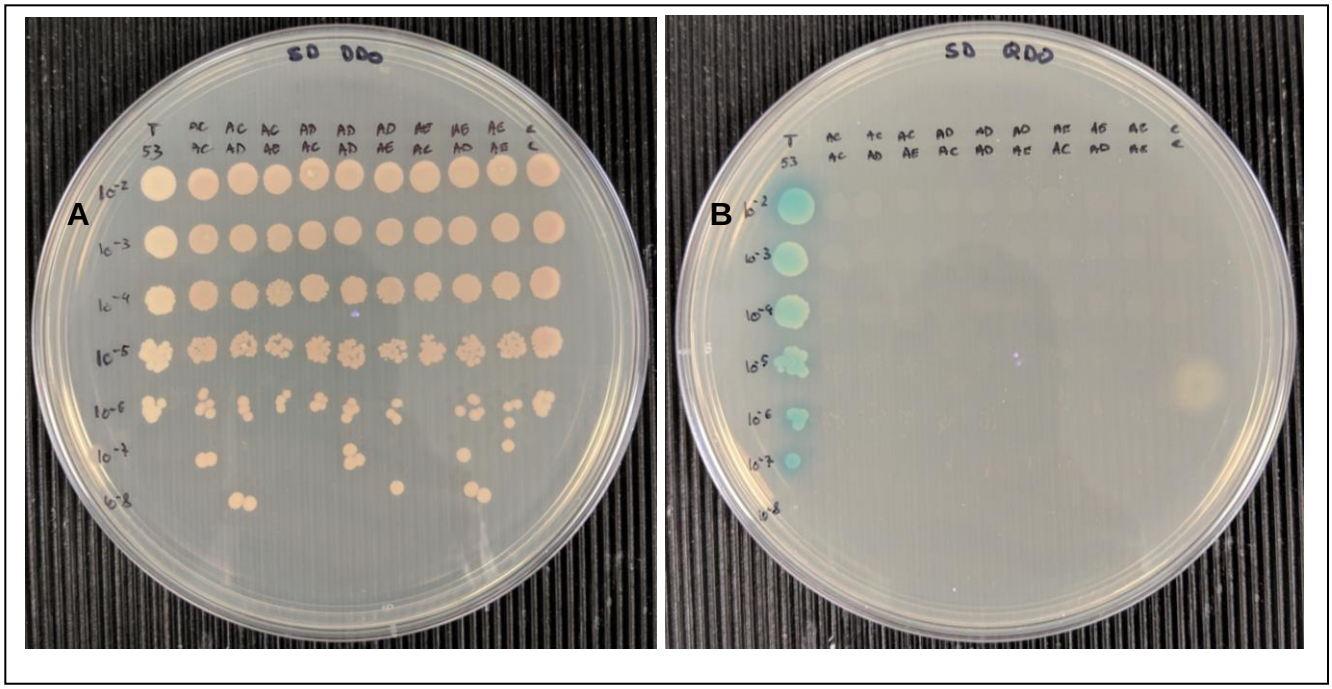

Figure 5.2. Yeast-2-hybrid assay

Yeast reporter strain was double-transformed with plasmids harboring potential interaction partners, serially diluted and plate on double-dropout (DDO) or quadruple-dropout (QDO) media. (A) Serial dilutions on DDO media, confirming the presence of interacting plasmids. Leftmost column is strain transformed with pGBKT7-53 and pGADT7-T, serving as the positive control. Rightmost column is strain transformed with empty vectors, serving as the negative control. Interacting partners are plated between. (B) Same strains as in (A), plated on QDO. Only the positive control shows growth and blue colonies indicating interaction.

Our Y2H assays detected no interaction between the plasmids harboring C-terminal fusions of *spoVAC, spoVAD, spoVAE* to either Gal4 DNA-BD or AD, regardless of whether the fusion was made in pGBKT7 or pGADT7. We can discount the possibility that the fusion proteins are toxic to Y2HGold yeast strains since we observed good growth on DDO media. It is possible that SpoVAC, SpoVAD, and SpoVAE are not expressed in their native conformation in yeast cells, preventing their interaction, or that the interaction levels are too low to be detected by this assay.